Studies on the Self-association, biological activity and DNA binding properties of a series of water soluble, mixed ligand [Pt(diimine)*N*,*N*-dihydroxyethyl-*N*'-benzoylthioureato]Cl complexes

A dissertation submitted to the

UNIVERSITY OF CAPE TOWN

In fulfilment of the requirements for the degree of

DOCTOR OF PHILOSOPHY

By

Yu-Shan Wu

B.Sc., Hons. (University of Cape Town)

Department of Chemistry
University of Cape Town
Rondebosch
7701
South Africa

March 2002

ACKNOWLEDGEMENTS

I would like to thank :

- My supervisors, Prof. Klaus Koch, Prof. Horst Klump, Dr. Val Abratt and Dr. Tim Egan for their enthusiasm and guidance throughout this study.

- My colleagues, Dr. Jorn Miller, Claire Lawrence, Oren Hallale and Paul Swan for their invaluable advices.

- My parents and my brother Paul for their encouragement throughout my study and especially during the time of writing up.

- Dr. Krassie Dimitrova, Mr. Noel Hendricks and Mr. Pete Roberts for their assistance with the NMR experiments.

- Dr. Tinus van der Merwe for his help in *ESI*-Mass spectroscopy.

- The staff in EM unit for their interest and assistance.

- All the staff and students in Department of Chemistry and Department of Molecular and Cell Biology. Special thanks to the students in Dr. Abratt's research group for their patience in helping me with different research techniques.

- My good friends, Clement Lo, Heidi Lin, Terry Lu and Eric Lien for always being there for me.

- The University of Cape Town and the National Research Foundation for the financial assistance.

ABSTRACT

A series of mixed-ligand [Pt(diimine)(*N,N*-di(hydroxyethyl)-*N'*-bezoylthioureato)]$^{+}$A^{-} complexes have been synthesised and fully characterised (where diimine is 1,10-phenanthroline; 2,2'-bipyridyl; 4,4'-dimethyl-2,2'-bipyridyl; 4,4'-di-*tert*-butyl-2,2'-bipyridyl and A is Cl; Br and ClO_4.)

The study of the ^{1}H NMR resonance spectra of these complexes in 50% (v/v) acetonitrile-d_3 and D_2O revealed a pronounced concentratioin effect which indicates that self-association is occuring in solution. It was assumed that in dilute concentrations, these complexes form dimer species. For each complex, dimerisation constants (K^D) were calculated from significant chemical shift changes as a function of concentration. Large upfield shifts are observed for the diimine protons which suggest that the self-association is regioselective. The upfield shift of protons can be attributed to the anisotropic effect of the ring current from one diimine upon its neighbour. The effect of solvent on the self-association of these complexes was also investigated. The extent of self-association was found to increase as the H_2O content in the solvent mixture increases.

The experimental results were analysed using a computer program which allowed for the best estimation of the association constant (K^D) as well as the chemical shift values at infinite dilution (δ_0-monomer) and high concentration (δ_∞-dimer). These values were optimised simultaneously using a linear regression of the chemical shift *vs.* concentration data. In the 50% (v/v) mixture of acetonitrile-d_3/D_2O, dimerisation constants are in the range of 21.3±2.7 for [Pt(bipy)H_2L]Cl and 36.4±11.8 for [Pt(diMebipy)H_2L]Cl.

In pure aqueous solutions, larger aggreates were observed by the transmission electron microscopy. It was spectulated that [Pt(diimine)(*N,N*-di(hydroxyethyl)-*N'*-bezoylthioureato)]$^{+}$A^{-} complexes formed supra molecular aggregates similar to that of lipid bilayers.

These complexes were found to bind strongly to DNA. Experiments such as UV-thermal melting, Circular Dichoism and DNA Mobility study were carried out in attempt to elucideate the binding mode of DNA to [Pt(diimine)(*N,N*-di(hydroxyethyl)-N'-benzoylthioureato)]$^{+}A^{-}$ complexes. Complexes such as [Pt(bipy)H_2L]Cl, [Pt(diMebipy)H_2L]Cl, [Pt(phen)H_2L]Cl were found to intercalate into DNA whilst the tertiary butyl moiety on [Pt(di-*tert*-butylbipy)H_2L]Cl provided a steric hindrance for intercalation.

The *in vivo* study of these complexes shown that only [Pt(bipy)H_2L]Cl complex is biologically active. The survival study using a wild type strain of E.*coli* (AB1157) and a *uvrA*$^{-}$ mutant (AB1886) showed that [Pt(bipy)H_2L]Cl is more than 100 fold more toxic to the *uvrA*$^{-}$ mutant strain than the wild type strain of E.*coli.* This result strongly suggest that [Pt(bipy)H_2L]Cl causes damages directly to the DNA.

TABLE OF CONTENTS

CHAPTER 2: SYNTHESIS AND CHARACTERISATION

CHAPTER 3: SELF ASSOCIATION

CHAPTER 4: BINDING STUDIES ON BIOLOGICAL SYSTEM

Metal ions play a vital role in numerous biological processes[1]. Their chemistry offers many opportunities to the medicinal chemists. Transition metals have labile *d*-electron systems, and are most suitable to catalyse redox reactions for the following reasons: (1) A range of accessible oxidation states enables them to transfer electrons. (2) The redox potentials (E_o) for such transfer can be varied by alteration of ligand type or geometry. (3) Metal ions can mediate atom transfer reactions. (4) Stable paramagnetic states are common, facilitating reaction with radical substrates. (5) Metals can bind neutral as well as anionic ligands[2]. They can also undergo ligand substitution with biological molecules with a specific stereochemistry about the metal centre and with a controlled reactivity. Some examples of the roles of metal ions in biological system are:

- Alkali and alkaline earth metals – responsible in carrying charges in the nervous system and muscle contraction. It also controls the ionic balance across the cell membrane.
- Transition metals – responsible for biological redox reactions. The heme iron proteins are associated with oxygen transport and storage, with electron transfer in the cytochromes, with catalysis of oxidations by oxygen and hydrogen peroxide. Cobalt containing B_{12} coenzymes is essential for the catalysis of reduction and methyl group transfer reactions.
- Some metals possess radioactive isotopes that have potential for tumour imaging or therapy.

Apart from being essential for the functioning of the body, metal coordination chemistry can also be used in the treatment, management, diagnosis of disease, or coordination complexes can be formed in the body to handle dysfunction due to metal poisoning.[3] Four principal areas of the use of transition metal compounds in medicine are: (1) The used of metal-based drugs to treat disease. Examples are the historical use of organoarsenicals in the treatment of syphilis, the use of *cis*-dichlorodiammineplatinum(II) (cisplatin) in the treatment of cancer and the use of gold complexes in the treatment of rheumatoid arthritis. (2) The use of chelating or complexing agents to treat metabolic dysfunction. The classical example is the

use of D-penicillamine to treat Wilson's disease, which is caused by an inability of the body to metabolise copper in the normal way. Another example is the use of desferrioxamine for iron overload in Cooley's anaemia, which is caused by a fault in haemoglobin synthesis. (3) The use of complexing, chelating or sequestering agents to remove heavy metal poisons from the body. (4) The use of coordination complexes to transport metals to specific sites in the body to aid in imaging.

In the following sections we will discuss the current development of anticancer drugs and their different mode of interactions with DNA.

1.1 PLATINUM ANTICANCER DRUGS

The biological properties of *cis*-diamminedichloroplatinum(II) (cisplatin) were discovered serendipitously by Barnett Rosenberg[4] in the mid-1960s during experiments studying the effect of electric fields on the growth of *E. coli* bacteria. The platinum electrodes which were used in the experiment reacted with the bacterial growth media to produce Pt(II) and Pt(IV) compounds, including *cis*-$[Pt(NH_3)_2Cl_2]$, which inhibited cell division causing the bacteria to become long and filamentous. Since inhibition of cell division has often been associated with anticancer agents, the platinum compounds were examined for antitumour activity in mice. Based on these studies *cis*-diammine dichloroplatinum(II), now known as cisplatin, was found to be very effective against a variety of solid tumours, whereas its *trans*-isomer was inactive.

When cisplatin initially entered clinical trials, the high levels of nephrotoxicity observed during drug administration almost prevented its further development[5]. However, prehydration therapy with intravenous saline and controlled dosage levels of less than 120 mg m^{-2} greatly reduced renal toxicity as a side effect of cisplatin treatment[6].

While cisplatin (Fig. 1.1) was entering the clinic for treatment against primarily testicular cancer, studies were ongoing to combat the numerous side effects of its chemotherapy. Several compounds have been identified which show better antitumour activity than cisplatin. Some have the advantage of higher water solubility and greater ease of administration. Sulphato-1,2-diaminocyclohexane platinum(II) is water soluble, active against at least three animal tumours and about 30 times as potent as cisplatin. Another similar complex, cis-diammine-1,1-cyclobutanedicarboxylateplatinum(II), commonly known as carboplatin (Fig. 1.1), was presumed to have the same active form of the drug as cisplatin, but the slower hydrolysis of the cyclobutanedicarboxylate leaving group of carboplatin allows a similar antitumour activity with reduced toxicity[7]. Carboplatin is now routinely used as an alternative to cisplatin in chemotherapy. A new compound, JM-216 (*cis, trans, cis*-$PtCl_2(Oac)_2(NH_3)(C_6H_{11}NH_2)$)[8] (Fig. 1.1), can be administered orally and this drug is metabolized into several active compounds in the gastrointestinal tract. This complex showed substantially greater cytotoxicity than cisplatin and carboplatin. It also showed a lack of cross-resistance with cisplatin in some cell lines, particularly in those where reduced platinum accumulation played a dominant role in resistance.

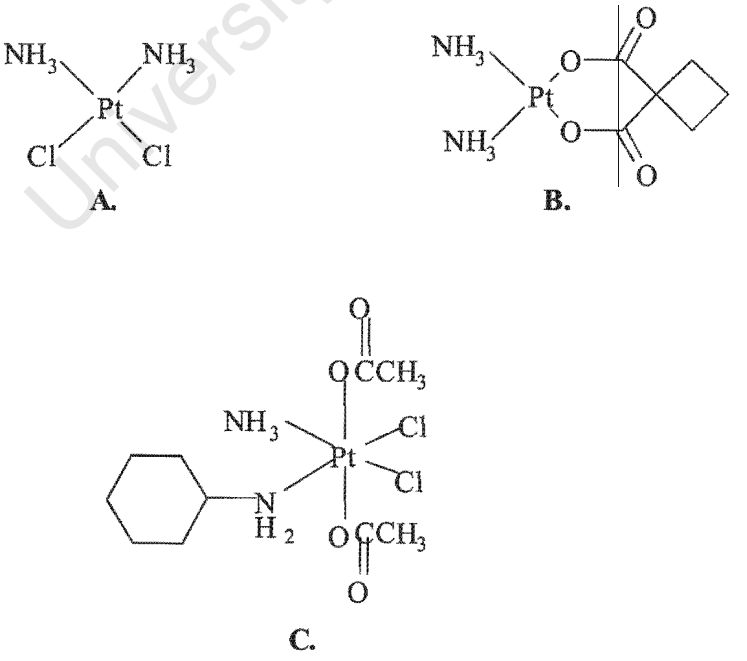

Fig.1.1 Structure of A. cisplatin, B. carboplatin, and C. JM216.

Tumour cells are distinguished from normal body cells by the loss of genetic control of their growth regulation during their life span. The feedback mechanisms of the neighbouring cells are therefore also impaired, which leads to the uncontrolled growth of tumour tissue. In normal cells, these processes are restrained and regulated by proto-oncogenes, and cancer may thus result from changes in their genetic expression. According to this basic concept of carcinogenesis, platinum anticancer drugs such as *cis*-diamminedichloroplatinum(II) (cisplatin) were believed to exert their cytostatic effect primarily through coordination with DNA in the cell nucleus while reactions in other regions cause undesired side effects. This will be discussed in greater detail under section 1.2.1 of this chapter. The pathways of cisplatin in human body are schematically outlined in Fig.1.2.[9]

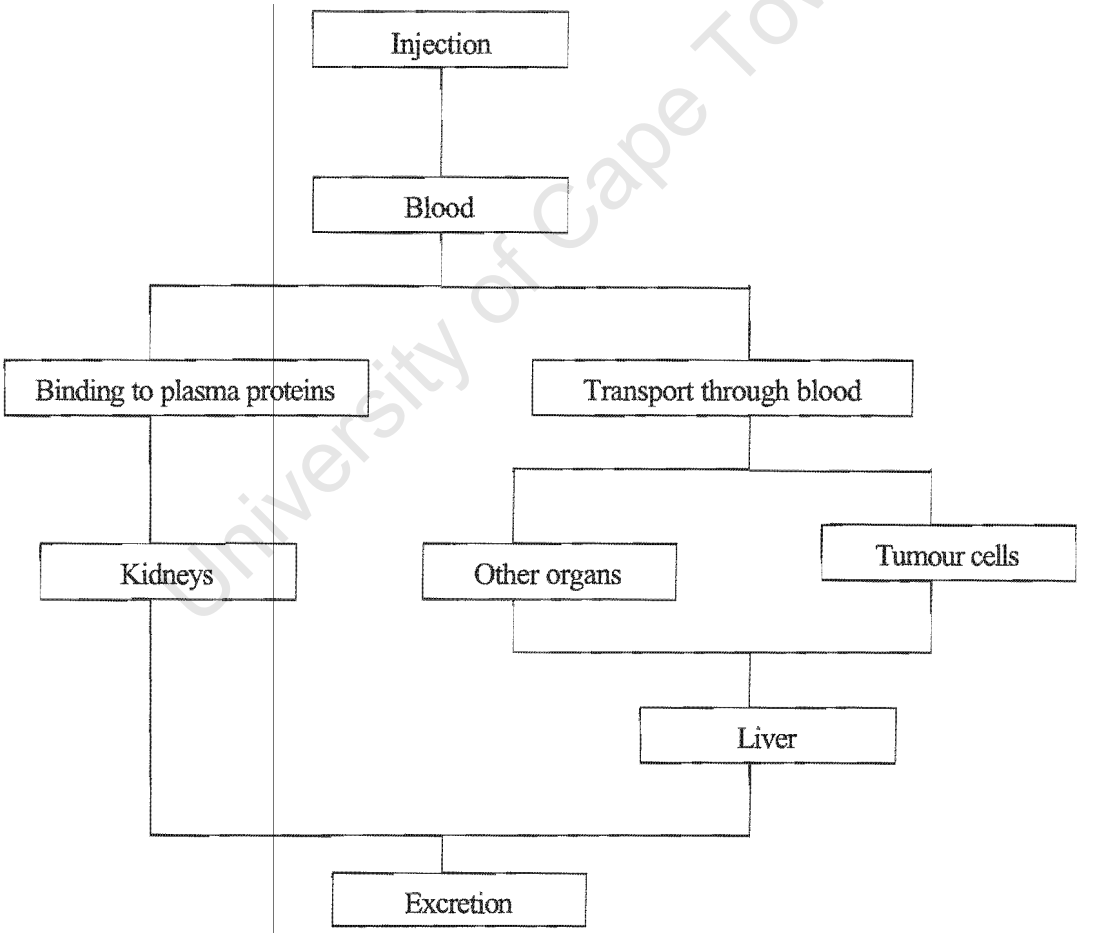

Fig. 1.2 The metabolic pathways of cisplatin in the human body.[9]

1.2 MODE OF INTERACTION OF PT ANTICANCER DRUGS WITH DNA

Nucleic acids interact reversibly with a broad range of chemical species that include water, metal ions and their complexes, small organic molecules and proteins, and their conformations are stabilised solely by these interactions.[10] Dramatic structural transitions in nucleic acids are generally brought about by changes in water activity, salt concentration (ionic strength), or by interaction with organic molecules. In medicine, the most important chemotherapeutic agents active against cancer, viral and some parasitic diseases, involves drugs that interact reversibly with nucleic acids. This results in the interest in understanding the mode of action of existing medicinal agents and in turn helps in developing a new generation of superior drugs.

1.2.1 DNA Structure

Nucleic acids are linear polymers of nucleotides whose phosphates bridge the 3' and 5' positions of successive sugar residues. The phosphates of these polynucleotides, the phosphodiester groups, are acidic so that at physiological pH's, nucleic acids are polyanions[11]. In 1953, Watson and Crick, based on chemical analysis of DNA base composition and on x-ray diffraction patterns, proposed the double helical structure of DNA. The evidence showed that DNA consists of two polynucleotide chains wrapped around each other to form a helix. The two chains are held together by hydrogen bonds between bases on opposite chains, with the paired bases lying in a plane perpendicular to the helical axis. The sugar-phosphate backbone is the outer part of the helix[12] (Fig. 1.3).

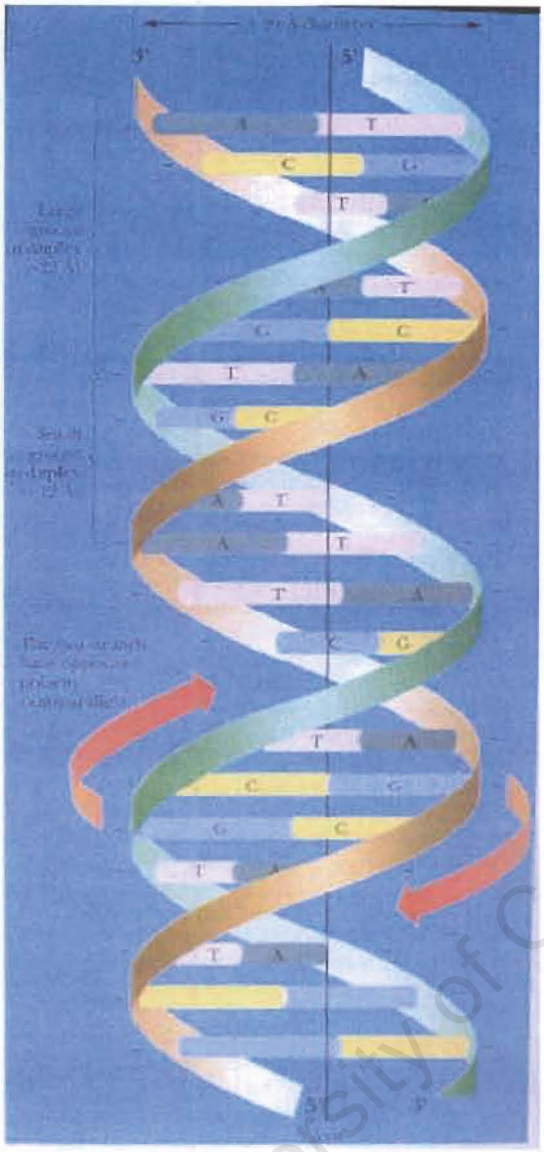

Fig. 1.3 The schematic diagram of DNA double helix.[9]

The base pairing in DNA is highly specific: the purine adenine pairs with the pyrimidine thymine (Fig. 1.4) and the purine guanine pairs with the pyrimidine cytosine. A stereochemical consequence of the way A:T and G:C base pairs form is that the sugars of the respective nucleotides have opposite orientations, and thus the sugar-phosphate backbones of the two chains run in opposite or "antiparallel" directions. The bases in a base pair are not directly across the helix axis from one another along some diameter but rather slightly displaced. This displacement and the relative orientation of the glycosidic phosphate backbone, leads to differently sized grooves in the cylindrical column created by the double helix. The base pair portions that are exposed to the major and minor grooves afford specific binding affinity to different molecules.

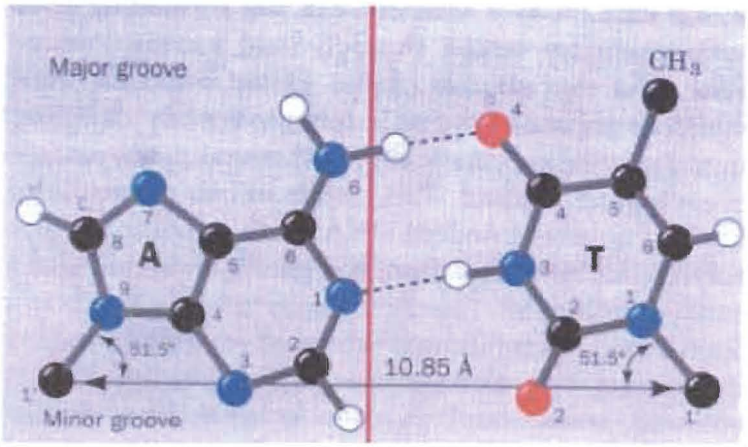

Fig. 1.4 The Watson-Crick base pairs[9].

There are several possible modes of interaction of metal ions and their complexes with DNA. In general these are intrastrand chelation, intercalation of planar complexes, groove binding and electrostatic interaction, each of which will be discussed in some detail below.

1.2.2 Intrastrand chelation (covalent binding)- cisplatin

When *cis*-$[PtCl_2(NH_3)_2]$ enters into the bloodstream, it encounters a relatively high concentration of chloride ions that suppresses hydrolysis and maintains the compound in a neutral state. Uncharged *cis*-$[PtCl_2(NH_3)_2]$ complex then passes through cell membranes of different cells or tumour cells via passive transport[13]. It is rapidly hydrolysed due to the markedly lower chloride concentration in intracellular regions. Within cells, about 40% of the platinum are present as *cis*-$Pt(NH_3)_2Cl(H_2O)^+$. This hydrolysis product of cisplatin is kinetically labile since H_2O is a much better leaving group with respect to Pt(II) than Cl^-; it is thus assumed that *cis*-$Pt(NH_3)_2Cl(H_2O)^+$ is a particularly active form of the cytostatic agent. The positive charge of this substituted complex supports such an assumption because it would be more likely to approach and coordinate to the negatively charged DNA. After loss of Cl^-, the *cis*-$Pt(NH_3)_2Cl(H_2O)^+$ has been shown to form coordinative bonds to nitrogen atoms of nucleobases; in *in vitro* these include bonds to N7 of guanine, N1 and N7 of adenine and N3 of cytosine. N1 of adenine and N3 of cytosine are engaged in hydrogen

bonding within the DNA framework; for various nucleotide oligomers serving as DNA models, the highest binding affinity was found between N7 of guanine and platinum.[14]

Four other types of reactive species in the body which compete for cisplatin include 1) the rescue agent, 2) the cell membrane ligands, 3) the peptides and proteins, and 4) the cellular DNA[15]. After hydrolysis and transport, the binding to DNA is assumed to take place. For cisplatin and related species, a specific binding occurs at G-N7 site, resulting in a specific distortion of DNA, changing its interaction with proteins. In theory, basic coordination chemistry predicts that S-donor ligands such as methionine and cystein residues present in tissues, and in particular in proteins would rapidly bind and generate the most stable platinum complexes. Furthermore, the strong interaction of Pt ions with S-donor will leave hardly any reactivity for the N-donor ligands such as adenine and guanosine. However, in reality cisplatin is found to bind at N7 atoms of guanine. Competition studies for Pt-amine compounds with S-donor ligands have shown that transfer occurs easily from an S ligand to guanine-N7 site and that S-donor ligands, including those of protecting agents, may be involved as reaction intermediates for Pt (G-N7) (G-N7) target.[15] In such Pt-sulphur interactions perhaps serve as a drug reservoir for platination at DNA. Two reaction pathways are possible, either the spontaneous release of platinum from the sulphur followed by a subsequent reaction with DNA fragment or the direct nucleophilic displacement of platinum from sulphur by the guanine-N7 group. Studies with S-guanosyl-L-homocysteine reveal that indeed, isomerization with coordination at N7 of guanine does occur at pH values above 7, and thus confirm that N7 donor atom can indeed replace the sulphur atom in a platinum-sulphur adduct. Studies with Met-d(TpGpG) , which contains one end resembling the methionine residues of proteins (S-donor) and the other end resembling DNA (N-7), have shown initial S-coordinated complex formation (2 hours) and slow isomerization. However, after 6 days, no Pt-S adducts could be detected , and all platinum was found to be coordinated to N7 site. This illustrates the kinetic preference of platinum for sulphur donor atom but thermodynamic preference for N7 binding.

The chelation of cisplatin to two neighbouring guanines has been speculated in the early stage of mechanistic investigations. The possible binding can be shown schematically as in Fig. 1.5. In simple single strand DNA studies (pGpG , CpGpG), NMR, and two X-ray structural studies, confirmed the postulated formation of bis-N7 chelate between the neighbouring guanine bases and also that distortion to the two originally parallel guanine planes.[5] Studies on monofunctional Pt binding to ds DNA showed distortions in form or bending of the DNA, although the degree of distortion depends on the actual sequence, and the base pairs remain intact. Studies involving bifunctional binding to ds DNA by den Hartog *et al.*[16] using two-dimensional NMR analysis, proved that chelation of cisplatin to two neighbouring guanine indeed occurs, and further deduced that the DNA bends or kinks by an angle of 40-50 degrees. During recent years this picture has hardly changed and has been confirmed by several other sequences from other laboratories. The weak point in the use of two-dimensional NMR for determination of such structure is that no direct measurement of bending angle can be obtained and only by the use of XRD in solid state can provide this precise information. The major breakthrough came when Takahara and Lippard successfully determined the double stranded synthetic dodecamer d(CCTCTG*G*TCTCC)/ d(GGAGACCAGAGG) . The structure is kinked as was predicted by earlier studies, with a bending angle of the helix of about 45 degrees. (in fact only a small difference to two-dimensional NMR solution. It appears that the angle between the planes of the two chelating guanines is rather small and as a consequence the Pt ion lies about 1 Å out of the guanine plane. DNA conformation at the 5' side from Pt has changed from B-DNA to A-DNA.

After the Pt chelation to the neighbouring guanines, work by Lippard and others have shown that bent DNA is recognised by DNA repair system, such as the uvr system in prokaryotes and the high mobility group (HMG) proteins in eukaryotes. In early stages, it was proven that progression of DNA polymerase along the DNA chain is blocked at GpG-Pt sites. Also the progression of *E.coli* RNA polymerase was shown to be blocked, indicating that platination has an effect on both replication and transcription. Later work has shown that the effect of repair is fundamental for the mechanism. Experiment with mutants lacking the genes for excision repair or recombination, has shown high sensitivity for cisplatin.

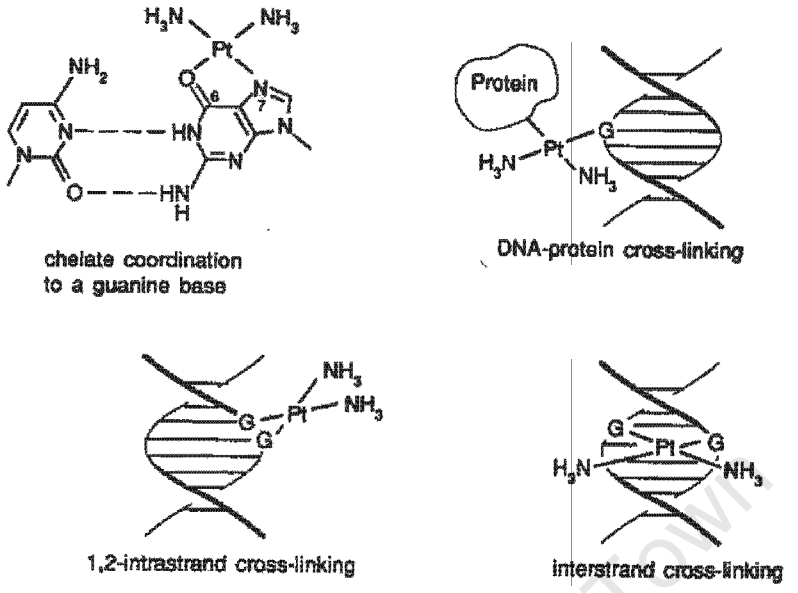

Fig. 1.5 Possible bindings between *cis*-$Pt(NH_3)_2^{2+}$ and guanosine (G) in double-stranded DNA.[11]

1.2.3 Intercalation

In the early 1960s, Lerman[17] described a number of physical studies on the interactions of DNA with planar aromatic cations. He concluded that from these studies that planar aromatic molecules could bind to DNA by a process which he termed intercalation. Typical intercalators are planar aromatic cations that bind by insertion of the aromatic ring systems between DNA base pairs. Intercalation distorts the torsional bonds in the DNA backbone, and causes separation of base pairs and a lengthening of the double helix. The DNA double helix has base pairs stacked along the helical axis at 3.4 intervals. The thickness of typical aromatic ring system should in principle lengthen the helix by 3.4Å However, in practice, the observed length increase of the DNA complex is generally less than the 3.4Å This is due to the unwinding of helix at the site of an intercalation complex and normally approximately 36° rotation of one base-pair with respect to the next is decreased as a result of intercalation. The amount of unwinding depends considerably on the intercalator structure and also with the DNA sequence in a manner.

Daunomycin and adriamycin are two anticancer drugs that currently used in the clinical treatment of human cancers. These molecules contain four fused rings and an amino sugar as seen in Fig. 1.6.[18]

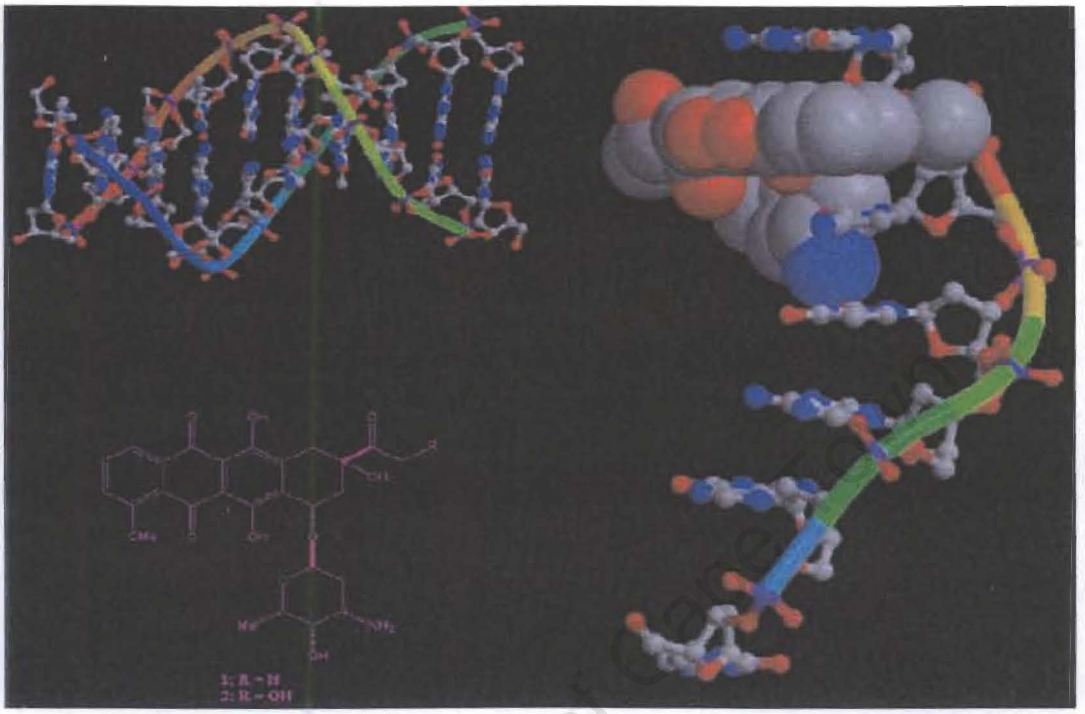

Fig. 1.6 Structure of Daunomycin and its intercalation into DNA.

It has been shown that the fused aromatic rings favourably intercalate between DNA base pairs. Wang, Rich and co-workers[19] determined the first crystal structure of daunomycin and the oligonucleotide d(CGTACG). Daunomycin binds to the DNA helix with its long axis almost perpendicular to the long axes of adjacent base-pairs at the intercalation site. The hydroxyl group O9 of a daunomycin provides a specific anchor on DNA by forming hydrogen bonding with the base pairs above and below the intercalation site.

1.2.5 External Electrostatic Interactions

The anionic phosphate groups on the DNA helices play an important role in their structure and interactions. When the line charge spacing of a DNA helix becomes too narrow, the molecule becomes unstable.[10] Polymer conformations with charges that are more closely spaced must therefore associate with counterions from the solution to achieve stability. Cationic species, such as alkali metals, associate with nucleic acids as a function of the polymer charge density. The association of ions with the polyelectrolyte is called counterion condensation. Counterions condense until the charge density is reduced to the stable level. Additional counterions are associated with the remaining charges on the polyanion through Debye-Hückel type interactions. (Fig. 1.7) The associated counterions reduce the effective charge on nucleic acids and strongly affect the solution properties and binding interactions of the polymer. A significant portion of the binding free energy of species ranging from small cations to large proteins can result from the neutralisation of nucleic acid charges (ion pair formation) in the complex and the resulting favourable entropic effect of release of counterions. At a constant temperature, this entropic effect resulting from counterion release can lead to nucleic acid denaturation as well as to increased binding of cationic ligands as the bulk solution salt concentration is decreased. This is a reason why the denaturation (conformation change) of nucleic acids depends strongly on salt concentration.

Any ligand binding process which causes a conformational change will have an additional salt dependence. For example, intercalators generally lengthen the double helix of DNA and this causes release of counterions since the longer helix has a larger spacing between phosphate groups and resulting in lower intrinsic charge density. For the cationic intercalators, counterions from DNA are released as the result of both the conformational change and the neutralisation of charges through ion-pairing.

Since the condensation creates a non-specific, mobile type complex along the exterior of the double helix, the kinetics of association and dissociation of this complex are rather rapid. Kinetics studies indicate that complex cations, which either bind to DNA through groove or via intercalation, initially associate with the duplex through condensation.

Another type of electrostatic interaction is non-specific outside stacking. Planar aromatic molecules can stack on each other to form dimers and higher aggregates. The charged planar compounds normally repel each other electrostatically, however, if the cations stack along the anionic DNA backbone, the charge repulsion is decreased and this leads to the outside stacking of planar cations along the double helix. This binding mode is a type of extended self-association, and can be highly co-operative. Therefore it is more favourable at high ratios of the aromatic cation to DNA phosphate groups.

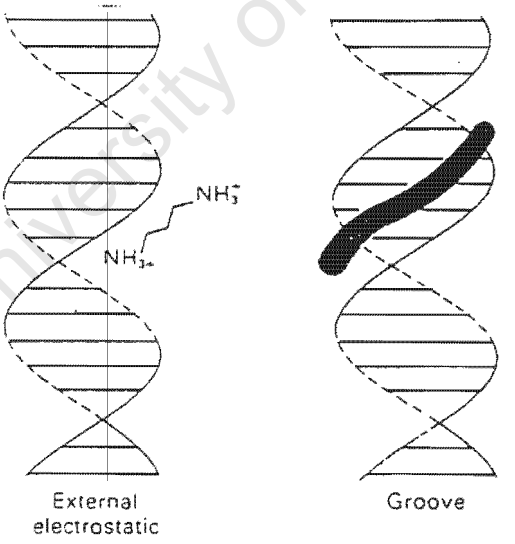

Fig. 1.7 Diagram showing the groove binding and electrostatic interaction with DNA[10].

1.3 RECENT DEVELOPMENT OF ANTICANCER DRUGS

Since the development of cisplatin as a successful antitumour drug, a large number of cancer patients that have been completely cured after cisplatin treatment. It is highly effective in treating testicular and ovarian cancers, and it contributes to the treatment of oropharyngeal carcinoma, bronchogenic carcinoma, cervical carcinoma, lymphoma, osteosarcoma, bladder carcinoma and neuroblastoma. Recent studies have shown that in combination with new drugs, cisplatin may be effective against particularly refractive disease including melanoma and breast cancer.[20]

Despite of the success of cisplatin in treating cancers, cisplatin and its closely related analogue carboplatin have two important shortcomings, namely (1) toxicity such as nephrotoxicity, neurotoxity, and emetogensis, which limits the dose that can be given to patients.[21] The toxic side effects are generally thought to be due to the platinum complexes binding to biomolecules in the blood stream and in cells instead of their supposedly DNA targets. Biomolecules such as methionine and glutathione (reduced GSH; oxidised G-S-D-G) interact with cisplatin because of the higher affinity of S-donor ligands to Pt metal. The use of rescue agents with antagonistic S-donor such as diethyldithiocarbamate and thiosulfate have been used to control cisplatin toxicity; (2) The development of drug resistance, which renders the drug less effective.

An even more important challenge is to overcome the development of resistance. This has resulted in development of new generations of mononuclear, dinuclear and even trinuclear platinum compounds, lacking cross-resistance with cisplatin/ carboplatin. One approach to overcome platin resistance is the preparation of drugs that bind to DNA in a structurally different way compared to cisplatin.

1.3.1 Structure-Activity relationships

Over the years, thousands of Pt compounds have been synthesized and tested as potential antitumour drugs in an attempt to overcome those problems mentioned above. In the earlier years, the development of new drugs adhered to structural analogues of cisplatin and also the rules that Cleare and Hoeschele[22,23] reported on the structural-activity relationship. These studies confirmed that complexes with the *trans* geometry were inactive and added other criteria, stating (i) that a pair of *cis* leaving groups was necessary but not sufficient; (ii) that the complex should be uncharged; (iii) that the leaving groups should be moderately strongly bound because those with highly labile leaving groups are toxic and those with tightly bound groups were less active, though significantly the point was made that complexes with dicarboxylate ligands such as malonate were active; and (iv) that higher activity is found for those complexes where the amine groups have fewer alkyl substituents. The structure-activity rules remained valid until relatively recently, since all the compounds that have entered clinical trials have conformed to these rules. However, these cisplatin analogues are limited in that they lack substantial advances over the existing drugs.

Recently, a number of compounds have emerged that do not conform to the structure/activity rules, and these compounds show different activity profiles to cisplatin and its analogues.

1.3.2 Covalently bound, cisplatin type of complexes

Sterically Hindered Pt Complexes

Studies have been done in the attempt to elucidate the mechanisms underlying tumour resistance to cisplatin, which have revealed that a combination of reduced platinum transport, increased cytoplasmic detoxification via elevated glutathione and/or metallothionein levels, enhanced DNA repair, and increased cellular tolerance to Pt-DNA adducts are the major

mechanisms underlying resistance. Complexes such as *cis*-amminedichloro(2-methylpyridine)platinum(II)[24] (Fig. 1.8) was designed to circumvent resistance by sterically hindering cellular detoxification by glutathione and other cellular thiols while still retaining the ability to form cytotoxic lesions with DNA. The 2-methyl group in the substituted pyridine ring causes the pyridine ring to tilt 102.7°. This places the 2-methyl group directly over platinum(II) square plane and introduces steric hindrance to an axial approach to the platinum metal from above. This compound was indeed found to be less reactive towards thiourea, pyridine, methionine and GMP than cisplatin and the pyridine analogue.

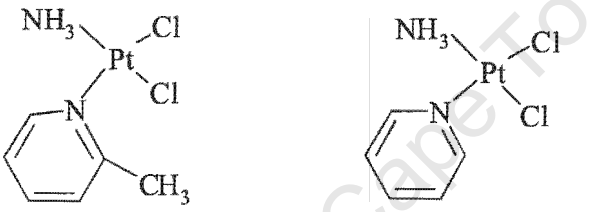

Fig. 1.8 Structures of *cis*-amminedichloro(2-methylpyridine)platinum (II) and *cis*-amminedichloro(pyridine)platinum (II)

Reedijk and Krebs[25] reported that complex *cis*-[Pt(bmic)Cl$_2$] has significant cytotoxicity while the less sterically hindered compound *cis*-[Pt(bmi)Cl$_2$] (Fig. 1.9A) was inactive. This was also illustrated by the difference in reactivity of these two complexes towards 5-GMP. The greater steric hindrance around the Pt metal renders it less susceptible to deactivation by cellular thiols. Another example was *cis*-bis(pyridine)platinum(II) complexes (Fig. 1.9B) reported by Deacon and co-worker.[26] They found that the replacement of Cl$_2$ group by the bulky organoamide ligand increases the cytotoxicity while still having comparable activity to cisplatin in L1210/1210cisR pair of cell lines.

A.

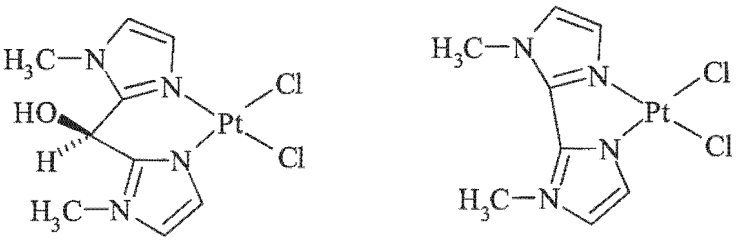

B.

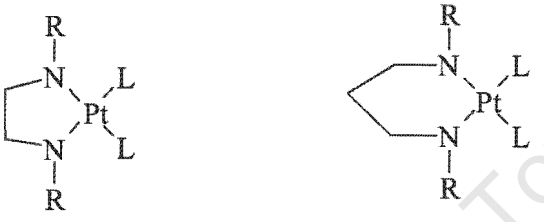

R = p-HC_6F_4, C_6F_5, p-ClC_6F_4, p-BrC_6F_4, p-IC_6F_4, 2,3,5-$F_3C_6H_2$, p-MeC_6F_4, p-$C_6F_5C_6F_4$

L = pyridine, substituted pyridines.

Fig. 1.9 Structures of A. *cis*-[Pt(bmic)Cl_2] and *cis*-[Pt(bmi)Cl_2]. B. *cis*-bis(pyridine) platinum(II) complexes.

Charged Complexes

Neutral compounds were believed to be essential for biological activity since platinum compounds were proposed to be taken up into cells by passive transport through the lipophilic cell wall. Apart from the pathway being less available to charged compounds, they are also generally eliminated by the body more rapidly.

Both [PPh_3Me][$PtCl_3$(caffeine)][27] (Fig. 1.10) and [$Pt(NH_3)Cl_3$]$^-$ are negatively charged and were found active against cancer cells. The possible reason for this was suggested by Cleare and Hoeschle where in biological environment, one Cl^- was substituted by a H_2O molecule

to form a neutral complex. Hollis and colleagues[28] prepared and investigated a series of 32 cationic complexes of the type *cis*-$[Pt(NH_3)_2(am)Cl]^+$ (Fig.1.10) where am was a pyridine , a pyrimidine, a purine, a piperidine or a saturated amine ligand. A number of the complexes demonstrated activity similar to or higher than that of cisplatin in vivo murine tumour models. The high activity of these charged agents were probably due to the loss of one ammine ligands to give neutral complexes *trans*-$[Pt(NH_3)(am)Cl_2]$.

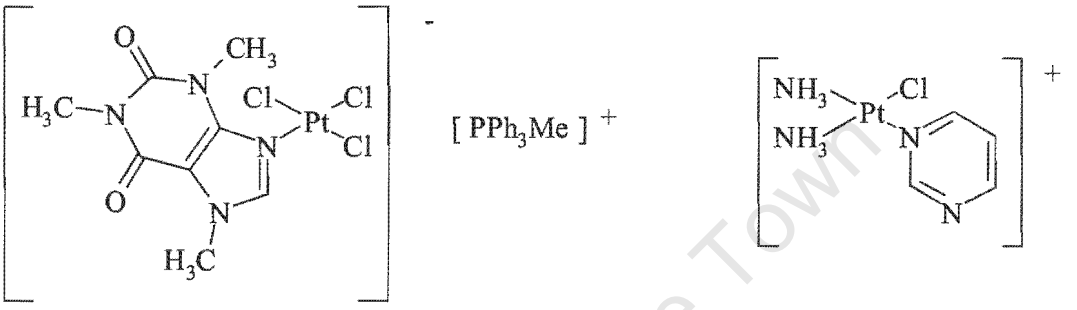

Fig. 1.10 Structure of $[PPh_3Me][PtCl_3(caffeine)]$ and *cis*-$[Pt(NH_3)_2(am)Cl]^+$

Platinum(IV) Complexes

Although much effort has been directed toward developing platinum(II) complexes, it needs to be recognized that the corresponding platinum(IV) homologs may have advantages from the viewpoint of stability to facilitate animal and potential clinical evaluations. In addition they modulate favourable interactions with the target DNA to increase the spectrum of antitumour activity.

Pt(IV) complexes are much more inert to ligand substitution reactions than their Pt(II) counterparts. It is generally believed that Pt(IV) complexes are reduced to Pt(II) by extracellular and intracellular agents prior to reaction with DNA. Iproplatin and ormaplatin were shown to be reduced intra-and extracellularly to their reactive Pt (II) counterparts.

1.2.4 Groove Binding

Groove binding interactions involve direct interactions of the bound molecule with the edges of base-pairs in either of the grooves of nucleic acids[10] (Fig. 1.7). The major and minor grooves differ significantly in electrostatic potential, hydrogen bonding characteristics, steric effects and hydration. Many protein and oligonucleotide molecules show binding specificity primarily through major groove interactions while small, groove-binding molecules in general prefer the minor groove. Typical minor groove-binding molecules have simple aromatic rings such as pyrrole, furan, or benzene connected by bonds with torsional freedom. These compounds can replace the water and fit into the helical curve of the minor groove with appropriate twist. In minor groove, molecules are more likely to hydrogen bond with A:T base-pairs since G:C base-pair regions contain a steric bulk of NH_2 group. A possibility with groove-binding molecules, which does not exist with intercalators, is that they can be extended to fit over many base-pairs along the groove and have very high sequence-specific recognition of nucleic acids. For example, an oligopyrimidine can be designed which forms a triple helix with a specific homopurine-homopyrimidine duplex sequence. By linking DNA cleavage reagents to the oligopyrimidine, a highly specific 'nuclease' can be created. Oligonucleotides are also being used as "antisense" antiviral and anticancer drugs which specifically recognise single-stranded cellular nucleic acids.

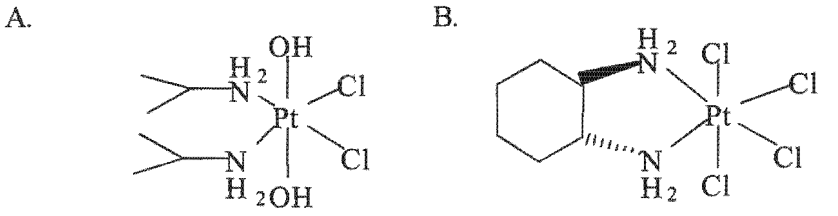

Fig 1.11 Structure of (A). iproplatin and (B). ormaplatin.

The kinetic stability of the axial ligand bonds in octahedral Pt(IV) complexes is known to strongly influence the reactions and reduction of the complexes. The important influence of the axial and carrier ligand on the in vivo redox process and on the overall biological activity of the complex has been studied by Hambley and co-workers.[29] The reduction rates depended on the electron withdrawing power and steric hindrance of the axial and carrier ligands. A comparison between the complexes with different carrier ligands but the same axial ligands revealed that a faster reduction rate coincided with a higher cytotoxic activity.

The clinical trial of the first orally active platinum drug, *cis,trans,cis*-$PtCl_2(Oac)_2(NH_3)(C_6H_{11}NH_2)$ (JM216), has revitalized the interest in Pt(IV) complexes, which had been diminished somewhat by the disappointing results with iproplatin and ormaplatin (Fig. 1.11). JM216 belongs to a class of amine dichloro dicarboxylate platinum(IV) complexes that were designed for oral activity.[30] The complex showed substantially greater cytotoxicity than cisplatin and carboplatin and also greater activity than ammine(cyclohexylamine)dichloro-platinum(II) (Fig. 1.12) and *cis,trans,cis*-amine (cyclohexylamine)dihydroxodichloroplatinum(IV).[31] This could be due to the Pt(IV) complexes having less vulnerability to deactivation in the case of ammine(cyclohexylamine)dichloroplatinum(II), the differences in activity could be due to differences in the reduction of complexes with carboxylate and hydroxo axial ligands. JM216 also showed a lack of cross-resistance with cisplatin in some cell lines, particularly in those where reduced platinum accumulation played a dominant role in resistance. This

suggests that the greater lipophilic nature of the complexes enable them to circumvent resistance due to decreased platinum accumulation.

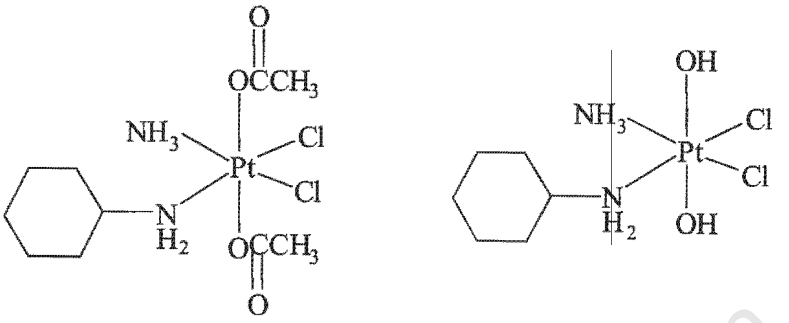

Fig. 1.12 Structure of JM216 and ammine(cyclohexylamine)dichloroplatinum(IV).

Active Trans Platinum Complexes

In the original empirical structure activity relationship, *trans* platinum complexes were considered to be inactive. However, several groups have shown that some of the *trans* compounds are active in vitro and in vivo.[32-35] While isomerization of the *trans* compound to an active cis isomer could account for some activity of *trans* isomers, in several cases, *cis* isomers are less active than the corresponding *trans* isomer. A distinct difference between cisplatin and transplatin is that transplatin is kinetically more reactive than cisplatin and more susceptible to deactivation.[36] Careful design using sterically hindered ligand may reduce the kinetic reactivity of *trans* Pt complexes. As transplatin forms different adduct with DNA to the cis adduct, it is hoped that the *trans* complexes can overcome the cisplatin resistance in certain tumours.

Farrell and colleagues examined and compared the cytotoxicity of three series of *trans* complexes with the general formula $[PtCl_2(L)(L')]$: (i) L = L' where L and L' are pyridine, N-methylimidazole and thiazole; (ii) L = quinoline and L' = RR' SO where R = methyl and R' = methyl, phenyl benzyl; (iii) L = quinoline and L' = NH_3 (Fig. 1.13). In cisplatin sensitive

and resistant cell lines, the trans Pt complexes in the three series showed comparable activity to cisplatin and greater activity than transplatin. In cisplatin sensitive and resistant cell lines, the trans isomers exhibited greater activities than their cis counterparts.[32,33]

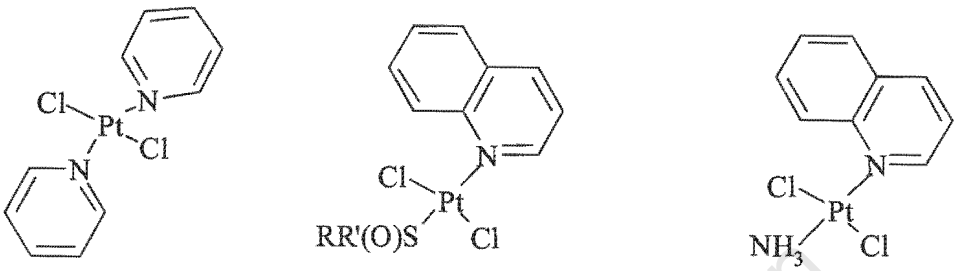

Fig. 1.13 Structure of $[PtCl_2(py)_2]$, $[PtCl_2(quinoline)(RR'SO)]$ where R= methyl; R' = methyl, phenyl or benzyl, and $[PtCl_2(quinoline)(NH_3)]$

A *trans* Pt(IV) complex *trans,trans,trans*-ammine(cyclohexylamine)dichlorodihydroxoplatinum(IV) was reported to have greater activity than transplatin and its cis analogue. Similar to other Pt(IV) complexes, lack of cross-resistance was observed in cell lines where resistance was mediated through reduced platinum accumulation. However, in contrast to the cis Pt(IV) ammine/amine complexes, lack of cross-resistance was attributed to enhanced repair and/or increased tolerance to Pt-DNA adducts.[34]

Multinuclear Platinum Complexes

An approach to the design of Pt drugs that can circumvent Pt resistance in tumour is to develop compounds that form radically different Pt-DNA adducts than the current Pt drugs. Activation of *trans* isomers with bulky ligands is an example of this approach. Another example of this strategy is multinuclear platinum complexes with bridging linkers. Farrell and colleagues have been the most active in this area and have extensively investigated binuclear

formulas $[\{PtCl_m(NH_3)_{3-m}\}i\text{-}H_2N\text{-}R\text{-}NH_2\text{-}\{PtCl_n(NH_3)_{3-n}\}]^{[(2-m)+(2-n)]+}$ (m or n = 0-3 and R is a linear or substituted aliphatic linker).[37-40] A host of complexes have been generated and some have shown activity in both cisplatin-sensitive and resistant cell lines. In complexes with two $[PtCl_2(NH_3)\text{-}(NH_2R\text{-})]$ centers (Fig. 1.14), a relationship between chain length and activity was observed. For diatomic complexes with two $[PtCl(NH_3)_2\text{-}(NH_2R\text{-})]$ centers, the *cis* or *trans* position of the leaving Cl group had an effect on activity. The binding of the binuclear Pt complexes to DNA were reported to be faster than for cisplatin. And a completely different array of Pt-DNA adducts that were totally inaccessible to mononuclear platinum complexes were observed.[39-42]

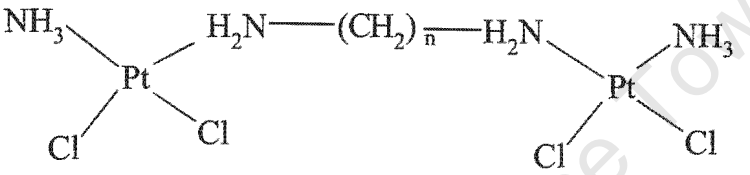

Fig. 1.14 Structure of a binuclear Pt complex.

Another group of binuclear Pt complexes with bifunctional thiourea,[43,44] spermine, spermidine and modified tetra-amine linkers[45] as well as some trinuclear[46-48] (Fig. 1.15) and tetra-nuclear[49] platinum complexes have been reported recently. The most important of these complexes is the trinuclear platinum compound. It exhibited a complete lack of cross-resistance to cisplatin resistant cell lines and it's also significantly more potent than cisplatin in vitro in an osteosarcoma cell line. The increased potency was attributed to increased cellular Pt uptake of this complex relative to cisplatin and the extent of DNA binding.

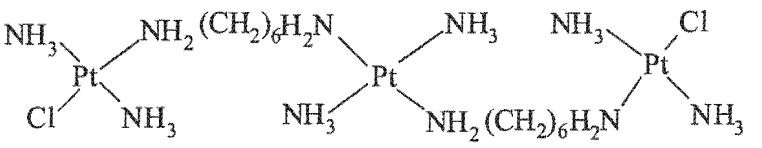

Fig. 1.15 Structure of a trinuclear platinum complex.

Water Soluble Complexes

The poor water solubility of cisplatin (~1 mg/ml) approaches the practical limit of solubility for a cytotoxic agent that can be administered parenterally. Orally administered compounds can be less soluble, although they must be soluble enough to be absorbed. Unfortunately, most Pt(II) dichloride complexes are substantially less soluble than cisplatin. The most common method of increasing water solubility has been replacing the chloride ligands with chelating carboxylates (such as cyclobutane dicarboxylate), oxalate and glycolate. Oxidation of Pt(II) to its Pt(IV) dihydroxo complex often increases water solubility too.[50]

A series of anionic phosphono-carboxylate complexes with high solubility and stability were found to exhibit pronounced activity in murine models (Fig. 1.16). Another unusual water soluble platinum compound can be prepared in a chelate opened zwitterionic form under acidic conditions. At physiological pH, the diamine chelate closes, forming a conventional platinum compound that has in vivo activity.

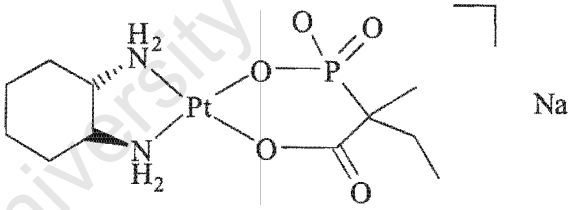

Fig. 1.16 Structure of a water soluble platinum amine phosphonocarboxylato complex.

Chiral Complexes

Differences in activity or toxicity arising from enantiomers of chiral compounds can be particularly informative with respect to the mechanisms involved because the differences are indicative of enantioselective interactions with chiral transport agents, deactivating agents or targets. The earliest of these were the cyclohexane-1,2-diamine complexes (Fig. 1.17) reported by Kidani and colleagues.[51,52] No significant differences in activity were observed. The Regensberg groups have reported enantioselective differences in activity for complexes of a number of variants of the substituted ethane-1,2-diamine ligands. The racemic stereoisomers (R,R and S,S) of [Pt (bis(3-hydroxyphenyl) ethane-1,2-diamine)Cl_2] and [Pt(bis(4-hydroxyphenyl)ethane-1,2-diamine)Cl_2] were more active than the meso isomer (R,S) and of these, the S,S enantiomers were the more active in terms of both in vitro activity against the breast cancer cell line and a number of leukaemia cells implanted in mice.[53]

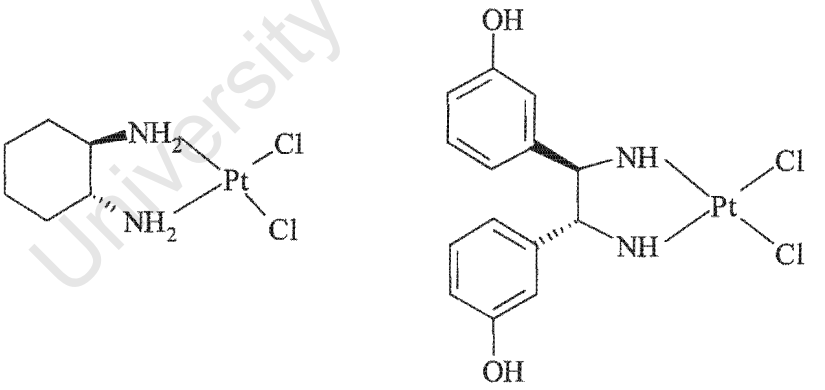

Fig. 1.17 Structure of cyclohexane-1,2-diamine platinum (II) and [Pt(bis(3-Hydroxyphenyl)ethane-1,2-diamine)]Cl_2.

1.3.3 Intercalative Binding

Organic intercalating agents have long been used as therapeutic agents. In 1940s, intercalating actinomycin antibiotics was discovered and it has been proven useful in the treatment of some childhood cancers. Later, other intercalating drugs such as daunomycin, adriamycin, amsacrine and mitoxantrone (Fig. 1.18) have also been used clinically as antitumour drugs. After the success of both cisplatin and organo-intercalators as antitumour drugs, research into metallointercalator starts to develop.

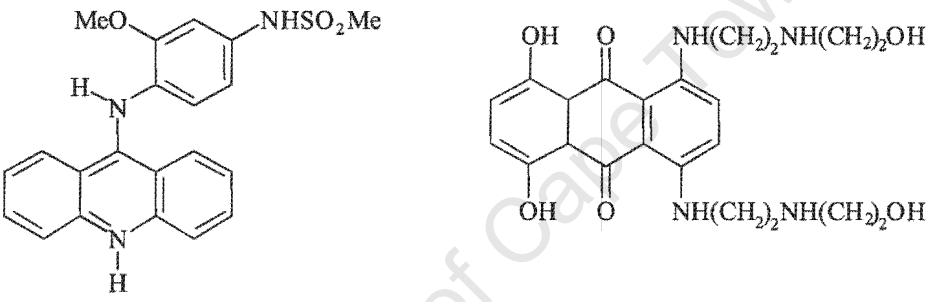

Fig. 1.18 Structures of Amsacrine and Mitoxantrone

Complexes with Biologically Active Carrier Ligands

Another approach to the design of novel Pt drugs is to target the Pt coordination moiety to DNA by attaching it to a suitable carrier ligand. Several groups have attempted to design new Pt compounds by attaching DNA intercalators to a Pt moiety with the expectation that the compounds would localize in the vicinity of the DNA. Denny and colleagues have prepared a series of complexes by attaching dichloro(1,2-diaminoethane)platinum(II) and dichloro(1,3-diaminoethane)platinum(II) to anilino-acridine and acridinecarboxamide[54-56] (Fig. 1.19). These complexes exhibited improved activity in cisplatin resistant cell lines

compared to the parent compounds, but there was no improvement relative to the carrier ligands. Other examples of Pt complexes with bioactive carrier groups include the attachment of a Pt moiety to chloroquine[57], ethidium bromide[58] and acridine orange.[59] The attachments of a Pt moiety to amino acids, sugars and antitrypanosomatid drugs have also been reported. Overall, studies of Pt compounds with biologically active carrier groups have yielded interesting results and there is potential for varying the biological activity of these compounds by altering the structure of the carrier group. However, there have not yet been clinically significant advances that have developed from this design approach. Gibson and colleagues have investigated a series of complexes with anthraquinone (Fig. 1.19) intercalator attached and have also reported promising activities.[60]

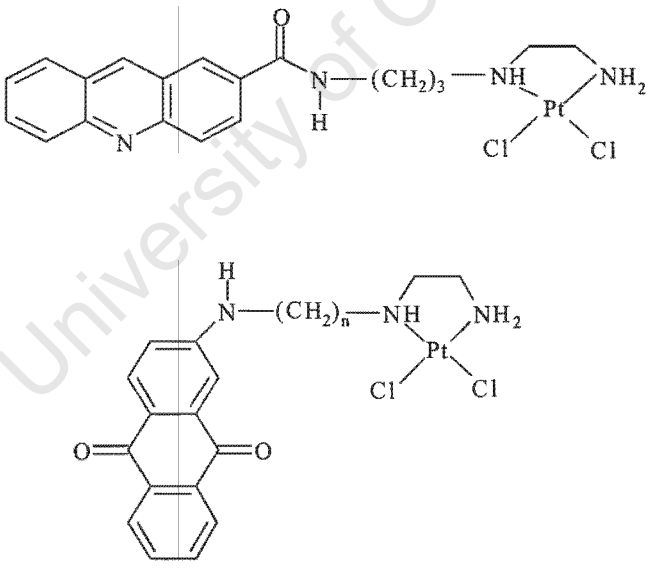

Fig. 1.19 Structures of acridinecarboxamide and anthraquinone attached to ethane-1,2-diamine.

Stereoselective and Site Specific Metallointercalators

This class of chiral Ruthenium complexes were designed by Barton and her research group to recognize difference structures along the DNA helix[61,62,63] (Fig. 1.20). The chirality of the metal complex and the various structural interactions of these rigid complexes with the asymmetric DNA helix dictate the modes of binding (stereoselective intercalation, groove binding and direct coordination).

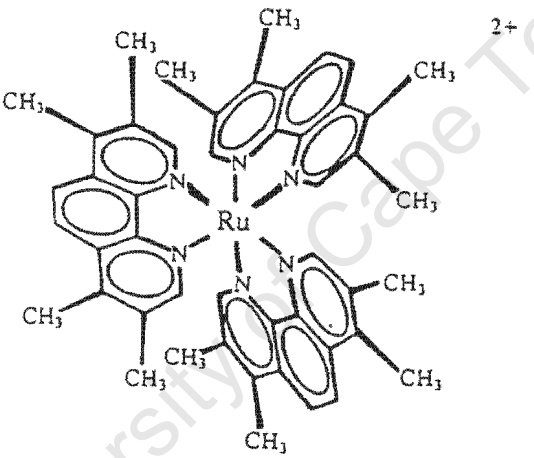

Fig. 1.20 Structure of Λ- and Δ- enantiomers of a tris(phenanthroline) metal complex.

1.4 OBJECTIVES

Due to all the shortcomings of currently available anticancer drugs, we are interested in the design of a series of water soluble potential metallointercalators. Recently, a series of platinum complexes as potential DNA intercalators have been prepared and these complexes were found to self-associate in organic solvents. Unfortunately, these complexes are not water soluble and therefore the biological properties could not be thoroughly studied. A new ligand then was re-designed to make the complex [Pt(diimine)L]Cl reasonably water soluble at physiological pHs.

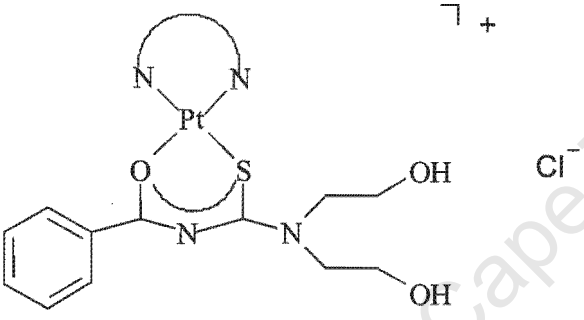

= 1,10-phenanthroline, 2,2'-bipyridyl, 4,4'-dimethyl-2,2'-bipyridyl and 4,4'-di-*tert*-butyl-2,2'-bipyridyl ligands

The objectives of this project include:

- Synthesis and characterisation of a series of mixed-ligand, water soluble [Pt(diimine)(*N,N*-dihydroxyethyl-*N'*-benzoylthioureato)]$^{+}$Cl^{-} complexes.
- To study their self association behaviour in water and mixed solvent system by physical techniques such as ^{1}H NMR spectroscopy, Electrospray Ionisation Mass Spectroscopy and Electron Microscopy.
- Study their DNA binding behaviour and determine their mode of binding by UV melting spectrophotometry, Circular Dichoism and Gel Mobility Study.
- Test their *in vivo* activities by doing a survival study on *E.coli* cells.

REFERENCES

1. M. N. Hughs, *Inorganic Chemistry of Biological Processes*, London: New York Wiley, 1972.
2. P. M. Harrison and R. J. Hoare, *Metals in Biochemistry*, London: Chapman & Hall, 1980.
3. H. E. Howard-Lock and C. J. L. Lock, *Semin Arthritis Rheum*, 1986, **15**(4), 261.
4. B. Rosenberg, L. Van Camp and T. Krigas, *Nature*, **205**, 698.
5. J. Reedijk, *J. Chem. Commun.* 1996, 801.
6. R. B. Weiss, M. C. Christian, *Drugs*, 1993, **46**, 360.
7. D. Lebwohl, R. Canetta, *Eur. J. Cancer*, 1998, **34**, 1522.
8. L. R. Kelland, B. A. Murrer, G. Abel, M. J. Mckeage, M. Jones, P. M. Goddard, M. Valenti and K. R. Harrap, *Cancer Res.*, 1993, **53**, 2581.
9. W. Kaim and B. Schwederski, *Bioinorganic Chemistry*: *Inorganic Elements in the Chemistry of Life*, John Wiley & Sons, 1991.
10. G. M. Blackburn and M. J. Gait, *Nucleic Acids in Chemistry and Biology*, IRL Press at Oxford University Press, 1990.
11. D. Voet and J. G. Voet, *Biochemistry*, New York: J. Wiley, 1995.
12. M. K. Campbell and I. Geis, Biochemistry, Philadelphia : Saunders College, 1991.
13. E. R. Jamieson and S. J. Lippard, *Chem. Rev*. 1999, **99**, 2467.
14. C. F. J. Barnard, *Plat. Met. Rev*. 1989, **33**, 162.
15. J. Reedijk, *Chem. Rev*., 1999, **99**, 2499.
16. J. H. J. den Hartog, C. Altona, J. H. van Boom, G. A. van der Marel, C. A. G. Haasnoot and J. Reedijk, *J. Biomol. Struct. Dyn*., 1985, **2**, 1137.
17. L. S. Lerman, *J. Mol. Biol.*, 1961, **3**, 18.
18. *Nucleic Acids and Molecular Biology*, **6**, 1992, Springer Verlag, 54.
19. A. H-J. Wang, G. Ughetto, G. J. Quigley and A. Rich, *Biochemistry*, 1987, **26**, 1152.
20. T. W. Hambley, *Coord. Chem. Rev*., 1997, **166**, 181.
21. E. Wong and C. M. Giandomenico, *Chem. Rev*., 1999, **99**, 2451.
22. M. J. Cleare and J. D. Hoeschele, *Plat. Met. Rev*., 1973, **17**, 3.

23. M. J. Cleare and J. D. Hoeschele, *Bioinorg. Chem.*, 1973, **2**, 187.

24. Y. Chen, Z. Guo, S. Parsons and P. J. Sadler, *Chem. Eur. J.*, 1998, **4**, 672.

25. M. J. Bloemink, H. Engelking, S. Karentzopoulos, B. Kerbs and J. Reedijk, *J. Inorg. Chem.*, 1996, **35**, 619.

26. L. K. Webster, G. B. Deacon, D. P. Buxton, B. L. Hillcoat, A. M. James, I. A.G. Roos, R. J. Thomson, L. P. G. Wakelin and T. L. Williams, *J. Med. Chem.*, 1992, **35**, 3349.

27. R. E. Cramer, D. M. Ho, W. Vandoorne, J. A. Ibers, T. Norton and M. Kashiwagi, *Inorg. Chem.*, 1981, **20**, 2457.

28. L. S. Hollis, A. R. Amundsen, E. W. Stern, *J. Med. Chem.*, 1989, **32**, 128.

29. L. T. Ellis, H. M. Er. and T. W. Hambley, *Aust. J. Chem.*, 1995, **48**, 793.

30. S. Neidle, C. F. Snook, B. A. Murrer, C. F. Barnard, *J. Acta Crystallogr.*, 1995, C51, 822.

31. L. R. Kelland, B. A. Murrer, G. Abel, C. M. Giandomenico, P. Mistry and K. R. Harrap, *Cancer Res.*, 1992, **52**, 822.

32. M. van Beusichem and N. Farrell, *Inorg. Chem.*, 1992, 31, 634.

33. N. Farrell, T. B. Ha, J. P. Souchard, F. L. Wimmer, S. Cros and N. P. Johnson, *J. Med. Chem.*, 1989, **32** 2240.

34. L. R. Kelland, C. F. J. Barnard, K. J. Mellish, M. Jones, P. M. Goddard, M. Valenti, A. Bryant, B. A. Murrer and K. R. Harrap, *Cancer Res.*, 1994, **54**, 5618.

35. M. Coluccia, A. Nassi, F. Loseto, A. Boccareli, M. A. Mariggio, D. Giordano, F.P. Intini, P. Caputo and G. Natile, *J. Med. Chem.*, 1993, **36**, 510.

36. F. R. Hartley, *The Chemistry of Platinum and Palladium*, John Wiley and Sons: New York, 1973.

37. N. Farrell, Y. Qu and M. P. Hacker, *J. Med. Chem.*, 1990, **33**, 2179.

38. A. Johnson, Y. Qu, B. van Houten and N. Farrell, *Nucleic Acids Res.* 1992, **20**, 1697.

39. P. K. Wu, Y. Qu, B. Houten and N. Farrell, *J. Inorg. Biochem.*, 1994, **54**, 207.

40. P. K. Wu, M. Kharatishvili, Y. Qu and N. Farrell, *J. Inorg. Biochem.*, 1996, **63**, 9.

41. Y. Zou, B. Van Houten and N. Farrell, *Biochemistry*, 1994, **33**, 5404.

42. N. Farrell, T. G. Appleton, Y. Au, J. D. Roberts, A. P. Soares Fontes, K. A. Skov, P. Wu, Y. Zou, *Biochemistry*, 1995, **34**, 15480.

43. U. Bierbach, T. W. Hambley and N. Farrell, *Inorg. Chem.*, 1998, **37**, 708.

44. U. Bierbach, J. D. Roberts and N. Farrell, *Inorg. Chem.*, 1998, **37**, 717.

45. H. Rauter, R. Di Domenico, E. Menta, A. Oliva, Y. Qu and N. Farrell, *Inorg. Chem.*, 1997, **36**, 3919.

46. T. G. Appleton, Y. Qu, J.D. Hoeschele and N. Farrell, *Inorg. Chem.*, 1993, **32**, 2591.

47. Y. Qu, N. Farrell, J. Kasparkova and V. J. Brabec, *J. Inorg. Biochem.*, 1997, **67**, 174.

48. P. Di Blasi, A. Bernareggi, G. Beggiolin, L. Piazzoni, E. Menta and M. L. Formento, *Anticancer Res.*, 1998, **18**, 3113.

49. A.G. Qiorpga, J.M. Perez, J. Lopez-Solera, J. R. Masaguer, A. Luque, P. Roman, A. Edwards, C. Alonso and C. Navarro-Ranninger, *J. Med. Chem.*, 1998, **41**, 1399.

50. L. S. Hollis, A. V. Miller, A. R. Amundsen, J. E. Schurig and E. W. Stern. *J. Med. Chem*. 1990, **33**, 105.

51. Y. Kidani, K. Inagaki, *J. Med. Chem*., 1978, **21**, 1315.

52. M. Noji, K. Okamoto, Y. Kidani, *J. Med. Chem*., 1981, **24**, 508.

53. M. Jennerwein, R. Gust, R. Müller, H. Schönenberger, J. Engel, M.R. Berger, D. Schmähl, S. Seeber, R. Osieka, G. Atassi, D. M.-D. Bock, *Archiv Der Pharm*., 1989, **322**, 67.

54. B. D. Palmer, H. H. Lee, P. Johnson, B. X. Baguley, G. Wickham, L. P. G. Wakelin, W. D. McFadyen and W. A. Denny, *J. Med. Chem*. 1990, **33**, 3008.

55. H. H. Lee, B. D. Palmer, P. Johnson, B. X. Baguley, M. Chin, W. D. McFadyen, G. Wickham and W. A. Denny, *J. Med. Chem*. 1992, **35**, 2983.

56. V. Murray, H. Motyka, P. R. England, G. Wickham, H. H. Lee, W. A. Denny and W. D. McFadyen, *J. Biol. Chem*. 1992, **267**, 18805.

57. W. I. Sundquist, D. P. Bancroft and S. J. Lippard, *J. Am. Chem. Soc*., 1990, **112,** 1590.

58. W. I. Sundquist, D. P. Bancroft L. Chassot and S. J. Lippard, *J. Am. Chem. Soc*., 1990, **112,** 1590.

59. B. E. Bowler, K. J. Ahmed, W. I. Sundquist, L. S. Hollis, E. E. Whang and S. J. Lippard, *J. Am. Chem. Soc*., 1989, **111,** 1299.

60. K. F. Gean, R. Benshoshan, A. Ramu, I. Ringel, J. Katzhendler,Gibson, *Eur. J. Med. Chem*. 1991, **26**, 593.

61. J. K. Barton, *Science*, 1986, **233**, 727.

62. J. K. Barton, A. T. Danishefsky and J. M. Goldberg, *J. Am. Chem. Soc*., 1984, **106**, 2172.

63. H-Y Mei and J. K. Barton, *Proc. Natl. Acad. Sci*., 1988, **85**, 1339.

2.1 INTRODUCTION

2.1.1 General Coordination Chemistry of Platinum

The principal oxidation states of Pt are II and IV, but there is extensive chemistry in the I and III states where Pt-Pt bonds are involved.[1] Numerous complexes also exist in the 0 state when PR_3, CO or other π-acid ligands are present. The higher oxidation states, V and VI occur only in a few fluoro compounds.

In general, almost all Pt(II) complexes maintain a square planar geometry and only with few exceptions where 5 coordinate trignal bipyramidal coordination is observed.[2] Square planar complexes generally undergo bimolecular nucleophilic displacement reactions.[3] During the early study of platinum coordination chemistry, Chernyaev postulated that in the case of a trans isomer of platinum(II), a weakening of the bond between the two acid radicals (electronegative groups) and the central atom occurs.[4] The trans effects of atoms are inversely proportional to their metallic character, i.e., directly proportional to their electronegativities. His trans directing series has since been extended to include a variety of ligands: $CN^- \sim CO \sim C_2H_4 \sim NO\text{-}H^- > CH_3^- \sim SC(NH_2)_2 \sim SR_2 \sim PR_3 > SO_3H^- > NO_2\text{-}I \sim SCN^- > BR^- > Cl^- > C_5H_5N > RNH_2 \sim NH_3 > OH^- > H_2O$.[5] This finding not only explained the substitution behaviour of most platinum(II) reaction, it also made systematic planning of reactions possible.

Various metal ions fall into two categories: i) those binding strongly to base which would bind strongly to the proton; ii) those binding strongly to highly polarizable or unsaturated bases which often have negligible proton basicity. Soft acids and bases tend to be larger and more polarizable metal ions and ligands while hard acids and bases tend to be small, slightly polarizable species. Pearson[6] has suggested a simple rule for predicting the stability of complex formed between acids and bases: Hard acids prefer to bind to hard bases and soft acids prefer to bind to soft bases. Pt(II) ion forms most stable complexes with ligands that have "soft" donor atoms such as S, I and Br. Since Pt(II) ion is classified as a soft acid, it coordinates preferably to a soft base. The stability of the complex is

enhanced if the coordinating ligand can bind to the metal at more than one site, this is referred to as the chelate effect.

Two common aromatic nitrogen ligands which will form chelate complexes with platinum(II) are 2,2' -bipyridyl and 1,10-phenanthroline. They are known to form stable complexes with Pt(II) ion yielding poorly soluble yellow complexes such as [Pt(2,2'-bipy)Cl_2] and [Pt(1,10-phen)Cl_2]. There are two pathways leading to the formation of [M(diimine)X_2] : a direct pathway where diimine ligand reacts with the metal ion directly and a solvent pathway where solvolysis occurs prior to the attack by the diimine ligand.[5,6]

A detailed mechanism of Pt(II) reacting directly with 1,10-phenanthroline in aqueous solution was reported by Palocsay *et al.*[7] When Pt(II) X_4 reacts with a flexible bidentate ligand, the first X group is substituted by one end of the ligand to form a square pyramidal complex. The structure then was rearranged to a trigonal bipyrimidal conformation with Cl group at the axial position and it eventually leaves the complex. This is a slow, rate determining step since the molecular model indicated that when a diimine ligand occupies only one coordination position on a metal ion, the complex is extremely crowded. The other donor atom of the bidentate ligand then displaces a second X group in a faster step. The mechanism is similar to the substitution of a monodentate ligand, however, the inflexibility of the molecule and the closeness of its donor "N" seemed to preclude the possibility of binding through just one nitrogen centre. Flexibility in a bidentate ligand is a very important factor affecting the overall rate of reaction. Experimental results showed that bipyridyl ligand reacts faster than 1,10-phenanthroline ligand but significantly slower than ethylenediamine. The large difference in the rate of reaction was caused by the steric crowding in the initially formed monodentate intermediate. 1,10-phenanthroline posses a most rigid conformation and the closeness of the two nitrogen centres also force the metal-ligand to be in an unusual angle. This can be seen by comparing the bond angles N-Zn-N of $Zn(NH_3)_2Cl_2$ (108^o) and $Zn(phen)Cl_2$ (80^o).[7] Ethylenediammine on the other hand has the most flexible structure which allows

the formation of unidentate complex with Pt(II). This is the most likely explanation for the much higher reaction rate in comparison to both 1,10-phenathroline and 2,2' bipyridine.

Usually the solvent path of reaction involves a slow attack by the solvent followed by a rapid displacement of the solvent by the subsitituting ligand. In the formation of [M(diimine)X_2], however, the attack of the solvolyzed species by the phenanthroline was found to be slower than the solvolysis, giving a second order solvent path.[7] In the kinetic study of [Pt(diimine)Br_2] and [Pd(diimine)X_2], the rate of substitution for $M(H_2O)X_3^-$ complexes was also much greater than the substitution for MX_4^{2-} complexes by the diimine ligands.[8] This is most probably because water is a better leaving group than halide.[3]

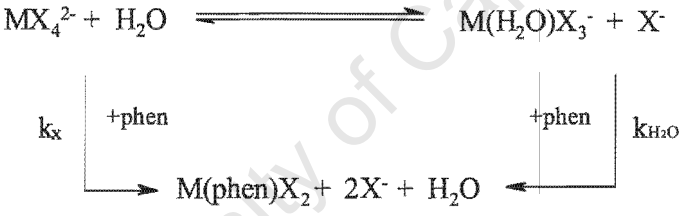

Fig. 2.1 Schematic Diagram showing the ligand and solvent paths of MX_4^- reacting with 1,10-phenanthroline ligand.

Monodentate 1,10-phenanthroline complexes have also been isolated and the first observation of this feature in the solid state was with *cis*-[PtCl(phen)$(PEt_3)_2$]BF_4.[9] In solution, the phenanthroline rapidly exchanges nitrogens bonded to platinum.[10] This fluxionality is somewhat general, being observed with platinum(II) complexes of phen, bipy, 4-Me-1,8-naphthyridine, pyridazine and phthalazine. The fluxionality of Pt(II) between the two nitrogen sites is dependent on the suitability of the nitrogen lone pair orientation for bidentate coordination.

2.1.2 Synthesis of *N,N*-dialkyl-*N'*-aroylthiourea ligands

The first reported *N*-acylthiourea was *N'*-substituted-*N*-aroylthiourea, synthesised and described by Neuki[11] in 1873. In 1895, Dixon [12] *et al* systematically studied the reactivity of a number of new acyl and aroyl isothiocyanate reagents. He used benzene as a solvent and adding slight excess of lead thiocyanate to an aroyl chloride to produce an aroyl isothiocyanate. The byproduct, lead chloride was removed by filtration before the addition of amine. Douglass and Dains in 1934,[13] followed the principal developed by Dixon, modified the method into an "one pot" synthesis. He used anhydrous acetone as a solvent, and ammonium or potassium thiocyanate instead of lead thiocyanate. This reaction involved the addition of acyl or aroyl chloride to a solution of NH_4SCN in acetone followed by the addition of amine. The nucleophile, thiocyanate, attacks the acyl chloride and the acylthiocyanate intermediate goes through thermal isomerisation to form an acylisothiocyanate (Fig.2.2). A primary or secondary amine then undergoes nucleophilic addition at the thiocarbonyl carbon of the acylisothiocynate.

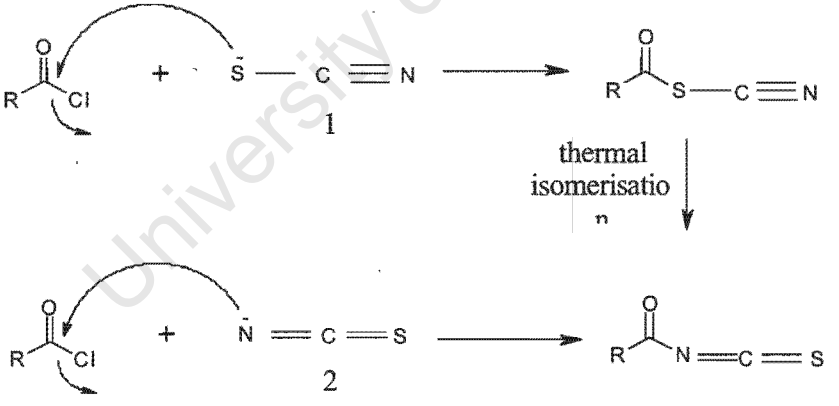

Figure 2.2 Reaction of thiocyanate with an acyl chloride

The reaction of potassium thiocyanate with an acyl chloride in acetone studied by Takamizawa *et al.*[14] in 1963 suggested that the thiocyanate ion can exist as two tautomeric forms, (1) and (2) in Fig. 2.2. Both the S and N sites are able to act as

nucleophile in attacking the carbonyl carbon of the acyl chloride to form acylthiocyanate or acylisothiocyanate. The acylthiocyanate, however, was found to be less stable and reacts with isothiocyanate to give acylisothiocyanate exclusively.

The formation of acylthiourea involves a nucleophilic addition of the amine at the thiocarbonyl carbon of the acylisothiocyanate. It was found that undesired product may also form from the nucleophilic attack of amine to the carbonyl carbon. (Fig. 2.3) This reaction has been investigated in earlier studies by Lozinsky *et al.*[15], who suggested that the rate of these reactions appear to depend on factors such as the polarity of the solvent, temperature, structure of the acylisothiocyante intermediates as well as the basicity of the amine. In a more recent study by Miller[16], it was discovered that the nature and structure of the amine plays the most important role in the outcome of this reaction. As the amine becomes more substituted, the steric bulk of the substituent groups drives the reaction to favour the attack at thiocarbonyl carbon instead of the carbonyl carbon. In the case of benzoylioso-thiocyanate, the phenyl group acts as a large steric hindrance for a bulky secondary amine to attack at carbonyl carbon, hence *benzoylthioureas* in general, can be synthesised with relatively high yield (80 – 100%). In contrast, *acylthioreas,* derived from acylchlorides are generally formed in lower yields together with significant amounts of amide as byproduct.

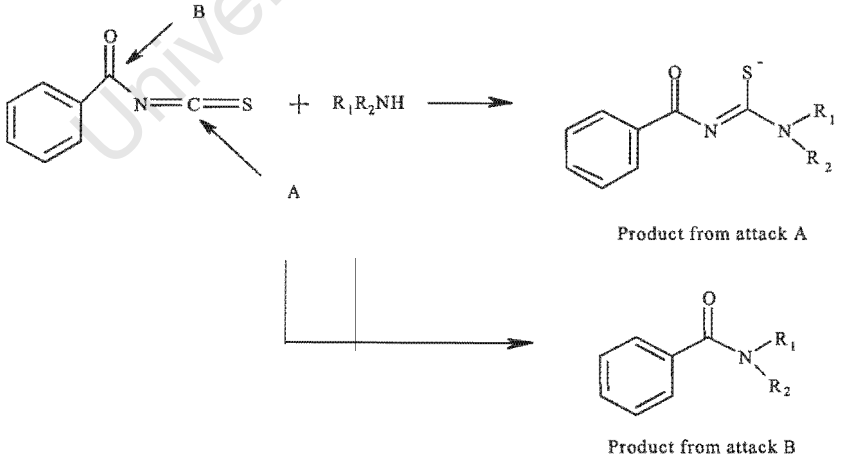

Fig. 2.3 Schematic diagram showing the two possible products from the nucleophilic attack of amine at the two reactive centres.

The co-ordination chemistry of *N*-acylthiourea ligands with various transition metals has been well investigated over the years. [9,10] A series of neutral Cu(II), Co(II), Ni(II), and Pd(II) complexes with *N,N*-dialkyl-*N'*-benzoylthiourea were studied by Beyer *et al.*[17-19] These ligands were also found to have exceptionally high affinity to the platinum group metals (PGMs), and their co-ordination is maintained even in strongly acidic environments. Other transition metal *N,N*-dialkyl-*N'*-benzoylthiourea complexes readily dissociate under acidic condition. This property afforded *N,N*-dialkyl-*N'*-benzoylthiourea ligands to be excellent agents for the pH-selective extraction of PGM from matrices with interfering metals.[20,21]

N,N-dialkyl-*N'*-aroylthiourea and *N*-alkyl-*N'*-aroylthiourea ligands coordinate to metals in different ways. While *N*-alkyl-*N'*-aroylthiourea ligand co-ordinates to metals via the sulphur atom, *N,N*-dialkyl-*N'*-aroylthiourea co-ordinate in bidentate or chelating fashion through the oxygen and sulphur atoms. In the case of *N*-alkyl-*N'*-aroylthiourea, the proton on *N* is hydrogen bonded to the oxygen atom, which locks the conformation into *E,Z'* form (Fig. 2.4A) and directs the coordination through S only. The bidentate co-ordination of *N,N*-dialkyl-*N'*-aroylthiourea to metal is made possible by the fact that the ligand conformation can change from the *E,Z'* form to a chelating complex with loss of the acidic *N'*-H proton; this can be encouraged with a weak base such as $NaCH_3COO$ (Fig. 2.4B). The ligand thus becomes charged, the nucleophilic O tautomeric form co-ordinating readily to the metal, forming a very stable, six-membered chelate ring, with fairly extensive electronic delocalisation[24].

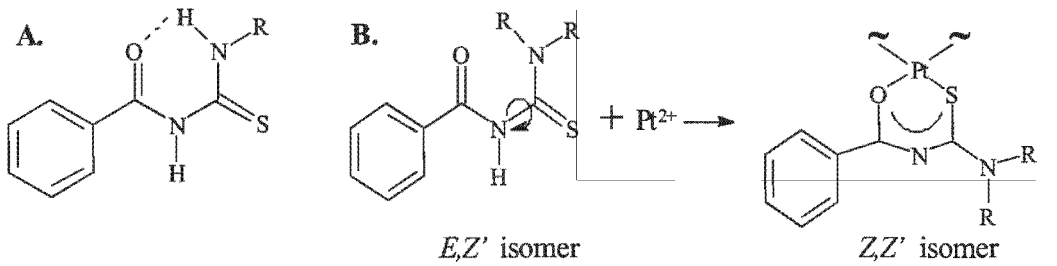

Fig. 2.4 Schematic illustration of a **A**. *N*-alkyl-*N'*-aroylthiourea ligand and **B**. *N,N*-substituted *N'*-benzoylthiourea ligand (in preferred *E,Z'* conformation) reacting with Pt(II)

In this chapter, a description of the synthesis and characterisation of a series of mixed ligand [Pt(diimine)(*N,N*-di(2-hydroxyethyl)-*N'*-benzoylthiourea]$^{+}$Cl^{-} complexes which are expected to be water soluble, is given. A list of abbreviations that are being used for this chapter as well as throughout this work is shown in Fig. 2.5 and Table 2.1.

		**Structure of the complex**
1	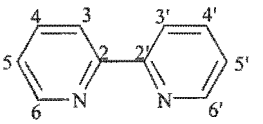	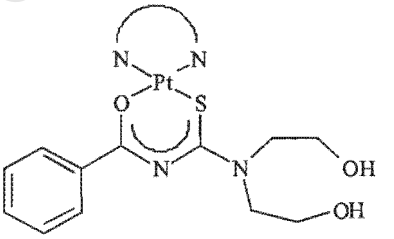
2	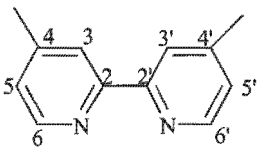	
3	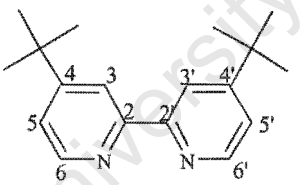	
4	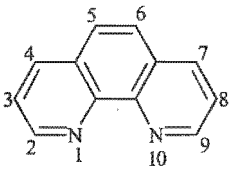	

Fig. 2.5 Schematic representation of [Pt(diimine)(*N,N*-di(2-hydroxyethyl)-*N'*–benzoyl-thioureato)]$^{+}$Cl^{-}

Full Name of the ligands or complexes	Abbreviations
N,N-di(2-hydroxyethyl)-*N'*-benzoylthiourea	H_3L
2,2'-bipyridyl	Bipy
4,4'-dimethyl-2,2'-bipyridyl	DiMebipy
4,4'-di-*tert*-butyl-2,2'-bipyridyl	Ditertbutylbipy
1,10-phenanthroline	Phen
2,2'-bipyridyl dichloroplatinum(II)	$Pt(bipy)Cl_2$
4,4'-dimethyl-2,2'-bipyridyl dichloroplatinum(II)	$Pt(diMebipy)Cl_2$
4,4'-di-*tert*-butyl-2,2'-bipyridyl dichloroplatinum(II)	$Pt(ditertbutylbipy)Cl_2$
1,10-phenanthroline dichloroplatinum(II)	$Pt(phen)Cl_2$
2,2'-bipyridyl dibromoplatinum(II)	$Pt(bipy)Br_2$
4,4'-dimethyl-2,2'-bipyridyl dibromoplatinum(II)	$Pt(diMebipy)Br_2$
2,2'bipyridyl-*N,N*-di(2-hydroxyethyl)-*N'*–benzoylthioureato(*S,O*)platinum(II) chloride	$[Pt(bipy)H_2L]Cl$
4,4'-dimethyl-2,2'bipyridyl-*N,N*-di(2-hydroxyethyl)-*N'*-benzoylthioureato(*S,O*)platinum(II) chloride	$[Pt(diMebipy)H_2L]Cl$
4,4'-di-*tert*-butyl-2,2'bipyridyl-*N,N*-di(2-hydroxyethyl) -*N'*–benzoylthioureato(*S,O*)platinum(II) chloride	$[Pt(ditertbutylbipy)H_2L]Cl$
1,10-phenanthroline-*N,N*-di(2-hydroxyethyl)-*N'*–benzoylthioureato(*S,O*)platinum (II) chloride	$[Pt(phen)H_2L]Cl$
2,2'bipyridyl-*N,N*-di(2-hydroxyethyl)-*N'*–benzoylthioureato (*S,O*)platinum(II) bromide	$[Pt(bipy)H_2L]Br$
4,4'-dimethyl-2,2'bipyridyl-*N,N*-di(2-hydroxyethyl)-*N'*–benzoylthioureato(*S,O*)platinum(II) bromide	$[Pt(diMebipy)H_2L]Br$
2,2'bipyridyl-*N,N*-di(2-hydroxyethyl)-*N'*–benzoylthioureato(*S,O*)platinum(II) perchlorate	$[Pt(bipy)H_2L]ClO_4$

Table 2.1 Full names and their abbreviations of complexes in this thesis

2.2 RESULTS AND DISCUSSION

The formation of [Pt(diimine)(*N,N*-di(2-hydroxyethyl)-*N'* -acylthioureato)]Cl complexes involved firstly in the synthesis of Pt(diimine)Cl_2 and subsequently the reaction with *N, N* di(2-hydroxyethyl)-*N'* -acylthiourea. (Fig. 2.6)

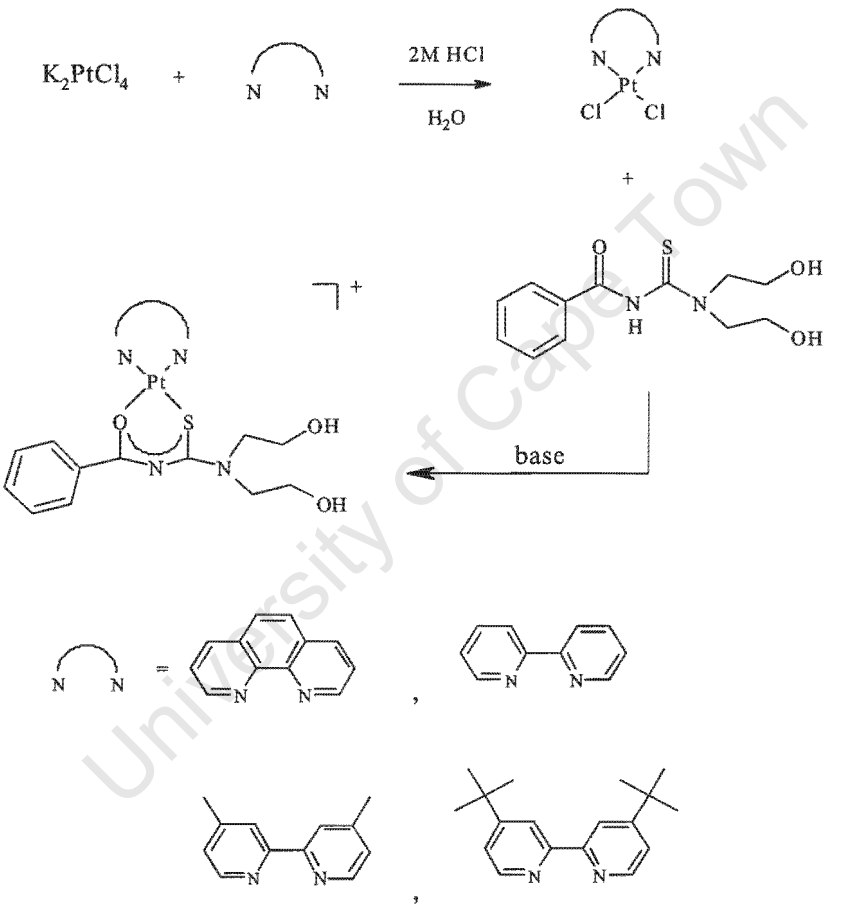

Fig. 2.6 The reaction scheme for the synthesis of [Pt(diimine)(*N,N*-di(2-hydroxyethyl)-*N'* -acylthioureato)]Cl complexes

2.2.1 Synthesis of Pt(diimine)Cl_2

The first reaction is the coordination of diimine ligands. The diimines used in the synthesis of [Pt(diimine)(*N,N*-di(2-hydroxyethyl)-*N'*-benzoylthioureato)]Cl complexes include 2,2'-bipyridyl, 1,10-phenanthroline; 4,4'-dimethyl-2,2'-bipyridyl and 4,4'-di-*tert*-butyl-2,2'-bipyridyl. Except for 4,4'-dimethyl-2,2'-bipyridyl which was synthesised according to the method of Hadda and Le Bozec[22], all the diimines were commercially available. The reaction was carried out in slightly acidic condition to prevent the platinum metal reduction as well as hydrolysis due to the nature of the diimine ligands. As reported by G.T. Morgan *et al.*,[23] addition of dilute HCl leads to the formation of a yellow form of the complex while addition of a concentrated acid would yield a reddish form of the complex. The differences in the two chlorides was thought to arise from some modification in the packing arrangements of molecules in crystal, rather than a difference in chemical structure because they could both undergo similar chemical reactions, have identical stoichiometries, and in solvents like dichloromethane and chloroform, the red form converts to the yellow form.

Although the starting material, K_2PtCl_4 was readily soluble in water, both the diimine ligands and Pt(diimine)Cl_2 were only sparingly soluble. Since the product, Pt(diimine)Cl_2, precipitated in water almost as soon as it was being formed, it was the driving force of this reaction, so that virtually quantitative yields of complex could be obtained. The diimine ligands with their relatively soft nitrogen donor atoms form stable complexes due to their ability to act as σ-bases as well as π-acids[24]. The σ-bonds appeared to be stabilised by the ability of the ligand to form π bonds with full metal d orbitals and their vacant π* orbitals.

The general course of this reaction can be seen in Fig. 2.7. When the $PtCl_4^{2-}$ anion reacted with a flexible bidentate diimine ligand, it was believed that one donor atom of the ligand first associates with the square planar complex, to form a transient (intermediate) square pyrimidal complex, which then rearranged to a trignal bipyrimidal structure with a Cl

group in the axial position, which subsequently left the complex. The displacement of the second Cl⁻ group was thought to take place much faster as a result of statistical advantage (anchimeric assistance) as the site of Cl⁻ ion displacement was adjacent to the already bound diimine in the complex.

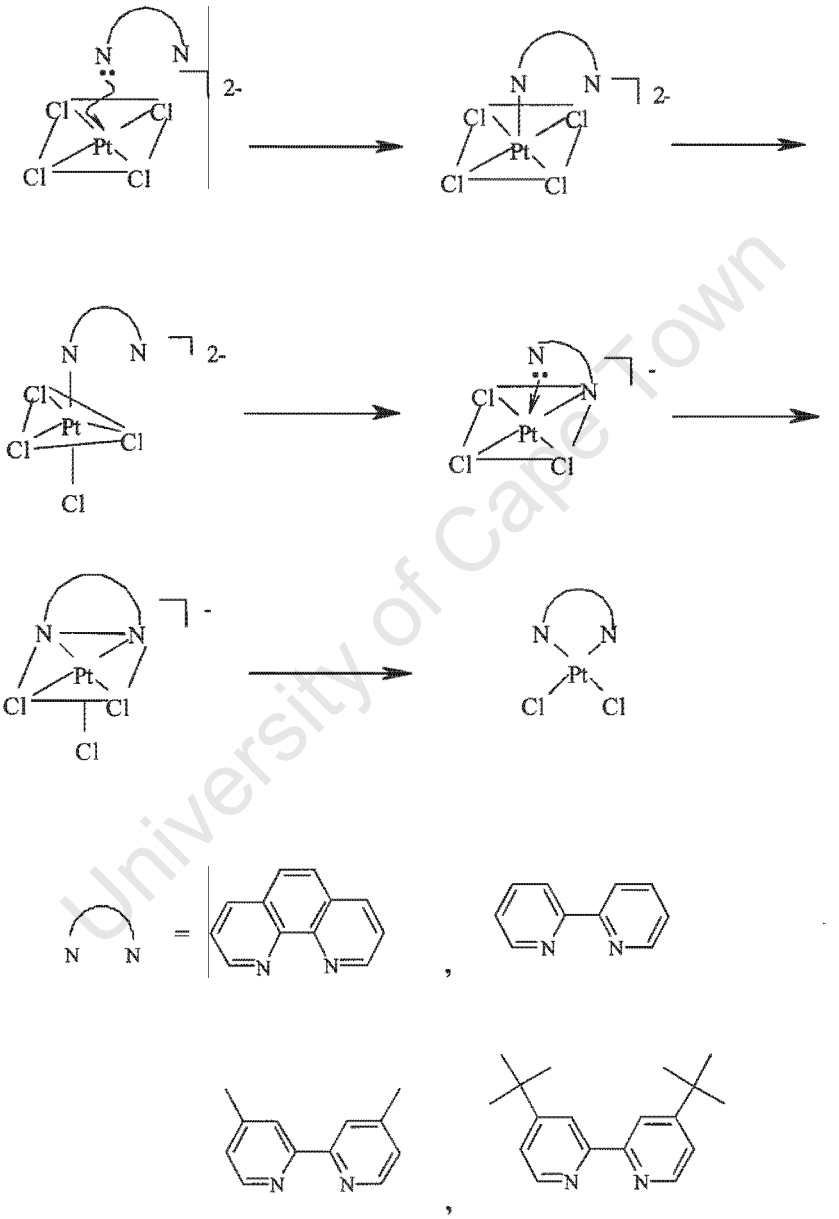

Fig. 2.7 The generally proposed mechanism for Pt(diimine)Cl_2 formation.

2.2.2 Mixed Ligand Synthesis

In general the ligand *N,N*-di(2-hydroxyethyl)-*N'*-benzoylthiourea was synthesised in high yield according to the method of Douglas and Dains to form white crystalline product. Fig. 2.8 demonstrated the reaction scheme of its synthesis.

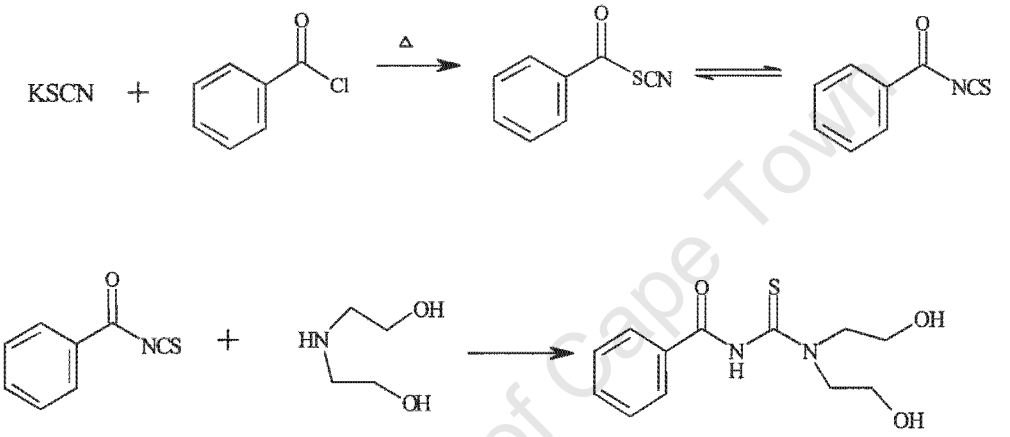

Fig. 2.8 Synthesis of *N,N*-di(2-hydroxyethyl)-*N'*- benzoylthiourea in anhydrous acetone.

The reaction of Pt(diimine)Cl_2 with *N,N*-di(2-hydroxyethyl)-*N'*-benzoylthiourea (H_3L) proceeded by co-ordination of the sulphur atom to platinum forming a complex [Pt(diimine)(H_3L)Cl]Cl with the subsequent loss of a chloride ion. This was followed by co-ordination to oxygen due to the chelate effect. The addition of base resulted in deprotonation of the amide nitrogen. The delocalisation of the negative charge caused the carboxyl oxygen atom to be more nucleophilic towards the platinum(II) centre. This procedure was summarised in Fig. 2.9.

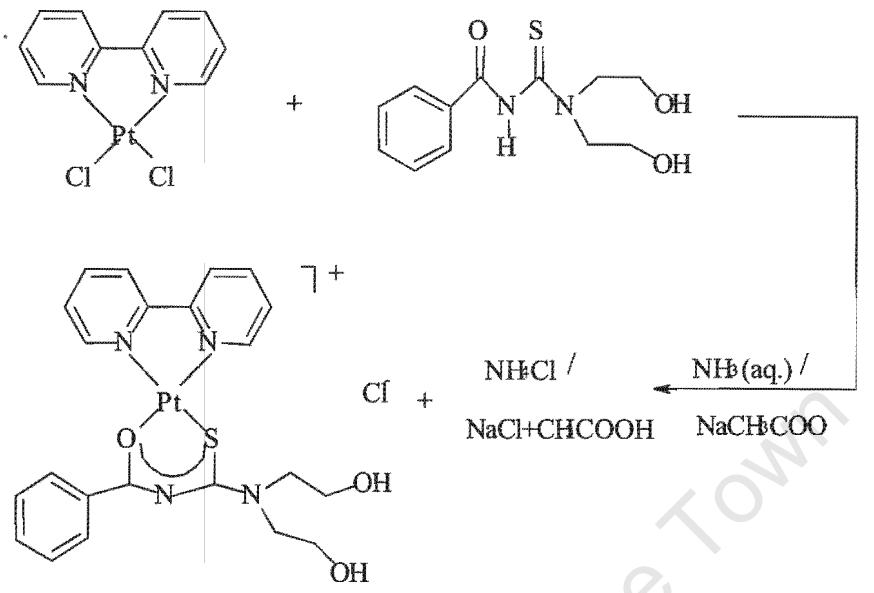

Fig. 2.9 The formation of water soluble salts together with the desired product [Pt(bipy)H_2L]Cl.

N,N-di(2-hydroxyethyl)-*N'*-benzoylthiourea (H_3L) ligand incorporated a 'soft' sulphur donor and a 'hard' oxygen donor atom. According to the rules suggested by Pearson[6], platinum was characterised as being a 'soft' metal and thus very much preferred binding to ligands that have 'soft' donor atoms. However, from the crystallographical data of similar complexes, almost only complexes that bound through both sulphur donor atom and oxygen donor atom were observed with *N,N*-dialkyl-*N'*-aroylthiourea.[25-27] This could be attributed to the chelate effect, which stated that complexes with bidentate ligands exhibit a greater stability in comparison to their non-chelated analogues. Hence the 'hard' oxygen donor atom was able to bind to the 'soft' metal, platinum forming a bidentate complex through both sulphur and oxygen donor atoms.

Mixed-ligand complexes with diimine and *N,N*-di(n-butyl)-*N'*-aroyl-thiourea were synthesised by Lawrence *et al.*[28] in the form of [Pt(diimine)(*S,O*)*N,N*-di(n-butyl)-*N'*-aroyl-thioureato]$^{+}PF_6^{-}$. This complex was relatively insoluble in water due to the large PF_6 anion. Since it was best for a potential biologically active compound to be water soluble, the Cl analogues were synthesised. The synthesis of mixed-ligand [Pt(diimine)(*S,O*)*N,N*-di(2-hydroxyethyl)-*N'*-benzoylthioureato]$^{+}Cl^{-}$ complexes were carried out in a similar fashion. Pt(diimine)Cl_2 complexes were reacted with *N,N*-di(2-hydroxyethyl)-*N'*-benzoyl-thiourea (H_3L) ligand in acetonitrile and subsequently the mono coordinated with *N,N*-di(2-hydroxyethyl)-*N'*-benzoyl-thiourea ligand was deprotonated by addition of sodium acetate to form the product [Pt(diimine)(*S,O*)*N,N*-di(2-hydroxyethyl)-*N'*-benzoyl-thioureato]$^{+}Cl^{-}$ complexes.

The method of synthesis was deceptively simple, and several problems were encountered during the synthesis of the chloride analogues using the same method as Lawrence *et al.*[28] Firstly, the starting material, Pt(diimine)Cl_2, was poorly soluble in pure acetonitrile which implied large amount of solvent was required to dissolve the starting material. In the case of Pt(4,4'-dimethyl-2,2'-bipyridyl)Cl_2 and Pt(1,10-phenanthroline)Cl_2, the starting material failed to dissolve completely even with a large amount of acetonitrile added. Since the final product was rather insoluble in acetonitrile, the formation of product should theoretically encourage more of the starting material to solubilise in the solvent, leaving only the product. Unfortunately there were often some Pt(diimine)Cl_2 precipitated when the acetonitrile solution was cooled. Second problem was the salt formation after addition of the base. In the original synthesis, aqueous ammonia or sodium acetate was used as the base to extract the N-H proton of *N,N*-di(2-hydroxyethyl)-*N'*-benzoyl-thiourea ligand. As a result of this proton extraction, salts such as NH_4Cl and NaCl were readily formed and precipitated out together with the desired product. [Pt(diimine)(*S,O*)*N,N*-di(2-hydroxyethyl)-*N'*-benzoylthioureato]$^{+}Cl^{-}$, NH_4Cl and NaCl were all readily soluble in water. Although NH_4Cl or NaCl should be more soluble in water than [Pt(diimine)(*S,O*)*N,N*-di(2-hydroxyethyl)-*N'*-benzoylthioureato]$^{+}Cl^{-}$, attempt to wash off NH_4Cl and NaCl could not prevent the product from dissolving in water.

Several methods were employed in the attempt to separate the starting material from the desire product [Pt(diimine)H_2L]Cl. An attempt to use ion exchange chromatography, since Pt(diimine)Cl_2 was an uncharged complex, there should not be any retention on the column. The NaCl solution used for elution, however, resulted in the [Pt(diimine)(*S,O*)*N,N*-di(2-hydroxyethyl)-*N'*-benzoyl-thioureato]$^+Cl^-$ complex to precipitate on the ion exchange column and therefore this method failed. Attempts to use reverse phase HPLC to separate the mixture were also unsuccessful since they could not be eluted with a variety of water/acetonitrile mixtures from C_{18} RP-HPLC column. It appeared that the [Pt(diimine)H_2L]Cl complexes were strongly retained on a C_{18} phase, and could only be eluted after extended methanol wash.

In view of these unexpected problems in the synthesis of [Pt(diimine)H_2L]Cl complexes, the synthetic method was reviewed. Both the starting materials, Pt(diimine)Cl_2, and the end products, [Pt(diimine)H_2L]Cl, had different solubility properties, a solubility test was carried out for all the complexes. (Table 2.2) In theory, if one found a solvent in which the starting material was readily soluble and their final product was relatively insoluble, then the possible contamination from the unreacted starting material could be eliminated. From table 2.2, it was not difficult to see that either DMF or DMSO was the best solvent for the synthesis of [Pt(bipy)H_2L]Cl and [Pt(diMebipy)H_2L]Cl since only the starting material would be soluble (and the product was not) in DMF/DMSO. Based upon the same reasoning, acetone was chosen as the better solvent for [Pt(di-*tert*-butylbipy)H_2L]Cl. For the synthesis of [Pt(phen)H_2L]Cl, because Pt(phen)Cl_2 was hardly soluble in any of those solvents tested, the final product required further recrystallisation from methanol/acetonitrile to eliminate any unreacted starting material.

	1	2	3	4	5	6	7	8
Acetonitrile	*	×	Poorly	×	✔	✔	poorly	×
Acetone	×	×	×	×	✔	×	×	×
H_2O	×	✔	×	✔	×	✔	×	✔
DMF	✔	×	✔	×	✔	✔	slightly	Poorly
DMSO	✔	×	✔	×	✔	✔	slightly	Poorly

1. Pt(bipy)Cl_2
2. $[Pt(bipy)H_2L]^+Cl^-$
3. Pt(diMebipy)Cl_2
4. $[Pt(diMebipy)H_2L]^+Cl^-$
5. Pt(di-*tert*-butylbipy)Cl_2
6. $[Pt(di\text{-}tert\text{-}butylbipy)H_2L]^+Cl^-$
7. Pt(phen)Cl_2
8. $[Pt(phen)H_2L]^+Cl^-$

* Pt(bipy)Cl_2 is soluble in a large volume of acetonitrile.

Table 2.2 The solubility characteristics of Pt(diimine)Cl_2 and $[Pt(diimine)H_2L]^+Cl^-$ complexes.

Another challenge in the development of synthetic method was to find a suitable base to abstract the N-H proton for *N,N*-di(2-hydroxyethyl)-*N'*-benzoylthiourea ligand co-ordination. The use of both aqueous NH_3 and sodium acetate as base in this reaction, resulted in the formation of water soluble salts such as NH_4Cl and NaCl (Fig 2.10). These salts and the desired complex [Pt(diimine)H_2L]Cl would both be insoluble in organic solvent and thus soluble when a small amount of H_2O was added, which made the seperation virtually impossible. It was then essential to find a base that would form soluble salts after the proton extraction of the *N,N*-di(2-hydroxyethyl)-*N'*-benzoylthiourea ligand. Several organic bases were tested and it was found that triethylamine was the most suitable base as it had required basicity to extract the proton and its more "hydrophobic" character enabled the salt formed to remain soluble in most organic solvents.

2.3 EXPERIMENTAL

The diimine ligands (4,4' -dimethyl-2,2' -bipyridyl and 2,2' -bipyridyl) used in the preparation of Pt(diimine)Cl_2 were commercially available from Aldrich Chemicals. 4,4' -di-tertiary-butyl-2,2' -bipyridyl was synthesised using the method reported by Hadda *et al.*[10]

2.3.1 Preparation of 4,4' -di-tertiary-butyl-2,2' -bipyridyl[10]

4-*tert*-butyl-pyridine (25ml) was purified by distillation under vacuum. 1g of palladium (10% on charcoal) was degassed in a schlenk flask overnight using an oil pump at 180°C. The pyridine (23ml) was added dropwise to the palladium catalyst under an inert (nitrogen) atmosphere. The mixture was left to heat under reflux for six days with stirring. After cooling, dry THF (75ml) was added to the mixture before filtering (through celite) to remove the catalyst. Concentration of the solution to approximately 75 ml was followed by the addition of neutral alumina (30g), and then complete evaporation of the solvent. The solid alumina mixture was added to a sublimation apparatus connected to a trap and oil pump. Unreacted *tert*-butyl-pyridine was eliminated (approximately 8ml) under vacuum and 4,4' -di-*tert*-butyl-2,2' -bipyridyl was obtained by sublimation under vacuum. Further purification was carried out by recrystallising from ethanol and water mixture.

4,4' -di-*tert*-butyl-2,2' -bipyridyl (2.80 g, 20.55%) m.p. 156-159°C (lit.,156°C) (Found: C,80.7; H,8.9; N,9.8%; M 268. Calc. for $C_{18}H_{24}N_2$: C, 80.5; H, 9.0; N,10.4%; M 268.194); δ_H(200.06MHz; solvent $CDCl_3$; reference $SiMe_4$) 8.54 (2H,dd, J=5.23 and 0.68Hz, H_6, $H_{6'}$), 8.35 (2H, dd, J=1.98 and 0.63 Hz, H_3, $H_{3'}$), 7.24 (2H, dd, J=5.24 and 1.99 Hz, H_5,$H_{5'}$), 1.33 (18H, s, Me's); δ_C(50.31 MHz; solvent $CDCl_3$; reference $SiMe_4$) 149.02 (C_6,C6'), 120.70 (C_3,$C_{3'}$), 118.28 (C_5,$C_{5'}$), 30.63 (CH_3)$_6$, 160.96 (C_2,$C_{2'}$), 156.54 (C_4,$C_{4'}$), 34.99 (C_7,$C_{7'}$); *m/z* 268, 253, 237, 212, 119.

2.3.2 Preparation of *N,N*-di(2-hydroxyethyl)-*N'* -benzoylthiourea ligand

The *N,N*-di(2-hydroxyethyl)-*N'* -benzoylthiourea ligand was synthesised according to the method reported by Douglass and Dains.[13] The acetone solvent was dried by heating to reflux in the presence of type 4 ÅLinde molecular sieves and K_2CO_3, and distilled before use. Dry potassium thiocyanate (0.04 mol) was dissolved in dry acetone (25 ml) in a two neck round bottom flask. An equimolar amount of benzoyl chloride dissolved in approximately 10ml dry acetone was then added dropwise under a nitrogen atmosphere. The solution was heated to reflux under nitrogen for 30 minutes. Dihydroxyethylamine (0.04 mol), dissolved in 10 ml of acetone was added dropwise and the reaction mixture was allowed to heat under reflux for a further 30 minutes. The solution was allowed to cool and ice cold water was added just sufficient to dissolve KCl salt. Light yellowish precipitates formed after leaving the solution in the refrigerator overnight. The precipitated product was collected by filtration and dried. The ligands were recrystallised from ethanol to give a white crystalline material.

N,N-di(2-hydroxyethyl)-N' -benzoylthiourea (8.99 g; 83.8%) m.p. 119-121°C (Found: C, 54.2; H, 6.3; N, 10.5; S, 12.0%; Calc. for $C_{12}H_{15}N_2O_3S$: C, 53.7; H, 6.0; N, 10.5; S, 11.9%); δ_H(200.06MHz; solvent d-acetone; reference $SiMe_4$) 10.42 (1H, br s, N-H), 7.85-7.90 (2H, m, $H_{2''}$, $H_{6''}$), 7.62 (1H, tt, $H_{4''}$), 7.52 (2H, tt, $H_{3''}$, $H_{5''}$), 4.11 (1H, br s, O-H), 3.80-4.08 (8H, m, H_a, $H_{a'}$, H_b, $H_{b'}$), 3.24(1H, unresolved t, O-H); δ_C(50.31 MHz; solvent d-acetone; reference $SiMe_4$) 182.0 (C=S), 165.6 (C=O), 134.4 ($C_{1''}$), 132.7 ($C_{4''}$), 128.0, 129.0 ($C_{2''}$ and $C_{6''}$ / $C_{3''}$ and $C_{5''}$), 59.2, 60.3 (C_b, $C_{b'}$), 54.8, 54.9 (C_a, $C_{a'}$).

2.3.3 Preparation of Pt(diimine)Cl_2

The same general method has been used to synthesise all Pt(diimine)Cl_2 complexes[23]. Potassium tetrachloroplatinate (1 mmol) was dissolved in 50 ml of water. Diimine ligand (1 mmol) and 2 ml of dilute HCl (2M) was then added to the solution. The reaction was heated under reflux and stirred for 2 hours until the yellow precipitates, and

the orange mother liquor became completely clear. The yellow precipitates were collected by centrifugation and washed with H_2O several times, followed by diethyl ether before drying in vacuum. These were used without further purification.

1,10-phenanthrolinedichloroplatinum(II) (0.43 g, 96.4%) m.p. > 335°C (Found: C, 32.4; H, 1.7; N, 6.2%. Calc for $C_{12}H_8N_2PtCl_2$: C, 32.3; H, 1.8; N, 6.3%)

2,2' -bipyridyldichloroplatinum(II) (0.42 g, 99.5%) m.p. > 335°C (Found: C, 28.2; H, 1.8; N, 6.5%. Calc for $C_{10}H_8N_2PtCl_2$: C, 28.4; H, 1.9; N, 6.6%)

4,4' -dimethyl-2,2' -bipyridyldichloroplatinum(II) (0.44 g, 99.1%) m.p. > 335°C (Found: C, 32.1; H, 2.6; N, 6.2%. Calc for $C_{12}H_{12}N_2PtCl_2$: C, 32.0; H, 2.7; N, 6.2%)

4,4' -di-*tert*-butyl-2,2' -bipyridyldichloroplatinum(II) (0.52 g, 97.7%) m.p. > 335°C (Found: C, 40.4; H, 4.5; N, 5.2%. Calc for $C_{18}H_{24}N_2PtCl_2$: C, 40.5; H, 4.5; N, 5.2%)

2.3.4 Preparation of Pt(diimine)Br_2

K_2PtCl_4 (0.5mmol) and NaBr (12.5mmol) were dissolved in 40 ml of water and then 20 ml of 10% HBr was added. The solution was left to stirr for an hour. The diimine ligand was suspended in 40 ml of water and 20 ml of HBr mixture and added into the K_2PtCl_4 mixture. The reaction was allowed to proceed for 3 more hours then poured into cold water and placed in the refrigerator. The precipitates were filtered and washed with H_2O and cold ethanol.

2,2' -bipyridyldibromoplatinum(II) (0.19 g, 76.2%) m.p. > 335°C (Found: C, 23.5; H, 1.4; N, 5.4%. Calc for $C_{10}H_8N_2PtBr_2$: C, 23.5; H, 1.5; N, 5.5%)

4,4' -dimethyl-2,2' -bipyridyldibromoplatinum(II) (0.25 g, 92.8%) m.p. > 335°C (Found: C, 25.9; H, 2.0; N, 5.1%. Calc for $C_{12}H_{12}N_2PtBr_2$: C, 26.7; H, 2.2; N, 5.2%)

2.3.5 Preparation of [(2,2' -bipyridyl)-*N*,*N*-di(2-hydroxyethyl)-*N*' -benzoyl-thioureato-(*O*,*S*)-platinum(II)] chloride

Pt(bipy)Cl_2 (0.24 mmol) was dissolved in 12ml of DMF with heating. After cooling, 33µl of triethylamine was added. *N*,*N*-di(2-hydroxyethyl)-*N*' -benzoylthiourea ligand (0.07g) in 1.7ml of DMF was added drop wise. Reaction was first heated up to *ca.* 70°C and the solution turned from yellow to orange colour. Precipitates start to form after 15 minutes. The reaction was left to stir in room temperature overnight and precipitates were centrifuged then filtered.

[(2,2' -bipyridyl)-*N*,*N*-di(2-hydroxyethyl)-*N*' -benzoyl-thioureato-(*O*,*S*)-platinum(II)] chloride (88.1%) m.p. 207-208°C (Found: C, 40.76; H, 3.61; N, 8.64; S, 4.84. $C_{22}H_{23}N_4O_3SPtCl$ requires C, 40.40; H, 3.52; N, 8.57; S, 4.90%) δ_H(300.08 MHz; solvent 50% CD_3CN/D_2O reference $SiMe_4$) 3.68-3.90 (4H, m, H_a H_b $H_{a'}$ $H_{b'}$), 7.37 (1H, t, $H_{5'}$), 7.39 (2H, t, $H_{3''}$, $H_{5''}$), 7.59 (1H, t, $H_{4''}$), 7.71 (1H, t, H_5), 7.80 (2H, d, $H_{2''}$, $H_{6''}$), 7.97 (1H, d, $H_{3'}$), 8.04 (1H, d, H_3), 8.08 (1H, t, $H_{4'}$), 8.15 (1H, t, H_4), 8.27 (1H, d, $H_{6'}$), 8.67 (1H, d, H_6).

2.3.6 Preparation of [(1,10-phenanthroline)-*N*,*N*-di(2-hydroxyethyl)-*N*' -benzoyl-thioureato-(*O*,*S*)-platinum(II)] chloride

Pt(phen)Cl_2 (0.23 mmol) was suspended in 16.3 ml of DMF and the solution was left to stir and reflux at 100°C overnight. Triethylamine (0.03 ml) then was added to the starting material. *N*,*N*-di(2-hydroxyethyl)-*N*' -benzoylthiourea ligand (0.07g) in 1.7ml of DMF was added drop wise and the solution turns from bright yellow to light orange after an hour. The mixture was left to heat for 24 hours then filtered out. The precipitates then were recrystalised from methanol/acetonitrile.

Preparation of [(1,10-phenanthroline)-*N,N*-di(2-hydroxyethyl)-*N'*-benzoylthioureato-(*O,S*)-platinum(II)] chloride (84.0%) m.p. 204-207°C (Found: C, 41.67; H, 3.37; N, 8.06; S, 4.43. $C_{24}H_{23}N_4O_3SPtCl$ requires C, 42.51; H, 3.42; N, 8.27; S, 4.72%) δ_H(300.08 MHz; solvent 50% CD_3CN/D_2O reference $SiMe_4$) H_a H_b $H_{a'}$ $H_{b'}$, 7.14 (2H, t, $H_{3''}$, $H_{5''}$), 7.30 (2H, d, $H_{2''}$, $H_{6''}$), 7.39 (1H, dd, H_8), 7.39 (1H, t, $H_{4''}$), 7.47 (1H, d, H_6), 7.54 (1H, d, H_5), 7.78 (1H, dd, H_3), 8.05 (1H, d, H_9), 8.27 (1H, d, H_7), 8.33 (1H, d, H_2), 8.40 (1H, d, H_4).

2.3.7 Preparation of [(4,4'-di-*tert*-butyl-2,2'-bipyridyl)-*N,N*-di(2-hydroxyethyl)-*N'*-benzoylthioureato-(*O,S*)-platinum(II)] chloride

Pt(di-*tert*-butyl-bipy)Cl_2 (0.19 mmol) was dissolved in 55ml of warm acetone. 0.026ml of triethylamine and *N,N*-di(2-hydroxyethyl)-*N'*-benzoylthiourea ligand (0.058g) in 5ml acetone were in turn added into the reaction mixture. The reaction was refluxed overnight and the precipitates were filtered and dried.

[(4,4'-di-*tert*-butyl-2,2'-bipyridyl)-*N,N*-di(2-hydroxyethyl)-*N'*-benzoylthioureato-(*O,S*)-platinum(II)] chloride (82.9%) m.p.214-215°C (Found: C, 46.87; H, 4.95; N, 7.23; S, 4.15. $C_{30}H_{39}N_4O_3SPtCl$ requires C, 47.03; H, 5.04; N, 7.32; S, 4.18%) δ_H(399.95 MHz; solvent 50% CD_3CN/D_2O reference $SiMe_4$) 1.70 (9H, s, $H_{7'}$, $H_{8'}$, $H_{9'}$), 1.82 (9H, s, H_7, H_8, H_9), 4.12 (2H, t, H_a, $H_{a'}$), 4.21 (2H, t, H_b, $H_{b'}$), 7.71 (2H, t, $H_{3''}$, $H_{5''}$), 7.85 (1H, d, $H_{5'}$), 7.95 (1H, t, $H_{4''}$), 8.07 (1H, d, H_5), 8.11 (2H, d, $H_{2''}$, $H_{6''}$), 8.32 (1H, s, $H_{3'}$), 8.48 (1H, s, H_3), 8.65 (1H, d, $H_{6'}$), 8.87 (1H, d, H_6).

2.3.8 Preparation of [(4,4'-dimethyl-2,2'-bipyridyl)-*N,N*-di(2-hydroxyethyl)-*N'*-benzoylthioureato-(*O, S*)-platinum(II)] chloride

Pt(4,4'-dimethyl-2,2'bipyridyl)Cl_2 (0.23g; 0.5 mmol) dissolved in 25 ml of DMF with heating. After cooling, 70µl of triethylamine was added. *N,N*-di(2-hydroxyethyl)-*N'*-benzoylthiourea ligand (0.13g; 0.5 mmol) in 4 ml DMF was added slowly. The mixture

was allowed to stir at 70°C until most of the yellow precipitates were formed. The yellow precipitate was filtered off and dried in oven (60°C) for two hours.

[(4,4' -dimethyl-2,2' -bipyridyl)-*N*,*N*-di(2-hydroxyethyl)-*N*' -benzoylthioureato-(*O*, *S*)-platinum(II)] chloride (82.9%) m.p. 213-216°C (Found: C, 46.87; H, 4.95; N, 7.23; S, 4.15. $C_{30}H_{39}N_4O_3SPtCl$ requires C, 47.03; H, 5.04; N, 7.32; S, 4.18%) δ_H(399.95 MHz; solvent 50% CD_3CN/D_2O reference $SiMe_4$) 1.98 (3H, s, $H_{7'}$), 2.07 (3H, s, H_7), 4.12 (2H, t, H_a, $H_{a'}$), 4.21 (2H, t, H_b, $H_{b'}$), 7.71 (2H, t, $H_{3''}$, $H_{5''}$), 7.85 (1H, d, $H_{5'}$), 7.95 (1H, t, $H_{4''}$), 8.07 (1H, d, H_5), 8.11 (2H, d, $H_{2''}$, $H_{6''}$), 8.32 (1H, s, $H_{3'}$), 8.48 (1H, s, H_3), 8.65 (1H, d, $H_{6'}$), 8.87 (1H, d, H_6).

2.3.9 Preparation of [(2,2' -bipyridyl)(*N*,*N*-di(2-hydroxyethyl)-*N*' -benzoylthio ureato-(*O*,*S*)-platinum(II)] bromide

$Pt(bipy)Br_2$ (0.124 mmol) was dissolved in 10ml of DMF with heating. After cooling, 20µl of triethylamine was added. *N*,*N*-di(2-hydroxyethyl)-*N*' -benzoylthiourea ligand (0.032g) in 1.0ml of DMF was added drop wise. Reaction was first heated up to *ca.* 70°C and the solution turned from yellow to orange colour. The reaction was left to stir in room temperature overnight and precipitates were centrifuged then filtered.

[(2,2' -bipyridyl)(*N*,*N*-di(2-hydroxyethyl)-*N*' -benzoylthioureato-(*O*,*S*)-platinum(II)] bromide (85%) m.p. 204-206 °C (Found: C, 37.50; H, 3.31; N, 7.78; S, 4.32. $C_{22}H_{23}N_4O_3SPtBr$ requires C, 37.82; H, 3.30; N, 8.02; S, 4.58%) δ_H(400 MHz; solvent 50% CD_3CN/D_2O reference $SiMe_4$) 3.68-3.36 (4H, m, H_a H_b $H_{a'}$ $H_{b'}$), 6.96 (1H, t, $H_{5'}$), 7.09 (2H, t, $H_{3''}$, $H_{5''}$), 7.19 (2H, d, $H_{2''}$, $H_{6''}$), 7.23 (1H, t, $H_{4''}$), 7.36 (1H, d, $H_{3'}$), 7.39 (1H, t, H_5), 7.43 (1H, d, H_3), 7.59 (1H, d, $H_{6'}$), 7.65 (1H, t, $H_{4'}$), 7.68 (1H, t, H_4), 7.91 (1H, d, H_6).

2.3.10 Preparation of [(4,4' -dimethyl-2,2' -bipyridyl)(*N*,*N*-di(2-hydroxyethyl)-*N*' -benzoylthioureato-(*O*,*S*)-platinum(II)] bromide

Pt(4,4' -dimethyl-2,2' bipyridyl)Br_2 (0.068g; 0.126 mmol) dissolved in 5 ml of DMF with heating. After cooling, 15µl of triethylamine was added. *N*,*N*-di(2-hydroxyethyl)-*N*' -benzoylthiourea ligand (0.034g; 0.126 mmol) in 4 ml DMF was added slowly. The mixture was allowed to stir at 70°C until most of the yellow precipitates were formed. The precipitate was filtered off and dried in oven (60°C) for two hours.

[(4,4' -dimethyl-2,2' -bipyridyl)(*N*,*N*-di(2-hydroxyethyl)-*N*' -benzoylthioureato-(*O*,*S*)-platinum(II)] bromide (78.5 %) m.p. 228-229°C (Found: C, 44.10; H, 4.78; N, 6.57; S, 3.85. $C_{30}H_{39}N_4O_3SPtBr$ requires C, 44.44; H, 4.81; N, 6.91; S, 3.95%) δ_H(399.95 MHz; solvent 50% CD_3CN/D_2O reference $SiMe_4$) 1.80 (3H, s, $H_{7'}$), 1.88 (3H, s, H_7), 3.50-3.28 (4H, m, H_a, $H_{a'}$, H_b, $H_{b'}$), 6.88 (1H, d, $H_{5'}$), 7.07 (1H, d, H_5), 7.23 (1H, s, $H_{3'}$), 7.23 (1H, s, H_3), 7.27 (2H, t, $H_{3''}$, $H_{5''}$), 7.33 (2H, d, $H_{2''}$, $H_{6''}$), 7.54 (1H, t, $H_{4''}$), 7.60 (1H, d, $H_{6'}$), 7.74 (1H, d, H_6).

2.4 CHARACTERISATION

These water soluble compounds were characterised by mass spectrometry, ^{1}H NMR, ^{13}C NMR and C, H, N, S elemental analysis. The ^{1}H NMR spectrum compared favourably with that reported previously.

All the Pt(diimine)Cl_2 were synthesised in good yields. Due to their extremely high melting points (> 320°C), it was not possible to determine the purity of these complexes by melting point. The formation of Pt(diimine)Cl_2 therefore was confirmed by C, H, N, S elemental analysis.

The *N,N*-di(2-hydroxyethyl)-*N'*-benzoylthiourea ligand was recrystallised from ethanol and the structure was confirmed by ^{1}H and ^{13}C NMR spectroscopy. The C, H, N, S elemental analysis was found consistent with the calculated values and the melting points corresponded to literature values.

The ^{1}H and ^{13}C NMR of *N,N*-di(2-hydroxyethyl)-*N'*-benzoylthiourea were recorded in d-acetone and their assignments were similar to those reported by Koch *et. al.* [25] In the ^{9}C NMR spectrum, there is a thiocarbonyl carbon peak at 182.0 ppm and a carbonyl carbon peak at 165.6 ppm, which are the characteristic peaks for dialkyl-*N'*-benzoylthiourea series.

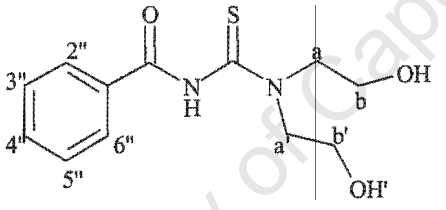

Fig. 2.11 Numbering of H atoms in *N,N*-di(2-hydroxyethyl)-*N'*-benzoylthiourea

The ^{1}H NMR spectrum was also relatively simple to assign. A broad N-H peak was observed at the most downfield region, 10.42, due to the two close by electron withdrawing C=O and C=S groups. The $H_{2"}$ and $H_{6"}$ protons of *N,N*-di(2-hydroxyethyl)-*N'*-benzoylthiourea were observed between 7.85 and 7.90 ppm. The $H_{4"}$ proton was observed as a triplet of triplet between 7.59 and 7.65 ppm. This was due to its coupling with $H_{3"}$, $H_{5"}$ and the long range W coupling with $H_{2"}$, $H_{6"}$. The $H_{3"}$ and $H_{5"}$ also appeared as a triplet of triplet at 7.52 ppm. The H_a, $H_{a'}$, H_b and $H_{b'}$ protons were observed as broad multiplets from 3.80 to 4.08 ppm and they were unable to be assigned unambiguously. In anhydrous DMSO-d_6, however, Koch *et al.* reported that two sets of resonances were being observed for H_a, $H_{a'}$, H_b and $H_{b'}$ protons. This was due to the restricted rotation

around the C-N bond between the thiocarbonyl group and nitrogen atom, which had significant double bond character. Similar pattern was also being observed in ^{13}C NMR spectra where there were two sets of peaks for C_a, $C_{a'}$ and C_b, $C_{b'}$. The two inequivalent O-H protons showed an interesting phenomenon: one of the O-H proton was observed as an unresolved triplet while the other one was a broad singlet. In anhydrous DMSO-*d*$_6$, the triplet of one O-H proton becomes well resolved. This can be accounted as the O-H proton can usually exchange rapidly with the protic solvent, when it is hydrogen bonded with other parts of the molecule, the exchange became significantly slower and thus produce a more well defined triplet. This observation confirmed that one of the O-H group is involved in hydrogen bonding with the rest of the molecule whilst the other O-H moves freely in the solvent.

Various $[Pt(diimine)H_2L]^+A^-$ complexes were synthesised with diimine ligands being 2,2'-bipyridyl, 4,4'-dimethyl-2,2'-bipyridyl, 4,4'-di-*tert*-butyl-2,2'-bipyridyl, 1,10-phenanthroline and the anion being chloride, bromide and perchlorate. (Fig. 2.12) These complexes were satisfactorily characterised by C, H, N and S elemental analysis and ^1H NMR spectroscopy (50% acetonitrile-d_3/ 50% D_2O)

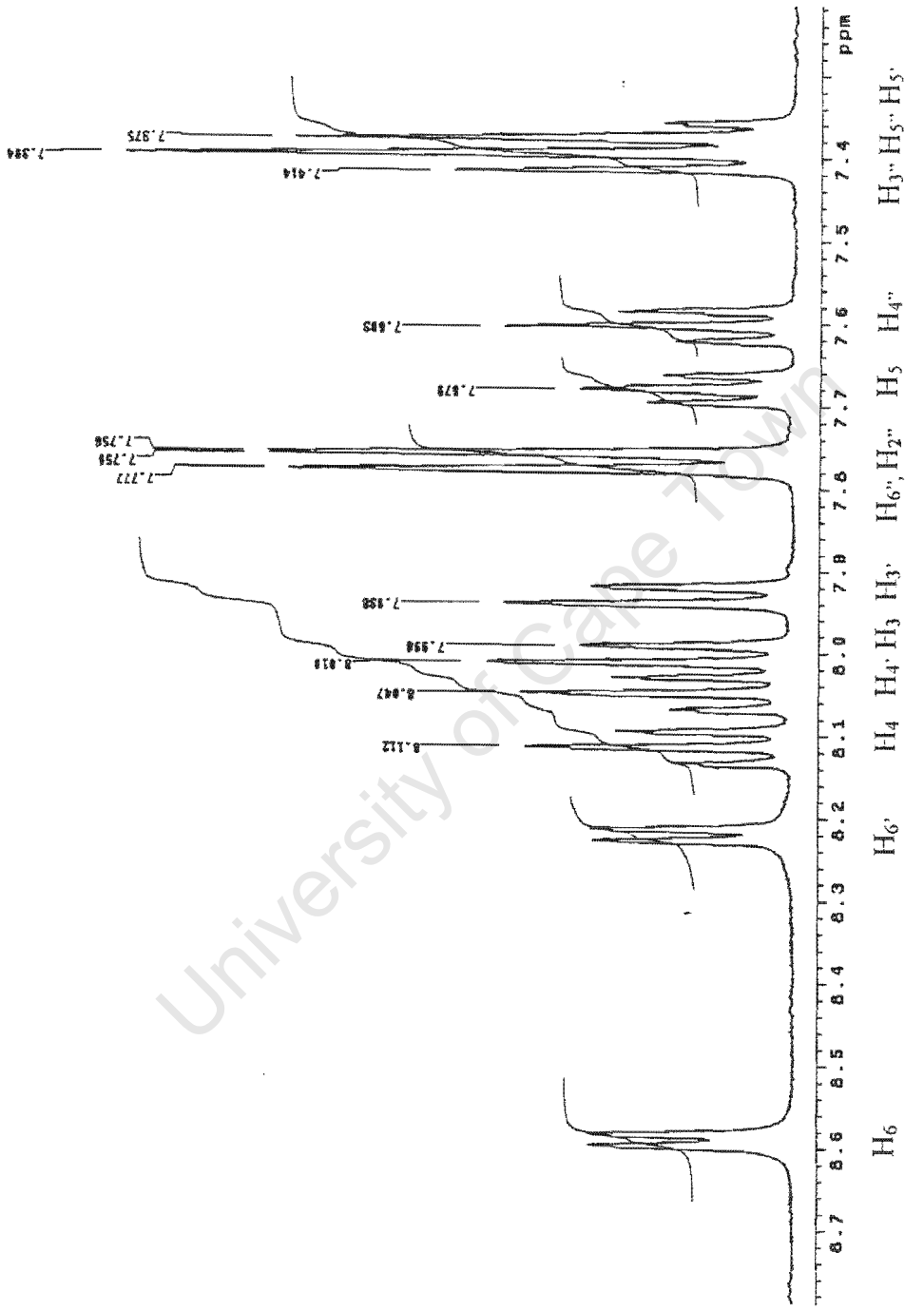

Fig. 2.12 The aromatic region of ^{1}H NMR Spectra of $[Pt(bipy)H_2L]Cl$.

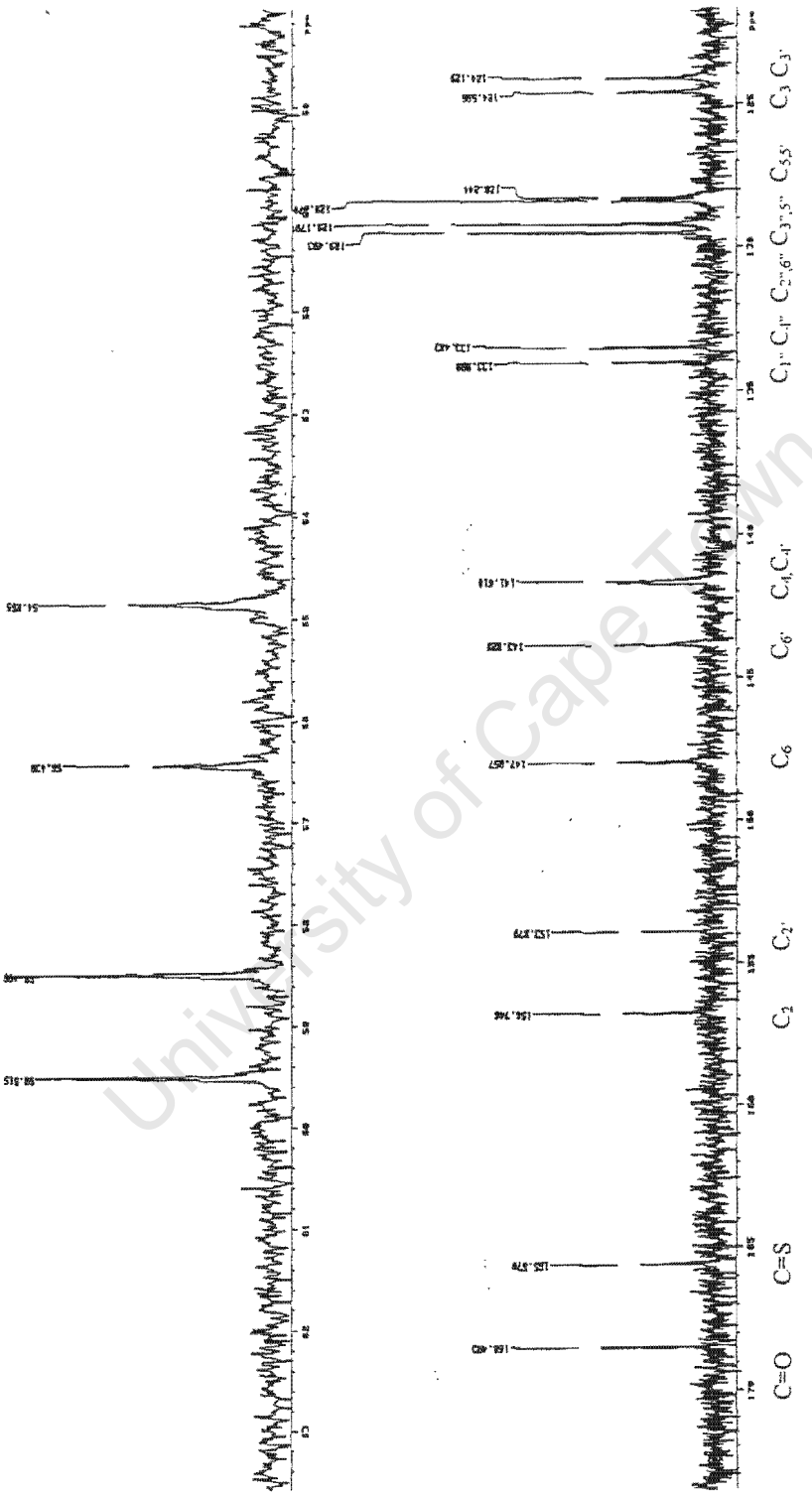

Fig. 2.12 ^{13}C NMR of $[Pt(bipy)H_2L]Cl$ complex

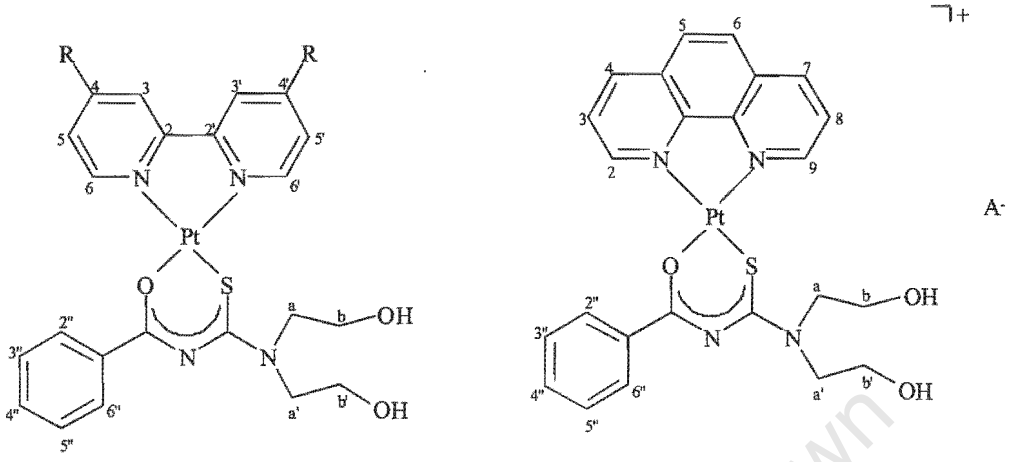

R= H, CH_3, *tert*-butyl

A= Cl, Br, ClO_3

Fig. 2.14 Diagram showing the $[Pt(diimine)H_2L]^+A^-$ synthesised and their numbering used in characterisation

The ^1H NMR spectra of $[Pt(diimine)H_2L]Cl$ complexes were originally done in D_2O and the resonances in the spectra showed extremely broad peaks. As soon as some acetonitrile was added to the solution, the resonace peaks sharpen up. This can be seen from Fig. 2.12 when we compare the spectra of the aromatic region for the complex in 100% D_2O ++that complexes of [Pt(diimine)(*N,N*-di(n-butyl)-*N'*-aroylthioureato)]PF_6 form dimmers in pure acetonitrile. The broadening of peaks in D_2O strongly suggest that these complexes not only have the tendency to self-associate into dimmers, they may also have the ability to form higher aggregates as the percentage of D_2O increases. A normal proton NMR spectrum gives sharp peaks. A small molecule tumbles rapidly in solution, so that magnetic energy exchange with the "lattice" is inefficient which result in short T_1 and T_2 times. When the molecular weight increase, the rate of tumbling decreases, so that T_1 and T_2 became even shorter. Since $\nu_{1/2} = 1 / T_2$, the smaller T_2 is, the larger $\nu_{1/2}$ becomes and

thus the resonances are broad. Large "aggregates" or "polymers" have short T_2, hence their $\nu_{1/2}$ is very large and broad resonances are observed. Further studies on this self-association phenonmenon can be found in chapter 3 of this thesis.

The ^1H chemical shift assignments were established with the aid of 2D-COSY NMR experiments. The ^1H NMR spectra of these complexes are characterised by the loss of the N-H resonance, which is convincing evidence that the *N,N*-di(2-hydroxyethyl)-*N'*-benzoylthiourea ligand has co-ordinated to platinum in a bidentate fashion. The 2,2'-bipyridyl and substituted bipyridyl moiety give rise to two sets of peaks in the aromatic region. This suggests that the two sets of protons in the two pyridine rings are in different environments and cannot be unambiguously distinguished. However, the assignments are based on the following reasoning: Pt-S bond is "stronger" than the Pt-O bond due to the fact that soft metal prefers bonding with soft atom, the Pt-N bond that is opposite to the Pt-S bond is weakened. Since H_6 was assigned to be the proton that is opposite to Pt-S bond and $H_{6'}$ is on the other pyridine ring trans to O atom, one might expect that the H_6 proton and the protons from the same ring are more deshielded than $H_{6'}$ and the rest of that ring. The same reasoning applied for a slight difference in the chemical shifts of protons on the phenantholine ring of $[Pt(phen)H_2L]Cl$ complexes. On this work, we assumed the convention of numbering the proton that is opposite to Pt-S as H_2, and the one opposite to Pt-O as H_9.

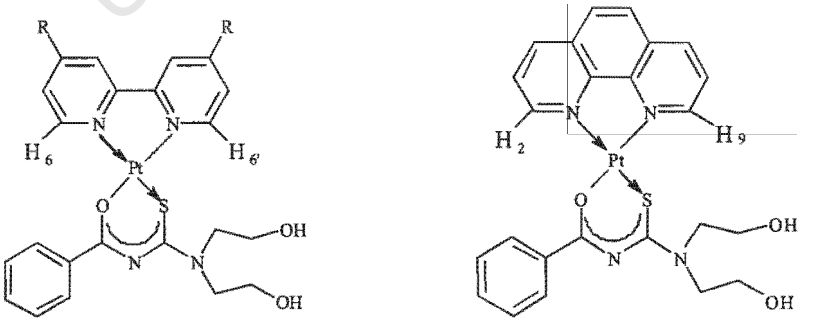

Fig. 2.13 The assignment of protons on the bipyridyl and phenanthroline rings.

REFERENCES

1. F. A.Cotton and G. Wilkinson, *Advanced Inorganic Chemistry*, John Wiley & Sons, 1988, 917.
2. S. Neidle and M. J. Waring (ed.), *Molecular Aspect of Anti-Cancer Drug Action*, Chapter 7, 183-186.
3. F. Basolo and R. G. Pearson, *Mechanisms of Inorganic Reactions*, John Wiley & Sons, Chapter 5, 351.
4. G. B. Kauffman, *J. Chem, Edu,* 1977, **54**, 87.
5. J. E. Huheey, Inorganic Chemistry: Principles of Structure and Reactivity, Harper and Row, 1972, 424.
6. R. G. Pearson, *J. Am. Chem. Soc*, 1963, **85**, 3533.
7. F. A. Palocsay and J. V. Rund, *Inorg. Chem*, 1969, **8**, 524.
8. J. V. Rund, *Inorg. Chem*, 1974, **13**, 738.
9. G.S. Bushnell, K.R. Dixon, and M. A. Khan, *Can.J.Chem*., **52**, 1367.
10. K. R. Dixon, *Inorg. Chem*, 1977, **16**, 2618.
11. K. Neuki, *Ber. dtsch. chem. Ges*., 1873, **6**, 598.
12. A. E. Dixon, *J. Chem. Soc*., 1895, **67**, 1040.
13. I. B. Douglass, F. B. Dains, *J. Am. Chem. Soc*., 1934, **56**, 719.
14. A. Takamizawa, K. Hira, K. Matsui, *Bull. Chem. Soc. Japan*., 1963, **36**, 1214.
15. M. O. Lozinskii, P. S. Pel' kis, *Russ. Chem. Rev. (Eng. Transl.),* 1968, **37**, 363.
16. J. D. Miller, PhD Thesis
17. L. Beyer, E. Hoyer, H. Hennig, R. Kirmse, *J. Prakt. Chem*., 1975, **317**, 829.
18. R. Richter, L. Beyer, J. Kaiser, Z. *Anorg. Allg. Chem*., 1980, **461**, 67.
19. G. Fitzl, L. Beyer, R. Richter, J. Kaiser, E. Hoyer and Z. *Anorg. Allg. Chem*., 1977, **433**, 237.
20. P. Vest, M. Schuster, K.-H König, *Fresenius, J. Anal. Chem*.,1991, **339**, 142.
21. P. Vest, M. Schuster, K.-H König, *Fresenius, J. Anal. Chem*.,1991, 341, 566.I.B. Douglass, F. B. Dains, *J. Am. Chem. Soc*., 1934, **56**, 719.

22. T. B. Hadda, H. Le Bozec, *Inorg. Chim. Acta.*, 1993, **204**, 103.

23. G. T. Morgan, F. H. Burstal, *J. Chem. Soc.*, 1934, 965.

24. D. F. Shriver, P. W. Atkins, C. H. Langford, *Inorganic Chemistry*, Oxford University Press, Oxford, 1990, Chapter 7.

25. K. R. Koch, C. Sacht, S. Bourne, *Inorganica Chimica Acta,* 1995, **232** 109.

26. S. Bourne and K. R. Koch, *J. Chem. Soc. Dalton Trans.* 1993, 2071.

27. K. R. Koch, J. du Toit, M. R. Caira and C. Sacht, *J. Chem. Soc. Dalton Trans.* 1994, 785.

28. K. R. Koch, C, Sacht and C. Lawrence, *J. Chem. Soc. Dalton Trans*. 1998, 689.

3.1 INTRODUCTION

Non-covalent intramolecular, intermolecular and hydrophobic interactions play an important role in biological systems. These include hydrogen bonding and vertical base-base interactions that stabilise the double helix of DNA[1], determining the tertiary structure of proteins[2], and in mediating processes such as receptor-ligand interactions[3], enzyme-substrate binding[4] and antigen-antibody recognition[5]. Applications of such non-covalent inter- and intramolecular interactions have also been extended further into the study of host-guest system[6], intercalation of drugs into DNA[7], studies of conformational preferences and binding properties of polyaromatic macrocycles[8], the packing of aromatic molecules in crystals[9], and the porphyrin aggregation[10]. The π-π interaction is a hydrophobic interaction that is not due to an attractive electronic interaction between the two π systems but occur when the attractive interactions between π-electrons and σ-framework outweigh unfavourable contributions such as π-electron repulsion[11].

Three important geometries have been identified for the aromatic π-π interactions; an edge-to-face (T-shaped) orientation where the positively charged hydrogen atoms on one ring interact with the negatively charged region on the second ring (A), a parallel face-to-face (B) and a centre-to-edge orientation (C) (Fig. 3.1). The C_6H_6/C_6F_6 heterodimer appears to prefer the face-to-face orientation in the solid state[12]. However, for the homodimer of benzene, edge-to-face orientation was favoured in place of face-to-face orientation due to the repulsion on the face-to-face stacked structure[13].

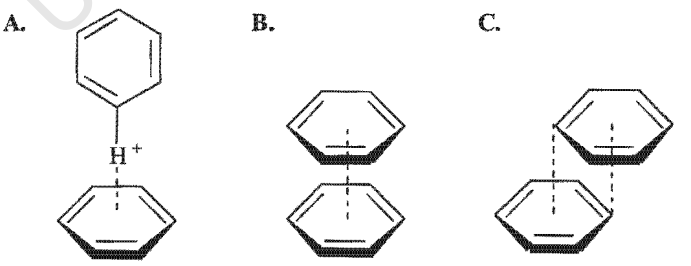

Fig. 3.1 Aromatic π-π interactions: **A**. face-to-edge, **B**. face-to-face and **C**. centre-to-edge orientation.

Early studies by Lippard *et al.*[14] have shown the tendency of some metal complexes having aromatic ligands (for example 2-hydroxyethanethiolato(HET)-(2,2',2"-terpyridine) platinum(II) nitrate complex) to self-associate in aqueous solution when the concentration is above 10^{-4}M. Two types of stacking interactions have been seen in the crystal structure of such systems, a direct head-to-tail overlap, and an overlap involving only two of the three aromatic rings of the terpyridine ligand (Fig. 3.2).

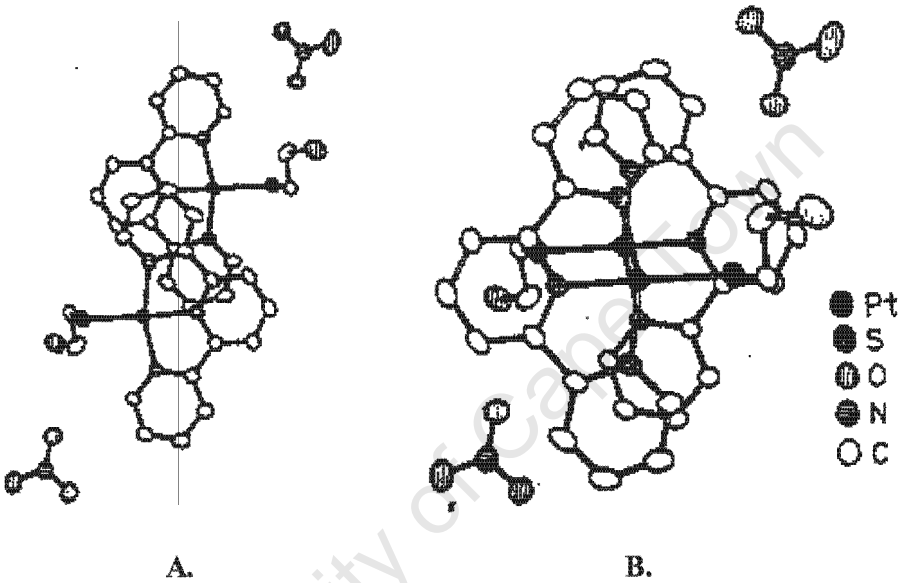

Fig. 3.2 The two different stacking interactions, viewed normal to the planes of the terpyridine ligand, found in the structure of [Pt(terpy)(HET)]NO_3[14].

A. overlapping with two ligand pyridine rings with each other.
B. head-to-tail-stacking.

Using the X-ray structure determined by Lippard *et al.*[14] on the stacking of $[Pt(terpy)(HET)]^+$ and ^1H NMR data, it was concluded that the dimer structure is the head-to-tail structure (Fig. 3.2B). At higher concentration, this complex was expected to form even larger polymeric structures since the concentration dependence became nonlinear. Romeo *et al.*[15] reported that complex such as (2,2':6',2"-terpyridine)methyl platinum(II) also shows extensive self-stacking in aqueous solution. It was found by various physical methods that even in a very dilute solution, this $[Pt(terpy)Me]^+$ complex would self-associate to form dimer species.

Self-association of metalloporphyrin complexes have also been known for a long time. Studies by NMR and EPR[16] demonstrated that metalloporphyrins with d^{10} central metal ions, such as zinc(II) or cadmium(II) behave like porphyrin dianions or divalent metal ions since there is no $d\pi$-$d\pi$ back-donation of electron density from the ring to the metal. Under such circumstances, the electrostatic difference between porphyrin and metal ion is counteracted by intermolecular rather than intramolecular interaction, i.e. by face-to-face aggregation (Fig. 3.3). For palladium(II) complexes, intramolecular $d\pi$-$p\pi$ interaction with empty d-orbitals on the metal results in less intermolecular donor-acceptor aggregation.

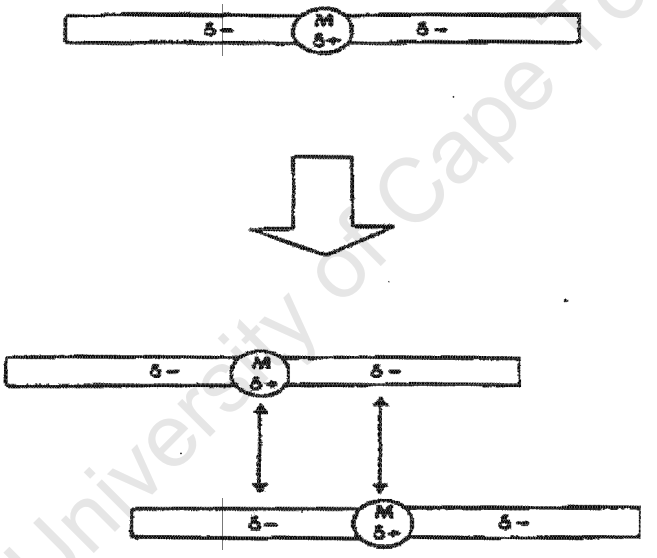

Fig. 3.3 Schematic diagram of interactions in metalloporphyrin π-π dimers. The partial negative charge refers to the pi-cloud of the aromatic portion of the ligand which interacts with the positively charged metal centre of the neighbouring complex in forming the dimer.

In a more recent study by Lawrence[16], it was found that Pt(II) complexes such as [Pt(diimine)(*N,N*-di(n-butyl)-*N'*-aroylthioureato)]PF_6 also self–associate in pure acetonitrile solution to form at least dimeric aggregates. It was thus no surprise to discover that the water soluble Pt(II) complexes, [Pt(diimine)H_2L]$^+A^-$ (where A^- = Cl^-, Br^-, ClO_4^-) studied in this work, also show a significant self-association in aqueous solution.

Studies were undertaken in an attempt to understand the self association behaviour of [Pt(diimine)H_2L]$^+A^-$ complexes, specifically the following factors were examined:

- The effect of complex concentration on the ^1H chemical shifts was investigated. (^1H NMR spectra for each complex were recorded over a concentration range of 10^{-4} to 10^{-2} mol dm^{-3}.)

- From the concentration dependence of the ^1H NMR spectra, "dimerisation" constants K^D for each [Pt(diimine)(*N,N*-di(2-hydroxyethyl)-*N'*-benzoyl-thioureato)]$^+A^-$ complex was estimated using the method of Horman and Dreux.

- Electrospray Ionization Mass Spectra (*ESI-MS*) for the platinum complexes were obtained to verify the existence of 'aggregate' species.

- Transmission electron microscopy (TEM) showed convincing images of supramolecular structures formed by these [Pt(diimine)(*N,N*-di(2-hydroxyethyl)-*N'*-benzoyl-thioureato)]$^+A^-$ complexes from aqueous solution.

3.1.1 Concentration Dependence and Estimation of Aggregation Constants

The concentration dependence of the chemical shifts of the diimine protons indicate extensive self-association of [Pt(diimine)(*N,N*-di(2-hydroxyethyl)-*N'*-benzoylthioureato)]$^+$ A^- complexes in aqueous solution. In view of the difficulties associated with characterising higher order aggregates, it was convenient to study the process of aggregation on the assumptions that initially only dimers are formed in dilute solutions.

We adopted the method developed by Horman and Dreux[17] for the estimation of dimerisation constants using the change in proton chemical shifts.

The dimerisation process of [Pt(diimine)(*N,N*-di(2-hydroxyethyl)-*N'*-benzoylthio-ureato)]$^+$ A^- complexes can be written as

$$2\,P \rightleftharpoons P_2 \qquad (1)$$

Where P = [Pt(diimine)H_2L]$^+A^-$

$$K^D = [P_2] / [P] \qquad (2)$$

If $[P]_0$ is the nominal concentration of P in solution, the equation can be expressed as

$$K^D = [P_2] / ([P]_0 - 2[P_2])^2 \qquad (3)$$

Where $[P_2]$ is the concentration of the dimer.
Equation (3) can be rearranged to give

$$1 / (2K^D [P]_0) = 2[P_2] / [P]_0 + [P]_0 / 2[P_2] - 2 \qquad (4)$$

If replace 2 [P_2] / [P]$_0$ by x, the fraction of P present as P_2, and replace 1 / (2 K^D [P]$_0$) by y, the resulting equation would be a hyperbola:

$$y = x + 1/x - 2 \qquad (5)$$

Therefore for a given y_i, the equation satisfies 2 x_i values : x_i and x_i^{-1} . The value of x_i for which $0 < x_i < 1$ is given by

$$x_i = (1 + y_i/2) - [(1 + y_i/2)^2 - 1]^{1/2} \qquad (6)$$

The fraction x_i is related to the measured chemical shift δ_i through the equation

$$x_i = (\delta_0 - \delta_i) / (\delta_0 - \delta_d) \qquad (7)$$

Where δ_0 = chemical shift of monomer and δ_d = chemical shift of dimer
Equation (7) can be rearranged to

$$\delta_i = \delta_0 - x_i (\delta_0 - \delta_d) \qquad (8)$$

This is the equation of a straight line relating δ_i to x_i , with slope – (δ_0 - δ_d) and intercept δ_0. For any given value of K^D, a set of x_i values corresponding to the different [P_i]$_0$ concentration in the set of experimental solutions of P can be calculated and plotted against the measured δ_i . The optimum K^D value is obtained where δ_i vs. x_i gives the best straight line.

3.1.2 Electrospray Ionization Mass Spectroscopy

Until recently only low molecular weight, volatile compounds were amenable to analysis by conventional mass spectrometric methods. Most larger species simply could not be promoted into the gas phase without substantial degradation and/or fragmentation. The characteristic feature of electrospray ionization (ESI) that distinguishes it from other

ionization techniques, is that it generally imparts multiple charges to larger water soluble analyte molecules, and the extent of multiple charging increases in approximate proportion with molecular weight. The resulting highly charged molecular ions exhibit little or no fragmentation resulting in ions with m/z value within the range of mass spectrometer, typically ≤ 4000 amu.

The ionization process in ESI is also "gentle" compared to thermal desorption or chemical ionization.[18] The electrospray mass spectrometry (ESI-MS) has been used to study compounds including proteins, DNA, synthetic polymers and inorganic transition metal complexes. Thus ESI-MS provides a gentle ionization that could produce intact ions from thermally labile molecules and noncovalent complexes.

The schematic representation of an electrospray source is shown in Fig. 3.4. The electrospray capillary consists of a small i.d. metal or glass capillary biased at ± 1-5 kV (+ve potential for cations, -ve potential for anions) relative to the desolvating capillary. A desolvation capillary often is added to expedite desolvation of the highly charged droplets generated in the electrospray plume. Glass inlet capillaries are emplyed widely in conjunction with a countercurrent flow of heated, dry nitrogen to enhance the rate of droplet desolvation and prevent large amounts of material from entering the spectrometer. A series of skimmer cones are used to transmit as many ions from the sample as possible to the mass decreasing the pressure in each subsequent vacuum stage of the chamber. An electrical bias on the skimmer cones serves to focus the ion beam and defines the average kinetic energy of the ion beam. If a sufficient potential difference is applied between the low pressure side of the desolvating capillary and the first skimmer cone, ions can be "heated" by high energy collisions with gas molecules to assist ion desolvation. Under appropriate conditions, ion fragmentation also will occur. Ion optics are the essential part of the electrospray ion sources because the ion lenses can enhance the ion transmission from the source to the mass analyser by focusing the ion beam into the mass spectrometer.

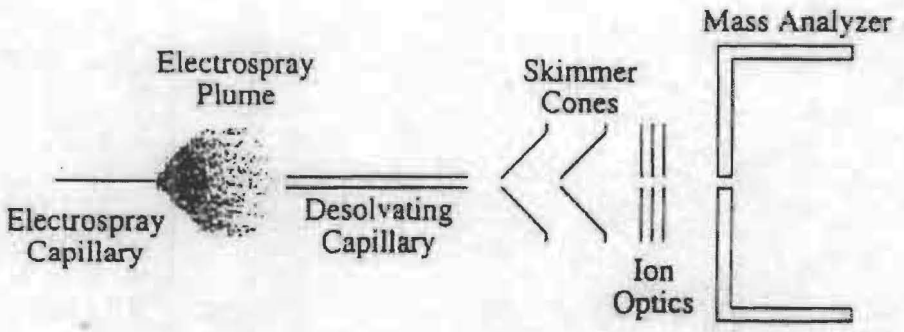

Fig. 3.4 A schematic representation of an electrospray source.

3.1.3 Nature of Self-Association: An Electrostatic Model

Hunter and Sanders[11] have proposed a model to explain the geometrical requirements for interactions between two π systems. They suggest that the geometry of the interaction is contributed by electrostatic interactions, while van der Waals interactions and solvophobic effects make the major contribution to the magnitude of the observed interaction.

The energy of interaction between two molecules can be represented as:

$$E_{\text{total}} = E_{\text{electrostatic}} + E_{\text{induction}} + E_{\text{dispersion}} + E_{\text{repulsion}}$$

The major contributions to the interaction energy com from the electrostatic and van der Waal's components. The energy of interaction between two molecules in solution includes association of the two molecules and displacement of solvent. The apparent energy of interaction between two molecules in solution includes association of the two molecules and displacement of solvent. In nonpolar organic solvents, the electrostatic interactions with the solvent will be negligible and so the dominant electrostatic

interaction will come from the association energy. Both the association and desolvation energies are likely to be associated with significant van der Waals interactions.

For crystals, the van der Waals interaction between molecules is roughly proportional to the area of π-overlap. In solution, however, solvent lowers the contribution of the van der Waals interactions to the total π-stacking energy. While van der Waals interactions can make some contribution to the magnitude of the π-π interaction, they cannot be the force which controls the experimentally observed geometry of interaction. We rarely see structures exist with maximum π-overlap, a cofacial arrangement with no offset. Therefore there must be a large electrostatic barrier to π-overlap which dominates the geometry of interaction. By estimating the electrostatic energy for the interacting systems and the van der Waals energies, the geometry and a quantitative value of the π-π interaction can be predicted.

A simple model of a π-system is illustrated in Fig.3.5. It consists of a positively charged σ-framework sandwiched between the two negatively charged π-electron clouds. It is not difficult to see that the repulsion would be dominant for the two closet approaching π-clouds.

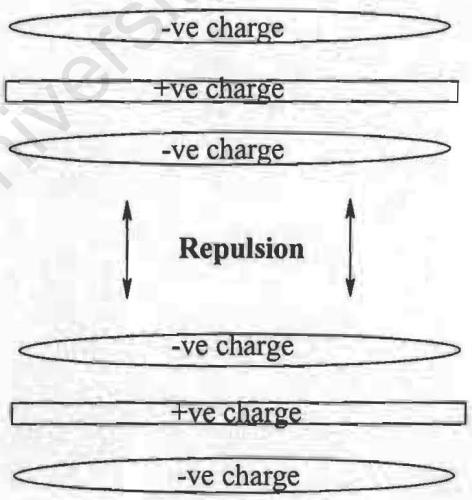

Fig. 3.5 The interaction between two face-to-face π-system.

Hunter and Sanders use a set of point charges to represent the electrostatic charge distribution of the molecules and calculate the elctrostatic interaction as the sum of the charge-charge interactions between two π-systems.[11] In their studies on porphyrin-porphyrin interactions, it was found that the optimum geometry for this system is when the pyrrole ring of one porphyrin directly above the π-cavity of one porphyrin with the π-electrons of the pyrrole ring immediately above (Fig. 3.6). This arrangement minimizes π-π repulsion and at the same time maximizes attraction between the σ-framework. When a metal is included into the system, the large positive charge in the central cavity of the porphyrin π-system leads to a favourable interaction with the π-electrons of the pyrrole of the other porphyrin.

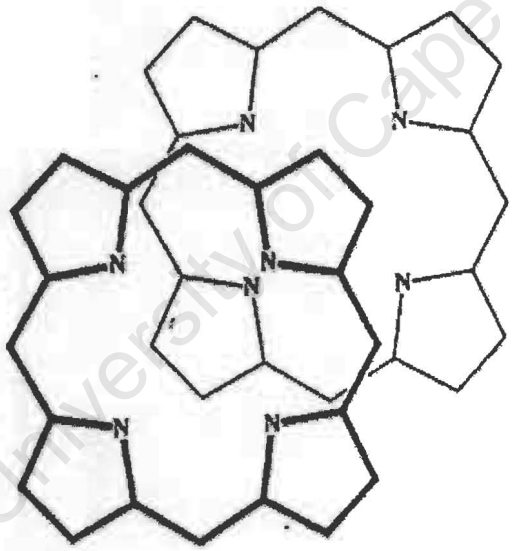

Fig. 3.6 The optinum geometry for the porphyrin-porphyrin interaction predicted.

For a nonpolarised π-system, π-π repulsion dominates in a face-to-face π-stacked geometry, therefore two types of preferred geometry observed are generally an edge-on relationship and a n offset π-stacked geometry since they have favourable π-σ attraction.

3.2 EXPERIMENTAL

3.2.1 ^{1}H NMR Concentration Dependence Study

^{1}H NMR concentration dependence experiments of [Pt(bipy)H_2L]Cl, [Pt(diMebipy)-H_2L]Cl, [Pt(diMebipy)H_2L]Br, [Pt(di-*tert*-butylbipy)H_2L]Cl, [Pt(phen)H_2L]Cl were carried out in 50% mixture of acetonitrile-d_3 and D_2O. For the solvent dependence study, the composition of solvent was varied from 20% to 60% of acetonitrile-d_3/D_2O.

A relatively concentrated solution (approximately 10^{-2} M) of each complex was prepared by weighing out an accurate mass of the complex and dissolving it in a measured volume of acetonitrile-d_3/D_2O mixture (typically 0,7 ml). 50µl aliquots of the more concentrated solution were transferred using a micropipette into the initial NMR tube. The ^{1}H NMR spectrum was recorded at 30°C after each addition of the concentrated solution.

3.2.2 ESI-Mass Spectroscopy

The complexes, [Pt(bipy)H_2L]Cl, [Pt(bipy)H_2L]Br, [Pt(diMebipy)H_2L]Cl, [Pt(diMebipy)-H_2L]Br, [Pt(diMebipy)-H_2L]ClO_4 and [Pt(di-*tert*-butylbipy)H_2L]Cl (3mg each) were dissolved in 50% (v/v) mixture of acetonitrile and water. 10µl of each solution was injected using acetonitrile/water, at 20 µl/minute, as carrier solvent. The carrier solvent was delivered by a LKB/Pharmacia 2249 gradient pump and the sample was injected through a Rheodyne injection valve. The Pt(II) solution was electrospray ionized in the positive mode using a Micromass (Manchester, UK) Quattro triple quadropole mass spectrometer.

3.2.3 Transmission Electron Microscopy

This study was undertaken by the Electron Microscope Unit at the University of Cape Town. Carbon coated copper grids were floated on 20 µl droplets of [Pt(diimine)H_2L]Cl samples for 10 minutes. Thereafter excess sample was removed by blotting with filter paper. The grids were then floated on a negative stain (2% uranyl acetate) for two minutes prior to viewing with a JEM 200CX transmission electron microscope (JEOL, Tokyo, Japan).

3.3 RESULTS AND DISCUSSION

3.3.1 ^{1}H NMR Spectroscopy

The proton NMR spectra of [Pt(bipy)H_2L]Cl complex in D_2O and 50% (v/v) mixture of D_2O and acetonitrile-d_3 are shown in Fig. 3.7. The resonances in the spectrum of the complex in pure D_2O are extremely broad whilst these in the 50% (v/v) of acetonitrile and water are quite sharp. This suggests that the complex aggregates in water to a larger extent than in the mixture of acetonitrile and water. A normal proton NMR spectrum gives sharp peaks because small molecules tumble rapidly in solution, so that magnetic energy exchange with the "lattice" is inefficient which leads to relatively long T_1 and T_2 times. When the molecular weight increases, the rate of tumbling decreases, so that T_1 and T_2 became shorter. Since $\nu_{1/2} \propto 1/\pi T_2$, the smaller T_2, the larger $\nu_{1/2}$ and therefore the peaks are broad. Large "aggregates" or "polymers" in solution show relatively slow molecules tumbling resulting in short T_2 times, hence their $\nu_{1/2}$ is very large and broad resonance is observed.

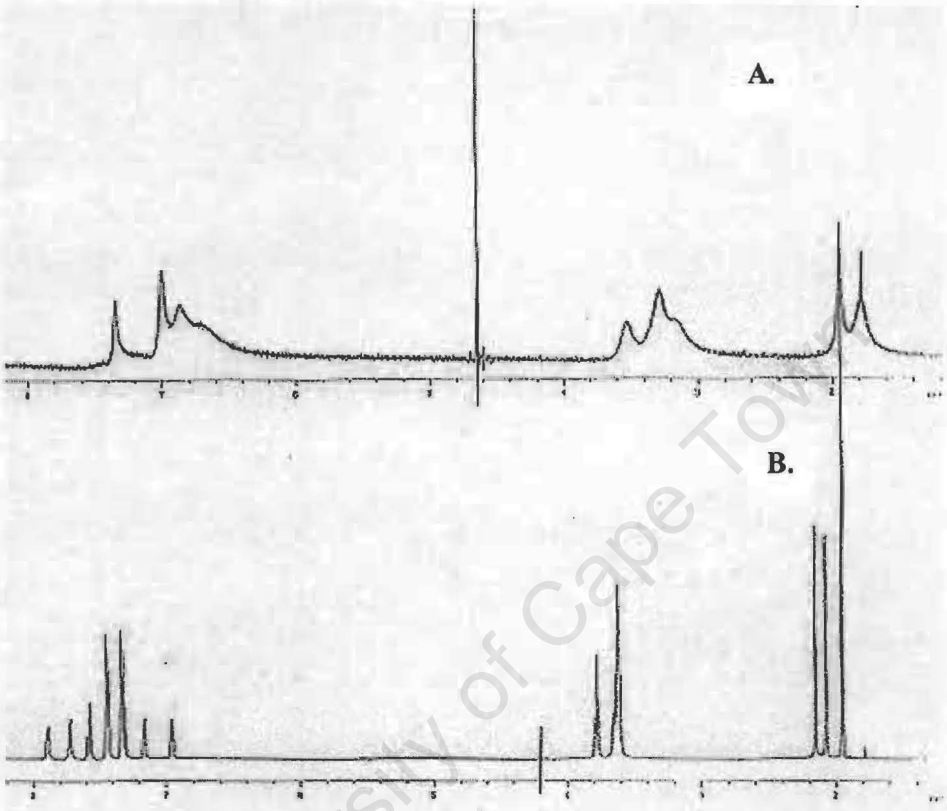

Fig 3.7 The ^{1}H NMR spectra of [Pt(diMebipy)H_2L]Cl in **A**. D_2O and **B**. 50% (v/v) CD_3CN/D_2O.

The ^{1}H NMR spectrum of [Pt(bipy)H_2L]Cl as a freshly made sample in 50% (v/v) mixture of CD_3CN and D_2O also showed some small 'spurious' peaks which were originally thought to be an impurity in the sample. The peaks in the spectrum were also rather broad. However, after approximately 6.5 hours, the ^{1}H NMR spectrum of same sample was again recorded showing that not only that all peaks were sharper, but that the ' spurious' peaks had also disappeared (Fig. 3.8)

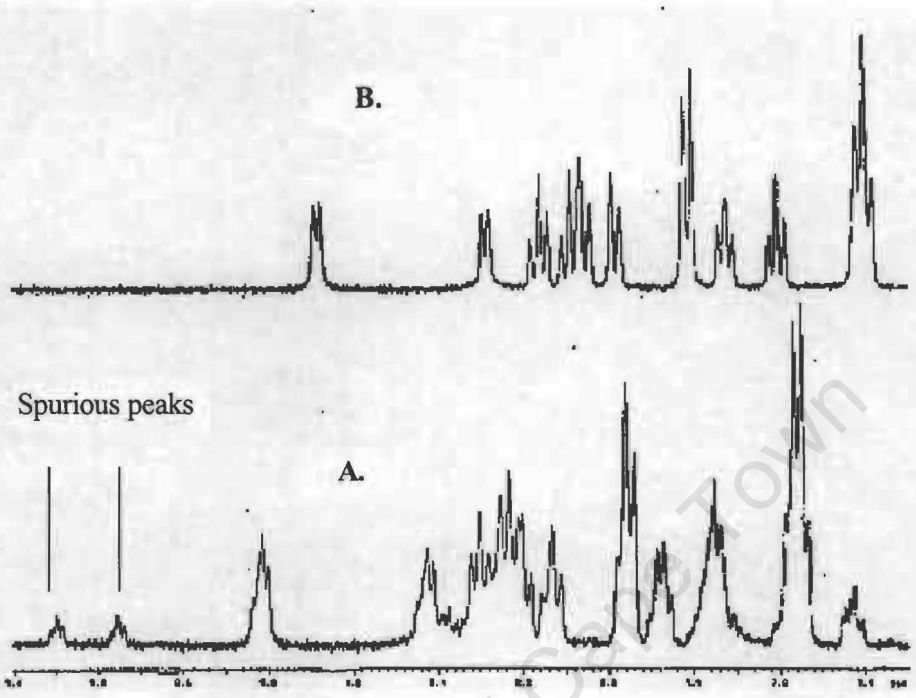

Fig. 3.8 The ^{1}H NMR spectra for the aromatic region of [Pt(bipy)H_2L]Cl complex in 50% CD_3CN/D_2O taken when A. sample was dissolved freshly. B. sample was left to stand for a futher 6.5 hours. (arrows showing spurious peaks)

This observation suggested that the distribution of complexes was not completely homogeneous when it was dissolved freshly in the 50% (v/v) acetonitrile and water mixture. Evidently, the redistribution/disaggregation of [Pt(diimine)H_2L]Cl complexes takes a surprisingly long time to reach an equilibrium state in which a truly homogeneous solution is obtained. A time-arrayed experiment was thus carried out, showing that the spectrum of freshly made samples of [Pt(bipy)H_2L]Cl contained the additional broad peaks. After approximately 40 minutes, all peaks became much sharper and the additional peaks had completely disappeared (Fig. 3.9). It appears that the [Pt(bipy)H_2L]Cl complex takes about 40 minutes to reach an equilibrium state in 50% (v/v) acetonitrile and water

mixture. All other experiments were thus performed after the solution had been allowed to reach equilibrium.

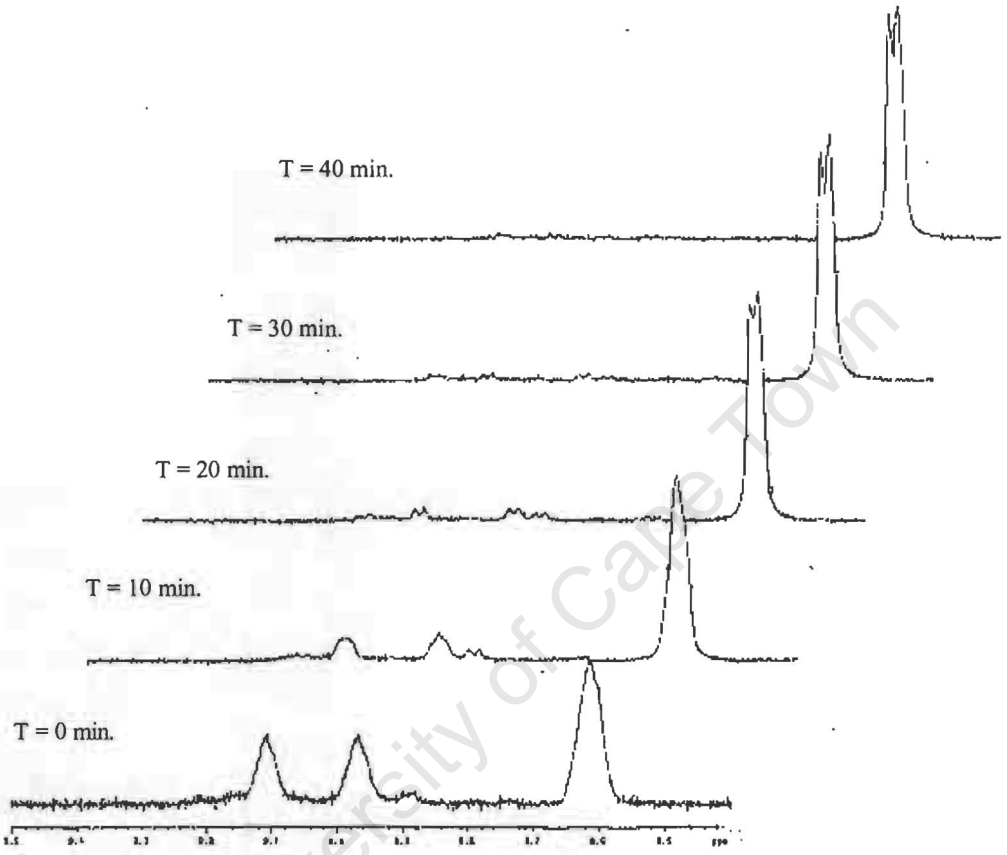

Fig. 3.9 A Section of ^{1}H NMR spectra for [Pt(bipy)H_2L]Cl complex at 10 minutes time intervals after making up the solution.

A comparitive study was carried out in 50% (v/v) mixture of DMSO-d_6 and water. The ^{1}H NMR spectra showed no broadening or additional peaks from the freshly made sample. This observation suggested that [Pt(bipy)H_2L]Cl was well solvated in this solvent mixture and an equilibrium state is reached soon after the addition of solvent.

3.3.2 Concentration Dependence Study by ^{1}H NMR

Concentration dependence studies were carried out to determine degree of intermolecular self-association of the [Pt(diimine)H_2L]A (A = Cl^-, Br^-, ClO_4^-) complexes by monitoring the chemical shifts of the various protons. An upfield shift of proton chemical shifts with increasing concentration was observed in all the complexes studied. This shift trend is well-known for the aromatic systems and it can be attributed to anisotropic shielding effects of one complex molecule upon its neighbour. Due to the mobile π electrons, a large diamagnetic current is induced in the plane of the ring by an external, perpendicular to the external magnetic field B_0. This ring current gives rise to a smaller, secondary magnetic field which can be approximated by the field of a dipole opposed to B_0 and centred in the middle of the ring. As the concentration of the complex increases and self-association takes place, the average distance between the aromatic rings decreases. Moreover, the upfield shifts indicate face-to-face offset centre-to-edge association. As a result, the protons of one aromatic ring are increasingly exposed to the secondary magnetic field produced by the ring current of an adjacent molecule.

The ^{1}H NMR chemical shift changes for [Pt(bipy)H_2L]Cl are given in Table 3.1 (over the specified concentration range). The results indicated that the diimine protons of the mixed-ligand platinum(II) complexes exhibited the most significant upfield resonance shifts with increasing concentration of the complex in 50% (v/v) of acetonitrile-d_3 and D_2O. The total magnitude of the concentration induced shifts experienced by these protons ranged from 0.113 ppm for $H_{4''}$ to 0.389 for H_6.

Conc. mol dm^{-3}	^{1}H NMR Chemical Shifts (ppm)					
	H_3	$H_{3'}$	H_4	$H_{4'}$	H_5	$H_{5'}$
4.37x10^{-3} *a*	8.06	7.99	8.16	8.09	7.72	7.41
2.50x10^{-2} *b*	7.75	7.68	7.93	7.88	7.50	7.19
Δδ	0.31	0.31	0.23	0.21	0.22	0.22
	H_6	$H_{6'}$	$H_{2''}/H_{6''}$	$H_{3''}/H_{5''}$	$H_{4''}$	
4.37x10^{-3} *a*	8.68	8.28	7.80	7.39	7.59	
2.50x10^{-2} *b*	8.29	7.91	7.49	7.24	7.47	
Δδ	0.39	0.37	0.32	0.14	0.11	

a: $C_{min.}$ = the lowest concentration at which ^1H chemical shift data is measured.

b: $C_{max.}$ = the highest concentration at which ^1H chemical shift data is measured.

$\Delta\delta$ chemical shift difference $\delta(C_{min}) - \delta(C_{max})$

Table 3.1 ^{1}H NMR Chemical shift data of [Pt(bipy)H$_2$L]Cl over the concentration range of 4.37x10^{-3} to 2.50x10^{-2} mol dm^{-3}.

It was observed in all [Pt(diimine)H$_2$L]Cl complexes that the magnitude of the chemical shift difference for the diimine protons varies roughly with the distance of the protons from the platinum atom. Thus the protons H_3, $H_{3'}$, H_6 and $H_{6'}$ of the bipyridyl ring experienced most shifts with the change in concentration while protons H_4, $H_{4'}$, H_5, $H_{5'}$ experienced the least. Furthermore, the proton chemical shifts of the diimine ligands undergo greater changes than the phenyl ring on the *N, N*-(dihydroxyethyl)-*N'*-benzoylthiourea moiety of the complexes. Hence only the diimine protons of the complexes are used for the investigation of concentration effects on the proton resonance shifts.

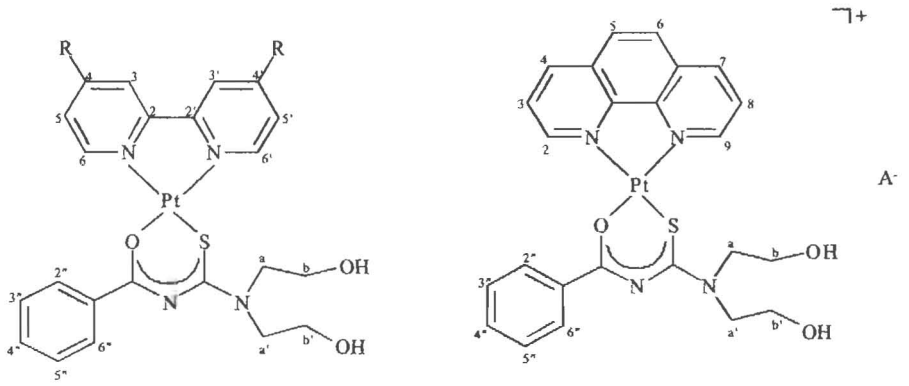

R= H, CH_3, *tert*-butyl ; A= Cl, Br, ClO_3

Fig. 3.10 Diagram showing the $[Pt(diimine)H_2L]^+A^-$ synthesised and their numbering used in characterisation

The concentration dependence can be represented by plotting chemical shift for the diimine protons *vs.* concentration, as illustrated in Figure 3.11 – 3.15 for $[Pt(bipy)H_2L]Cl$ $[Pt(diMebipy)H_2L]Cl$, $[Pt(diMebipy)H_2L]Br$, $[Pt(di\text{-}tert\text{-}butylbipy)H_2L]Cl$ and $[Pt(phen)\text{-}H_2L]Cl$. Table 3.2 summarizes the upfield chemical shift trends for all diimine protons with increased concentration.

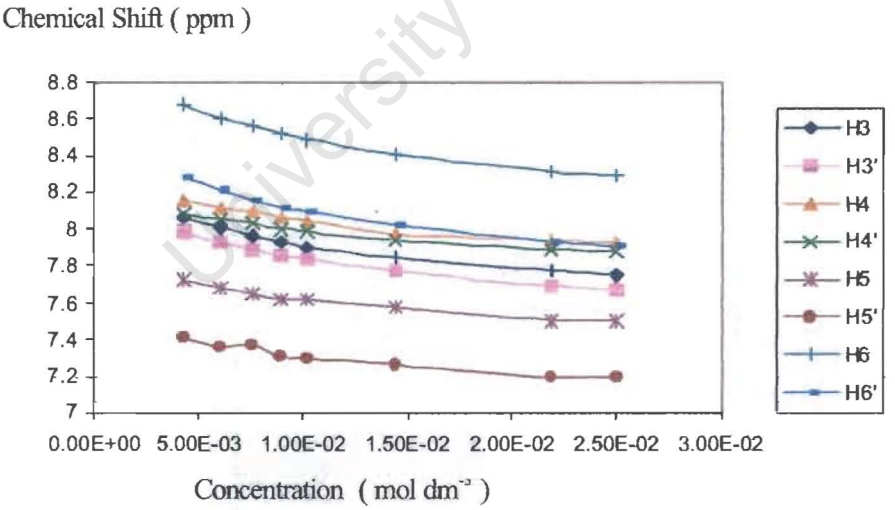

Fig. 3.11 Graphical representation of chemical shift (ppm) *vs.* concentration (mol dm^{-3}) for $[Pt(bipy)H_2L]^+Cl^-$ in 50% (v/v) mixture of D_2O/CD_3CN at 30°C, illustrating the upfield chemical shift of the diimine proton resonances.

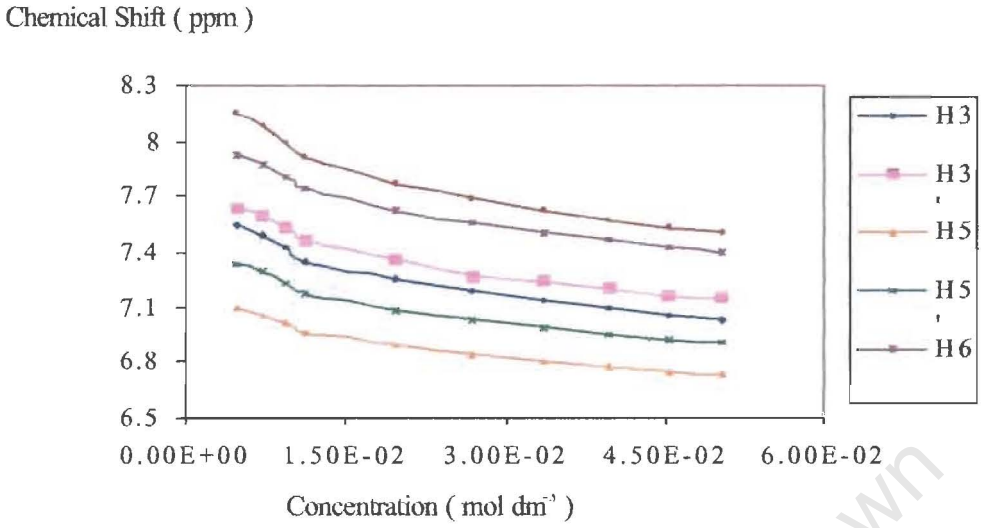

Fig. 3.12 Graphical representation of chemical shift (ppm) *vs.* concentration (mol dm^{-3}) for $[Pt(diMebipy)H_2L]^+Cl^-$ in 50% (v/v) mixture of D_2O/CD_3CN at 30°C.

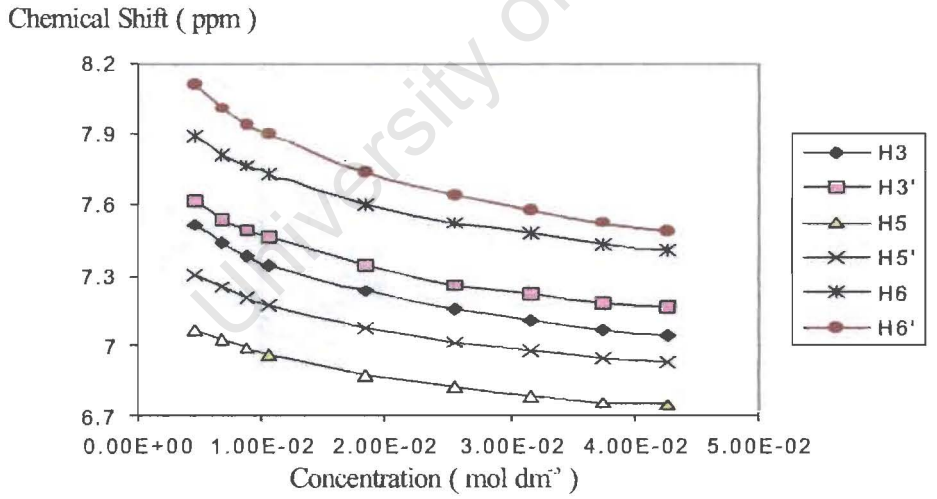

Fig. 3.13 Graphical representation of chemical shift (ppm) *vs.* concentration (mol dm^{-3}) for $[Pt(diMebipy)H_2L]^+Br^-$ in 50% (v/v) mixture of D_2O/CD_3CN at 30°C.

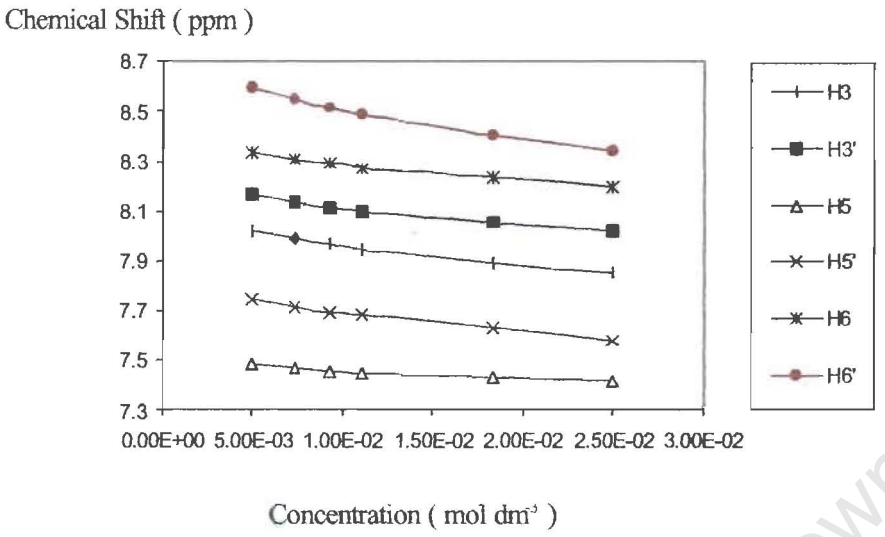

Fig. 3.14 Graphical representation of chemical shift (ppm) *vs.* concentration (mol dm^{-3}) for $[Pt(di\text{-}tert\text{-}butylbipy)H_2L]^+Cl^-$ in 50% (v/v) mixture of D_2O/CD_3CN at 30°C.

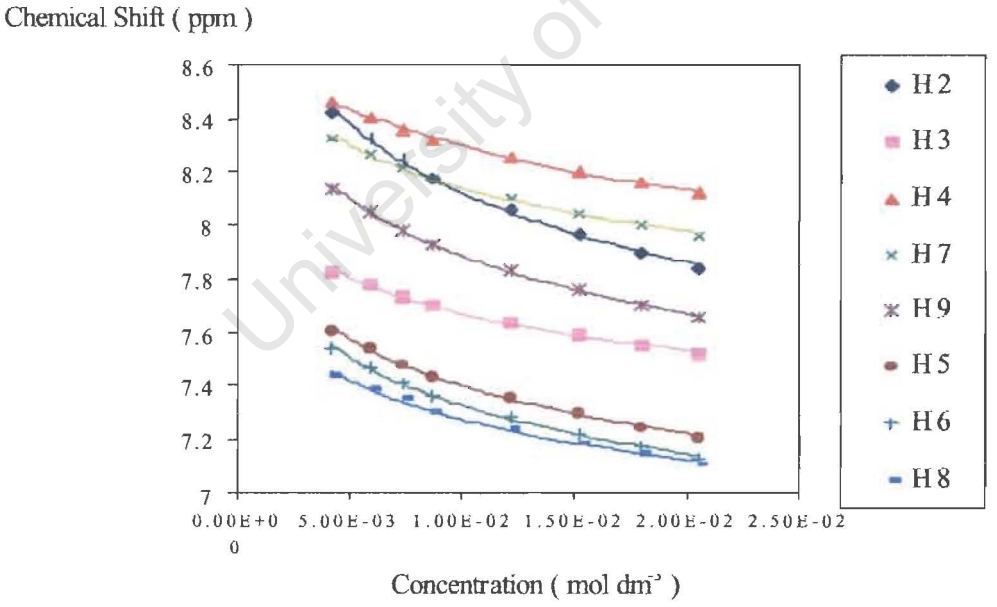

Fig. 3.15 Graphical representation of chemical shift (ppm) *vs.* concentration (mol dm^{-3}) for $[Pt(phen)H_2L]^+Cl^-$ in 50% (v/v) mixture of D_2O/CD_3CN at 30°C.

Complex	^{1}H NMR Chemical Shifts (ppm)							
	H_2	H_3	H_4	H_5	H_6	H_7	H_8	H_9
[Pt(phen)H_2L]Cl Δδ [a]4.22×10^{-3} – [b]2.05×10^{-2} M	0.584	0.310	0.337	0.400	0.408	0.362	0.331	0.486
	H_3	$H_{3'}$	H_4	$H_{4'}$	H_5	$H_{5'}$	H_6	$H_{6'}$
[Pt(bipy)H_2L]Cl Δδ [a]4.37×10^{-3} - [b]2.50×10^{-2} M	0.313	0.313	0.233	0.208	0.224	0.219	0.389	0.368
[Pt(diMebipy)H_2L]Cl Δδ [a]4.82×10^{-3} - [b]2.70×10^{-2} M	0.361	0.380	-	-	0.247	0.299	0.368	0.454
[Pt(di-tert-butylbipy)H_2L]Cl Δδ [a]5.04×10^{-3} - [b]2.50×10^{-2} M	0.168	0.141	-	-	0.066	0.159	0.138	0.252

a: lowest concentration at which ^{1}H chemical shift data is measured.
b: highest concentration at which ^{1}H chemical shift data is measured.
Δδ = chemical shift difference δ(lowest concentration) - δ(highest concentration).
- : not applicable for substituted bipyridyl ligands.

Table 3.2 ^{1}H NMR chemical shift data showing the overall upfield chemical shifts with increased concentration in 50% CD_3CN/D_2O.

3.3.3 Calculation of Dimerisation Constant K^D

In this study, we initially assumed that only dimers formed in 50% (v/v) D_2O/CD_3CN, due to the difficulties associated with characterising higher order aggregates. By adopting a method developed by Horman and Dreux[17] for determination of "dimerisation" constants (K^D), it can be concluded that if the data fits the dimerisation model well, then mostly dimers are found in the solution. Conversely, if the data does not fit this model, it is reasonable to assume higher order species such as tetramers etc.exist in the solution.

The dimerisation of Pt(II) complexes can be best represented as follows:

$$2\ [Pt(diimine)H_2L]Cl \underset{}{\overset{K^D}{\rightleftharpoons}} \{[Pt(diimine)H_2L]_2\}^{2+}\ (Cl^-)_2$$

and therefore K^D can be defined as

$$K^D = \frac{\{[Pt(diimine)H_2L]_2\}^{2+}\ (Cl^-)_2}{\{[Pt(diimine)H_2L]Cl\}^2}$$

The chemical shift of a selected proton on the Pt(II) complexes represents a weighted average of that proton's chemical shifts in 2 possible environments – the chemical shift of the monomer and the chemical shift of the dimer. Self-association or dimerisation constants K^D can thus be calculated from the proton chemical shifts. For this calculation, a measurement of δ_0 is required as a reference to determine the complexation-induced chemical shift displacements, $(\delta_0 - \delta_i)$. The direct measurement for this δ_0 is not possible for dimer formation since even at the lowest concentration, a small quantity of dimer will always be present. In some NMR studies of dimerisation, δ_0 has been determined by manual extrapolation of δi *vs.* $[C_i]_0$ curves to zero concentration. Horman and Dreux employed a new method where the optimum δ_0, K^D and δ_∞ values were determined simultaneously. When the proton chemical shift values δi are plotted against x_i, the

optimum K^D is defined as that value which give the best straight line as described in equation $\delta_i = \delta_0 - x_i\ (\delta_0 - \delta_\infty)$.

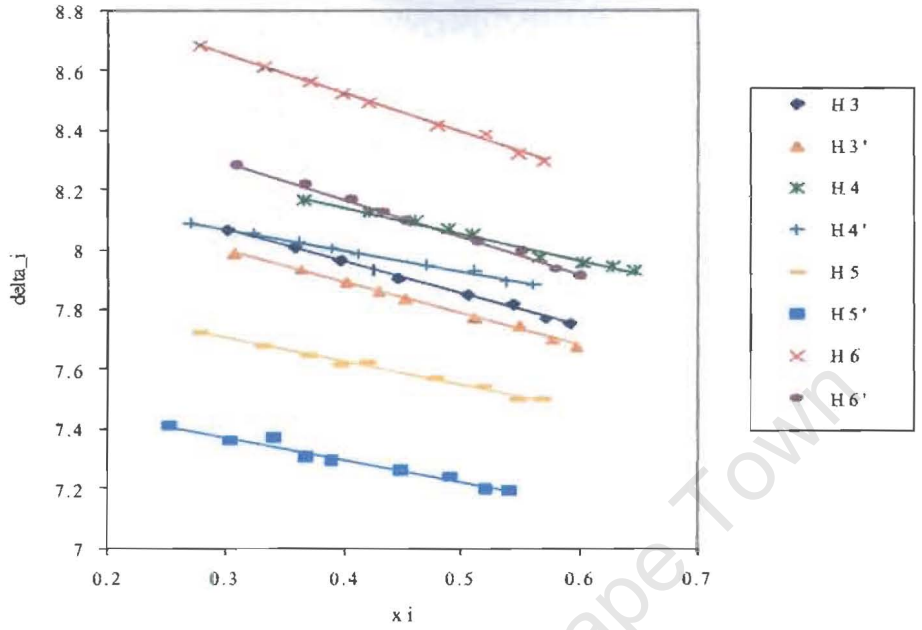

Fig 3.16 Graph showing the best fit straight line for the protons chemical shifts of [Pt(bipy)H_2L]Cl complex after the estimation of the optimum K^D value.

The calculated dimerisation constants for [Pt(bipy)H_2L]Cl, [Pt(diMebipy)H_2L]Cl, [Pt(diMebipy)H_2L]Br, [Pt(di-*tert*-butylbipy)H_2L]Cl and [Pt(phen)H_2L]Cl in 50% of D_2O and CD_3CN are given in Table 3.3 – Table 3.7. Optimum values for δ_0 (the intrinsic chemical shift of the monomer) and $(\delta_0 - \delta_\infty)$ are also given together with their lower and upper limits (with 95% confidence limits).

Previous methods employing manual extrapolation of δ_0 values have assumed no error in measuring this quantity and used it as a reference point in determining $(\delta_0 - \delta_i)$ and other parameters. However, Horman and Dreux noticed that there is an average error of 0.06 Hz (maximum error of 0.3 Hz) on the dimerisation of caffeine. These minor errors can induce large errors in K^D, since the K^D value is indirectly proportional to δ_0-δ_∞. The K^D value was also found to be highly dependent on the concentration range and the number of data points acquired in the experiment. A larger number of data points and a wider δ_i

range could minimize the error since the error in δ_i would be comparably small. All the experimental solutions were therefore carefully prepared and the comparisons of all different complexes are carried out in a similar concentration range.

Conc. Range Mol dm^{-3}	H	Optimum calculated complex parameters with 95% limits		
		min. $< \delta_0 <$ *max.* ppm	*Min.* $< K^D <$ *max.* $dm^3\ mol^{-1}$	*min.* $< \delta_0 - \delta_\infty <$ *max.* ppm
	3	8.226 – 8.233 – 8.240	21.54 – 22.94 – 24.37	1.356 – 1.375 – 1.396
4.37×10^{-3}	3'	8.148 – 8.155 – 8.162	20.24 – 21.62 – 23.02	1.372 – 1.392 – 1.416
-	4	8.276 – 8.281 – 8.286	17.56 – 18.79 – 20.06	1.086 – 1.106 – 1.129
2.50×10^{-2}	4'	8.190 – 8.195 – 8.200	17.64 – 19.00 – 20.39	0.961 – 0.980 – 1.001
	6	8.896 – 8.904 – 8.912	19.98 – 21.20 – 22.44	1.726 – 1.750 – 1.778
	6'	8.514 – 8.522 – 8.529	24.70 – 25.99 – 27.30	1.560 – 1.575 – 1.591

Table 3.3 The complex parameters for the formation of $[Pt(bipy)H_2L]Cl$ dimers in 50% CD_3CN/D_2O at 30°C.

Conc. Range Mol dm^{-3}	H	Optimum calculated complex parameters with 95% limits		
		min. $< \delta_0 <$ *max.* ppm	*min.* $< K^D <$ *max.* $dm^3\ mol^{-1}$	*min.* $< \delta_0 - \delta_\infty <$ *max.* ppm
	3	7.796 – 7.832 – 7.868	28.75 – 34.65 – 41.02	1.343 – 1.344 – 1.353
	3'	7.894 – 7.925 – 7.958	28.17 – 33.43 – 39.08	1.329 – 1.330 – 1.343
4.82×10^{-3}	5	7.237 – 7.256 – 7.274	19.84 – 23.58 – 27.59	0.960 – 0.976 – 0.998
-	5'	7.524 – 7.547 – 7.570	24.46 – 28.80 – 33.44	1.129 – 1.139 – 1.155
2.70×10^{-2}	6	8.163 – 8.187 – 8.211	24.54 – 28.16 – 31.99	1.389 – 1.400 – 1.417
	6'	8.477 – 8.507 – 8.539	28.50 – 32.42 – 36.54	1.724 – 1.727 – 1.740

Table 3.4 The complex parameters for the formation of $[Pt(diMebipy)H_2L]Cl$ dimers in 50% CD_3CN/D_2O at 30°C.

Conc. Range Mol dm^{-3}	H	Optimum calculated complex parameters with 95% limits		
		min. < δ_0 < *max.* ppm	*min.* < K^D < *max.* dm^3 mol^{-1}	*min.* < $\delta_0 - \delta_\infty$ < *max.* ppm
	3	7.764 – 7.774 – 7.783	33.54 – 35.43 – 37.37	1.278 – 1.283 – 1.286
	3'	7.835 – 7.852 – 7.869	28.13 – 31.27 – 34.54	1.261 – 1.269 – 1.282
4.53×10^{-3}	5	7.224 – 7.232 – 7.241	24.96 – 26.84 – 28.77	0.934 – 0.940 – 0.948
-	5'	7.498 – 7.506 – 7.513	29.59 – 31.18 – 32.80	1.063 – 1.068 – 1.071
2.54×10^{-2}	6	8.117 – 8.124 – 8.131	25.99 – 27.03 – 28.08	1.369 – 1.373 – 1.379
	6'	8.419 – 8.427 – 8.435	29.56 – 30.61 – 31.68	1.718 – 1.721 – 1.725

Table 3.5 The complex parameters for the formation of [Pt(diMebipy)H_2L]Br dimers in 50% CD_3CN/D_2O at 30°C.

Conc. Range Mol dm^{-3}	H	Optimum calculated complex parameters with 95% limits		
		min. < δ_0 < *max.* ppm	*min.* < K^D < *max.* dm^3 mol^{-1}	*min.* < $\delta_0 - \delta_\infty$ < *max.* ppm
	3	8.131 – 8.140 – 8.149	21.90 – 25.18 – 28.63	0.660 – 0.673 – 0.693
	3'	8.245 – 8.252 – 8.259	17.60 – 20.63 – 23.83	0.569 – 0.587 – 0.612
5.04×10^{-3}	5	7.550 – 7.561 – 7.572	55.01 – 70.81 – 88.36	0.239 – 0.241 – 0.245
-	5'	7.784 – 7.799 – 7.812	2.169 – 5.50 – 9.42	0.854 – 1.148 – 2.200
2.50×10^{-2}	6	8.424 – 8.431 – 8.438	23.74 – 27.50 – 31.47	0.541 – 0.551 – 0.566
	6'	8.725 – 8.737 – 8.748	13.48 – 15.79 – 18.23	1.078 – 1.122 – 1.182

Table 3.6 The complex parameters for the formation of [Pt(di-*tert*-butylbipy)H_2L]Cl dimers in 50% CD_3CN/D_2O at 30°C.

Conc. Range Mol dm^{-3}	H	Optimum calculated complex parameters with 95% limits		
		min. $< \delta_0 <$ *max.* ppm	*min.* $< K^D <$ *max.* $dm^3\ mol^{-1}$	*min.* $< \delta_0 - \delta_\infty <$ *max.* ppm
4.22×10^{-3} - 2.05×10^{-2}	2	8.829 – 8.848 – 8.866	28.62 – 30.97 – 33.39	2.342 – 2.373 – 2.410
	3	8.016 – 8.024 – 8.032	22.35 – 24.15 – 26.01	1.297 – 1.320 – 1.347
	4	8.678 – 8.687 – 8.695	24.86 – 26.71 – 28.61	1.382 – 1.403 – 1.426
	5	7.867 – 7.879 – 7.892	25.67 – 27.87 – 30.13	1.627 – 1.653 – 1.684
	6	7.805 – 7.817 – 7.829	26.09 – 28.26 – 30.51	1.653 – 1.678 – 1.708
	7	8.560 – 8.571 – 8.581	25.33 – 27.43 – 29.59	1.475 – 1.499 – 1.526
	8	7.622 – 7.639 – 7.655	17.14 – 20.36 – 23.77	1.435 – 1.499 – 1.585
	9	8.500 – 8.514 – 8.529	33.23 – 35.56 – 37.96	1.901 – 1.918 – 1.938

Table 3.7 The complex parameters for the formation of $[Pt(phen)H_2L]Cl$ dimers in 50% CD_3CN/D_2O at 30°C.

Since similar type of complexes $[Pt(diimine)(L\text{-}S,O)]PF_6$ were reported by Lawrence *et al.* to form dimeric structure in acetonitrile, it was expected that complexes $[Pt(diimine)H_2L]Cl$ would also form dimers or higher aggregates in aqueous solution. Dimerisation constant K^D can generally be affected by two important factors: the steric factor and the inductive effect.

In this study, 4,4' dimethylbipy and 4,4' di-*tert*-butylbipy was used to investigate the effect of electron density on the self-association of $[Pt(diimine)H_2L]Cl$ complexes. The dimerisation constants determined are reported in Table 3.8.

Complex	Average K^D
[Pt(phen)H_2L]Cl	27.7± 4.5
[Pt(bipy)H_2L]Cl	21.6 ± 2.7
[Pt(diMebipy)H_2L]Cl	36.4 ± 11.8
[Pt(diMebipy)H_2L]Br	32.3 ± 9.1
[Pt(di-*tert*-butylbipy)H_2L]Cl	22.3 ± 5.2

Table 3.8 Average K^D values calculated from the protons on the diimine moiety of Pt(II) Complexes in 50% (v/v) mixture of acetonitrile-d_3 and D_2O at 30°C.

The experimental results showed that the dimerisation constant for both [Pt(diMebipy)-H_2L]Cl and [Pt(di-*tert*-butylbipy)H_2L]Cl are higher than that of [Pt(bipy)H_2L]Cl. This is highly unexpected since alkyl substitution at 4,4' positions should pose a significant steric hindrance for dimerisation. In reality, an inductive effect of the methyl and *tert*-butyl groups in the diimine seems to counteract the steric effect. The inductive effect of the 4,4' substituted alkyl group enhances the σ bonding arising from lone-pair donation between nitrogen atom on the diimine ligand and the platinum metal. This also allows for increased dπ-pπ back donation of electron density from the filled metal orbitals to the aromatic ring (Fig. 3.17). The platinum atom is therefore left with a large δ+ charge and the π-ring with a δ- charge. The increased electron density on the diimine moiety then resulting in increased dimerisation constants. This coincided with a study on intercalation of 2,2'-bipyridyl platinum(II) complexes with DNA bases where a platinum coordinated 2,2'-bipyridyl complex binds more effectively than the uncoordinated 2,2'-bipyridine ligand.

Although the inductive effect appears to override the steric factor, the effect is still apparent. When comparing the dimerisation constants of [Pt(diMebipy)H_2L]Cl and [Pt(di-*tert*-butylbipy)H_2L]Cl, it seems that the bulky tertiary butyl groups at 4,4' position greatly hinder the formation of dimers. The counter ions have little effect on the self association since the K^D value for bromide complex is not different from the chloride complex.

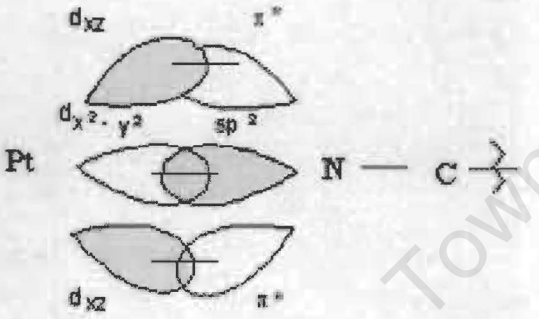

Fig. 3.17 Schematic diagram showing the π-back donation of electron density from platinum to the aromatic ring of the diimine ligand.

The ^{1}H NMR concentration dependence study and confirms the existence of dimer species in 50% mixture of acetonitrile and water. Using the general rules set by the studies of Hunter and Sanders[11], the most favourable geometry is that when the π-electron cloud is being stabilised by the positive metal charge. From this, we can propose possible conformations for the [Pt(diimine)H_2L]$^+$A$^-$ dimers (Fig. 3.18, 3.19). The structures for [Pt(bipy)H_2L]Cl, [Pt(diMebipy)H_2L]Cl and [Pt(di-tert-butylbipy)H_2L]Cl are proposed in which the bipyridyl rings of the two monomers overlap in an offset manner with one of the pyridine ring overlaps the electron deficient Pt metal centre. Since a single set of ^{1}H NMR resonances is observed, it suggests that only an average magnetic environment contributes to the observed resonance shift and the complexes must be fluctuating between the possible conformations. [Pt(phen)H_2L]Cl on the other hand has three possible structures, however, two of which would be less favourable due to the steric hindrance of the extra ring stacking on the *N,N*-dihydroxyethyl-*N'*-benzoylthiourea ligand.

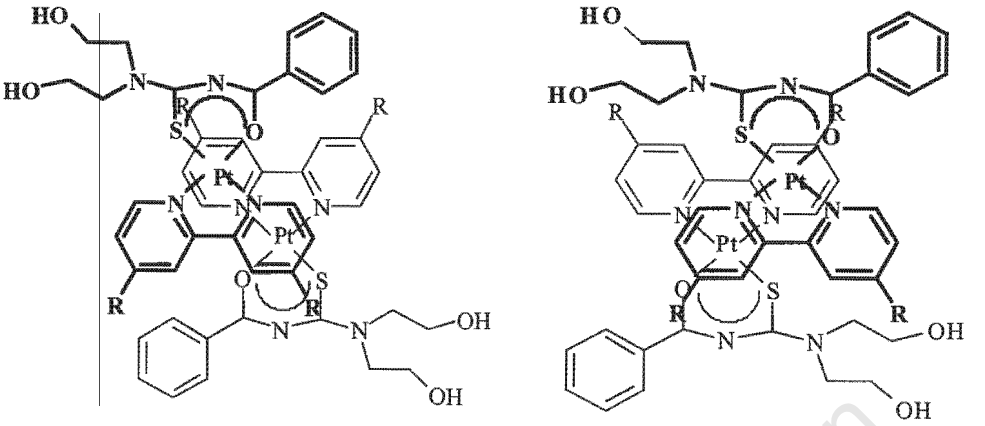

R = H, methyl, *tert*-butyl groups.

Fig 3.18 The proposed dimer structures for $[Pt(bipy)H_2L]^+$, $[Pt(diMebipy)H_2L]^+$ and [Pt (di-*tert*-butylbipy)$H_2L]^+$ complexes.

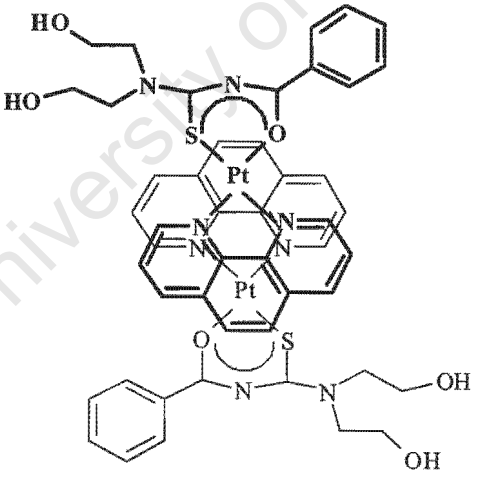

Fig 3.19 The proposed dimer structures for $[Pt(phen)H_2L]^+$. The other two possible structures that are similar to $[Pt(bipy)H_2L]^+$ are sterically unfavourable.

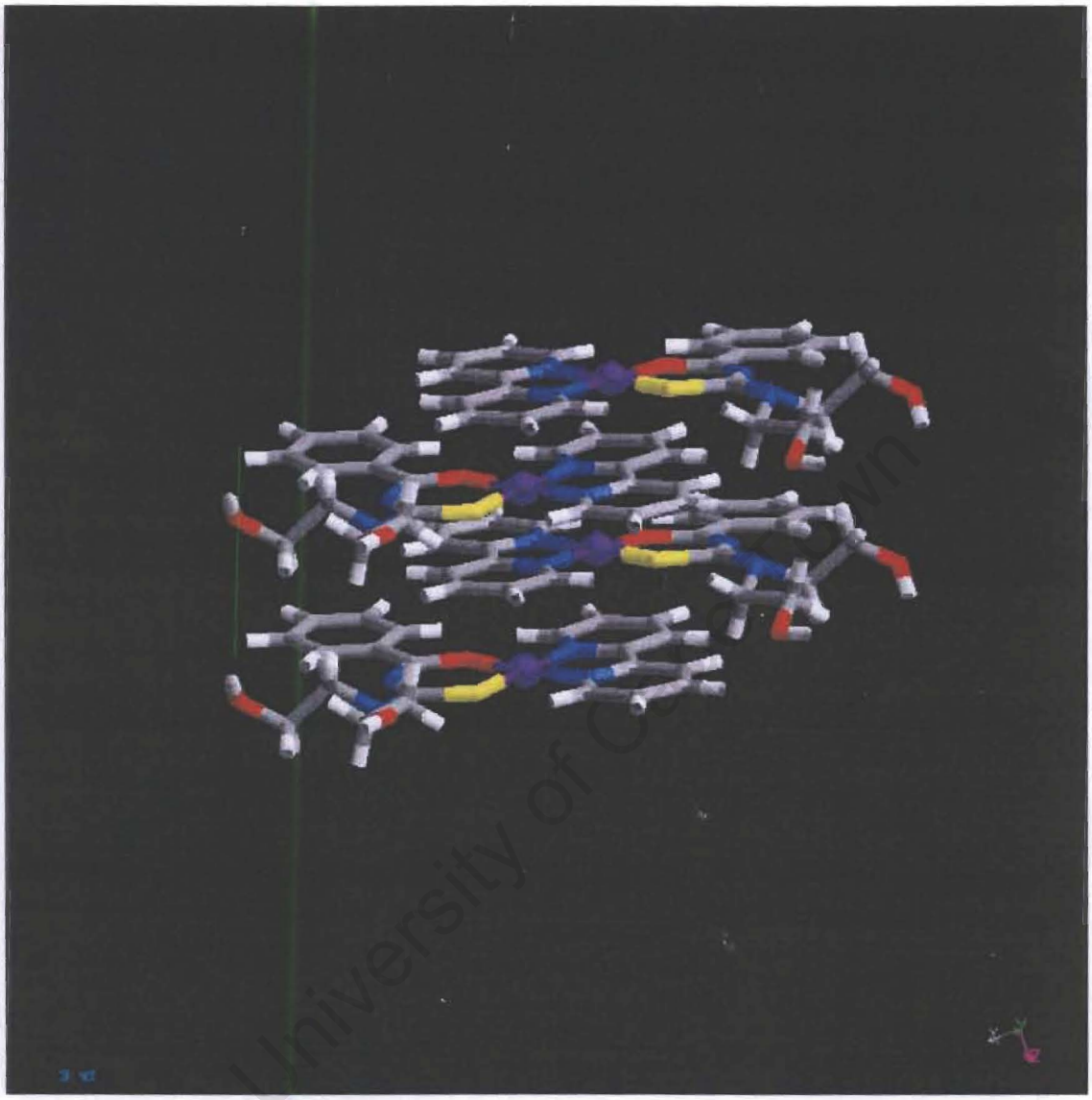

Fig. 3.20 The 3 dimensional representation of the [Pt(bipy)H_2L]Cl self-association.

3.3.4 Effect of Solvent Composition

Experiments were carried out with 40%, 50% and 80% (v/v) mixture of D_2O/CD_3CN to investigate the effect of solvent composition in self association. Since the chloride complexes are insoluble in pure acetonitrile-d_3, comparisons will be made with their corresponding PF_6 salts.

The calculated dimerisation constants for [Pt(diMebipy)H_2L]Cl, in 40%, 50% and 80% (v/v) mixture of D_2O to CD_3CN are given in Table 3.9 – Table 3.11. Optimum values for δ_0 (the intrinsic chemical shift of the monomer) and ($\delta_0 - \delta_\infty$) are also given together with their lower and upper limits (with 95% confidence limits).

Conc. Range mol dm^{-3}	H	Optimum calculated complex parameters with 95% limits		
		min. $< \delta_0 <$ *max.* ppm	*min.* $< K^D <$ *max.* $dm^3\ mol^{-1}$	*min.* $< \delta_0 - \delta_\infty <$ *max.* ppm
	3	7.656 – 7.700 – 7.744	2.94 – 6.54 – 10.91	1.867 – 2.308 – 3.671
	3'	7.748 – 7.791 – 7.834	2.33 – 5.74 – 9.93	1.918 – 2.446 – 4.284
$4.82x10^{-3}$	5	7.158 – 7.187 – 7.215	1.61 – 4.64 – 8.38	1.438 – 1.926 – 3.971
-	5'	7.411 – 7.447 – 7.484	2.33 – 5.80 – 10.06	1.589 – 2.027 – 3.572
$3.96x10^{-2}$	6	8.047 – 8.088 – 8.129	3.39 – 6.68 – 10.59	1.966 – 2.381 – 3.483
	6'	8.301 – 8.356 – 8.411	3.98 – 7.70 – 12.13	2.333 – 2.772 – 3.912

Table 3.9 The complex parameters for the formation of [Pt(diMebipy)H_2L]Cl dimers in 40% D_2O/CD_3CN at 30°C.

Conc. Range mol dm^{-3}	H	Optimum calculated complex parameters with 95% limits		
		min. < δ_0 < *max.* ppm	*min.* < K^D < *max.* $dm^3\ mol^{-1}$	*min.* < $\delta_0 - \delta_\infty$ < *max.* ppm
	3	7.823 – 7.873 – 7.924	33.83 – 43.65 – 54.54	1.319 – 1.326 – 1.329
	3'	7.875 – 7.917 – 7.960	24.56 – 31.77 – 39.73	1.325 – 1.339 – 1.374
$4.82x10^{-3}$	5	7.250 – 7.275 – 7.301	23.07 – 29.13 – 35.77	0.927 – 0.940 – 0.967
-	5'	7.537 – 7.570 – 7.603	27.45 – 34.40 – 42.02	1.106 – 1.113 – 1.133
$3.98x10^{-2}$	6	8.179 – 8.212 – 8.246	27.43 – 33.14 – 39.30	1.358 – 1.368 – 1.390
	6'	8.493 – 8.536 – 8.578	30.92 – 37.01 – 43.57	1.699 – 1.704 – 1.721

Table 3.10 The complex parameters for the formation of [Pt(diMebipy)H_2L]Cl dimers in 50% CD_3CN/D_2O at 30°C.

Conc. Range mol dm^{-3}	H	Optimum calculated complex parameters with 95% limits		
		min. < δ_0 < *max.* ppm	*min.* < K^D < *max.* $dm^3\ mol^{-1}$	*min.* < $\delta_0 - \delta_\infty$ < *max.* ppm
	3	7.323 – 7.336 – 7.349	34.72 – 38.60 – 42.66	0.857 – 0.858 – 0.862
	3'	7.430 – 7.451 – 7.473	34.42 – 41.11 – 48.31	0.808 – 0.808 – 0.812
$4.82x10^{-3}$	5	6.941 – 6.951 – 6.962	22.13 – 25.47 – 29.00	0.658 – 0.668 – 0.681
-	5'	7.159 – 7.169 – 7.178	26.87 – 29.79 – 32.84	0.738 – 0.744 – 0.752
$3.98x10^{-2}$	6	7.704 – 7.725 – 7.747	36.02 – 42.14 – 48.67	0.905 – 0.906 – 0.909
	6'	7.869 – 7.890 – 7.910	28.08 – 32.61 – 37.43	1.068 – 1.076 – 1.089

Table 3.11 The complex parameters for the formation of [Pt(diMebipy)H_2L]Cl dimers in 80% D_2O/CD_3CN at 30°C.

The average dimerisation constant K^D for $[Pt(diimine)H_2L]^+$ in different solvent composition is summarised in Table 3.12. The results showed that the addition of D_2O encourages in the dimer and presumably higher order aggregates formation. When the D_2O content in solvent mixture for $[Pt(diMebipy)\ H_2L]^+Cl^-$ was 40%, the dimerisation constant was only approximately 6. With the addition of more D_2O, the K^D value increased drastically up to 34.9. Similar behaviour was also observed between $[Pt(bipy)H_2L]Cl$ in 50:50 D_2O/CD_3CN and $[Pt(bipy)H_2L]PF_6$ in pure CD_3CN. Since the counter ions have little effect on the self-association, the addition of 50% D_2O must account for the large difference in the association constant. The addition of water into the mixture increases the polarity of the solvent. In a more polar solvent mixture, the aggregates have a greater propensity for intermolecular aromatic stacking since the stacked aggregate maximises the solvent interaction with the polar groups on the same molecule, and minimises interactions between the solvent and the hydrophobic aromatic π surfaces.

Complex		Average K^D
$[Pt(phen)\ H_2L]^+\ Cl$	in 50:50 D_2O/CD_3CN	27.7 ± 4.5
$[Pt(phen)\ H_2L]^+\ PF_6$ *	in pure CD_3CN	23.3 ± 3.3
$[Pt(bipy)\ H_2L]^+\ Cl$	in 50:50 D_2O/CD_3CN	21.6 ± 2.7
$[Pt(bipy)\ H_2L]^+\ PF_6$	in pure CD_3CN	2.7 ± 0.6
$[Pt(diMebipy)\ H_2L]^+\ Cl$	in 50:50 D_2O/CD_3CN	34.9 ± 5.1
$[Pt(diMebipy)\ H_2L]^+\ Cl$	in 40:60 D_2O/CD_3CN	6.2 ± 1.0
$[Pt(diMebipy)\ H_2L]^+\ Cl$	in 80:20 D_2O/CD_3CN	35.0 ± 6.7

*Results quoted from C. Lawrence, reference 16.

Table 3.12 The Average K^D calculated from the protons on the diimine moiety of Pt(II) complexes.

3.3.5 Electrospray Ionization Mass Spectroscopy (ESI-MS)

Electrospray mass spectra of [Pt(bipy)H_2L]Cl, [Pt(diMebipy)H_2L]Cl, [Pt(diMebipy)-H_2L]Br, [Pt(diMebipy)-H_2L]ClO_4, [Pt(di-*tert*-butylbipy)H_2L]Cl and [Pt(di-*tert*-butylbipy)H_2L]Br complexes were examined. Figure 3.17 shows an *ESI-MS* spectrum of [Pt(bipy)H_2L]Cl complexes in 50% (v/v) acetonitrile and water mixture. Table 3.13 summarises the calculated and observed peaks related [Pt(bipy)H_2L]Cl, [Pt(diMebipy)H_2L]Cl and [Pt(phen)H_2L]Cl complexes taking into account the different major naturally occur Pt isotopes.

[Pt (bipy) H_2L]$^+$			
Pt isotopes	Natural abundance	Calculated	Observed
193.96	32.90%	616.96	616.66
194.96	33.80%	617.96	617.88
195.97	25.50%	618.97	618.68
197.98	7.20%	620.98	620.91
[Pt (diMebipy) H_2L]$^+$			
Pt isotopes	Natural abundance	Calculated	Observed
193.96	32.90%	644.96	644.91
194.96	33.80%	645.96	645.90
195.97	25.50%	646.97	646.89
197.98	7.20%	648.98	647.88
[Pt (phen) H_2L]$^+$			
Pt isotopes	Natural abundance	Calculated	Observed
193.96	32.90%	641.49	640.96
194.96	33.80%	642.49	641.70
195.97	25.50%	643.5	642.69
197.98	7.20%	645.51	644.67

Table 3.13 The major peaks shown in the EMI-MS spectra for [Pt(bipy)H_2L]Cl, [Pt(diMebipy)H_2L]Cl and [Pt(phen)H_2L]Cl complexes.

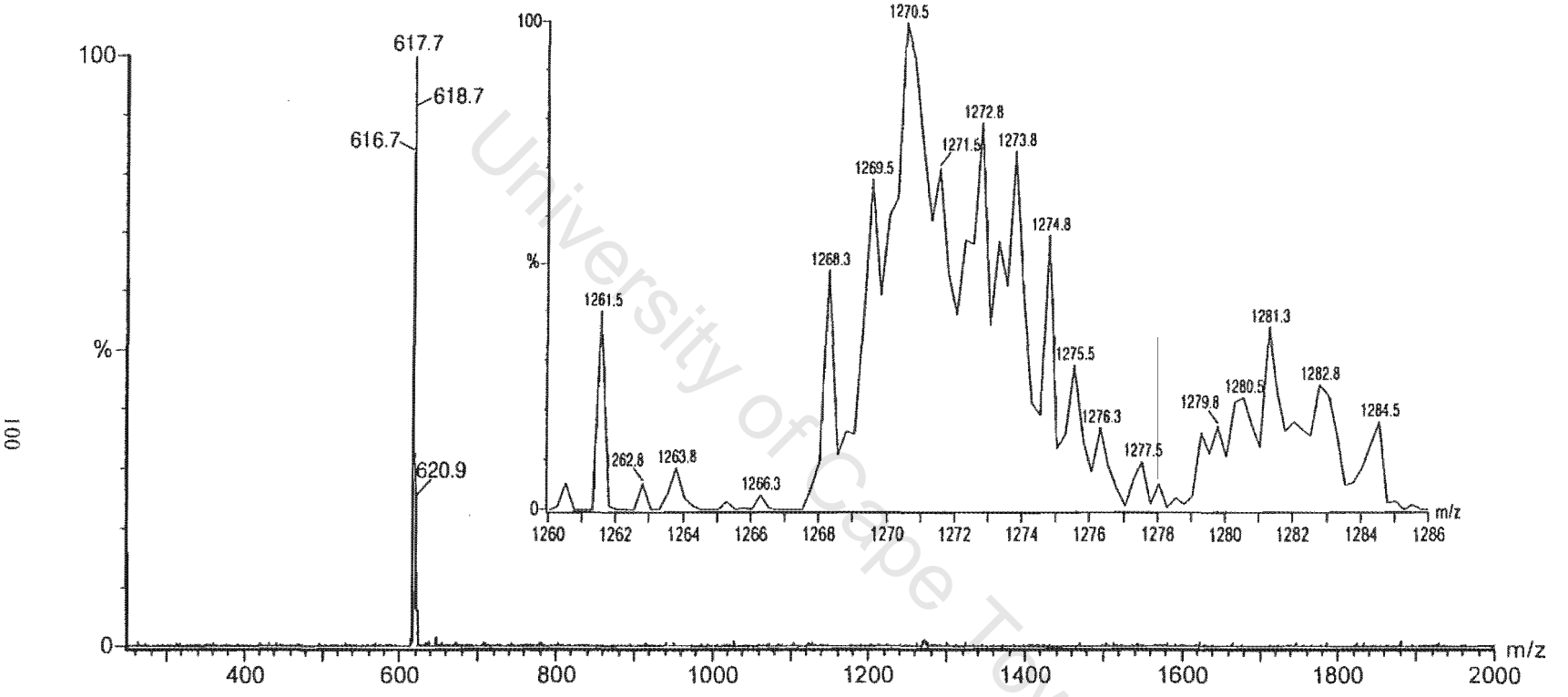

Fig. 3.21 The ESI-MS spectra showing the major peaks and the expanded section of minor peaks of [Pt(bipy)H_2L]Cl complex.

The spectra of all $[Pt(diimine)H_2L]^+A^-$ complexes not only confirmed that the structure of the $[Pt(diimine)H_2L]^+$ species exist in 50% (v/v) H_2O/acetonitrile mixture, but that there are also signals corresponding to species $\{[Pt(diimine)H_2L]_2A\}^+$. This observation further confirms the existence of at least dimers in these solutions. Unfortunately no evidence of higher order aggregates such as $\{[Pt(bipy)H_2L]_3Cl_2\}^+$ could be found. Table 3.14 shows the calculated and observed peaks for $\{[Pt(bipy)H_2L]_2Cl\}^+$ with all the possible isotopic combinations.

$\{[Pt(bipy)H_2L]_2Cl\}^+$			
Pt isotopes	Cl isotopes	Calculated	Observed
387.92	34.97	1268.89	1268.28
389.92	34.97	1270.89	1270.54
391.94	34.97	1272.91	1272.78
395.96	34.97	1276.93	-
388.92	34.97	1269.89	1269.54
389.93	34.97	1270.90	1270.54
391.94	34.97	1272.91	1272.78
390.93	34.97	1271.90	-
392.94	34.97	1273.91	1273.79
393.95	34.97	1274.92	1274.79
387.92	36.97	1270.89	1270.54
389.92	36.97	1272.89	1272.78
391.94	36.97	1274.91	1274.79
395.96	36.97	1278.93	1278.78
388.92	36.97	1271.89	-
389.93	36.97	1272.90	1272.78
391.94	36.97	1274.91	1274.79
390.93	36.97	1273.90	1273.79
392.94	36.97	1275.91	1275.54
393.95	36.97	1276.92	-

Table 3.14 The assignment on the minor peaks of $\{[Pt(bipy)H_2L]_2Cl\}^+$ in 50% (v/v) H_2O/acetonitrile mixture.

The dimers, $\{[Pt(bipy)H_2L]_2Cl\}^+$, each contain two Pt and due to the four different isotopes of Pt, there are many different possible combinations of these isotopes, accounting for the number of peaks observed for the dimer species. Similar results were obtained for [Pt(diMebipy)H_2L]Cl, [Pt(diMebipy)H_2L]Br, [Pt(diMebipy)H_2L]ClO_4, [Pt(di-*tert*-butylbipy)H_2L]Cl and [Pt(di-*tert*-butylbipy) H_2L]Br complexes. As a part of characterisation, the *ESI-MS* spectra of $[Pt(diMebipy)H_2L]^+$ with a different non-coordinating anion ClO_4^- was also acquired. This spectrum can be used to distinguish the difference between a fully coordinated *N, N*-dihydroxy-*N'*-benzoylthiourea $[Pt(diimine)H_2L]^+A^-$ complex and a partially coordinated [Pt(diimine) H_3L-*S*]$^+A^-$ complex. The spectra showed the same pattern as the rest of the series of complexes, both $[Pt(diimine)H_2L]^+$ and $\{[Pt(diimine)H_2L]_2A\}^+$, indicating the anion was not coordinated to the metal.

3.3.6 Electron Microscopy

It was shown in both ^{1}H NMR chemical shifts calculations and electrospray ionisation mass spectroscopy that $[Pt(diimine)H_2L]^+A^-$ complexes self-associate into dimers and possibly higher aggregates in a mixed solution of acetonitrile and water. Addition of water was also favours the formation of dimer or higher aggregates. This experiment was designed in an attempt to see whether higher aggregates can be observed in pure water by using the transmission electron microscope.

Fig 3.22 is the electron microscopic photo of the [Pt(bipy)H_2L]Cl solution. Some long, tangled tubes were observed for an unheated [Pt(bipy)H_2L]Cl solution indicating large tertiary structure was formed in water. After the sample being heated, it showed no presence of any structure. This can be explained by the breaking down of [Pt(bipy)H_2L]Cl "polymer" after heating. The electron microscopic photo was also taken for [Pt(diMebipy)H_2L]Cl solution and the same tube like structure was also observed (Fig. 3.23)

Fig. 3.22 The tubular structure of [Pt(bipy)H_2L]Cl as seen in a TEM Image (x 73000)

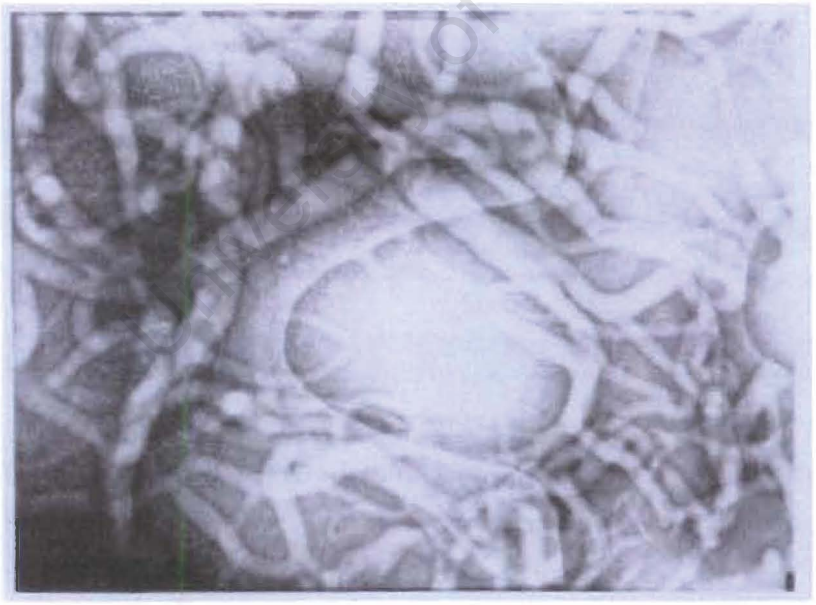

Fig. 3.23 The tubular structure of [Pt(diMebipy)H_2L]Cl as seen in a TEM Image. (x 73000)

The [Pt(di-*tert*-butylbipy)H_2L]Cl solutions were pre-heated to 50°, 80° and 100° to examine the effect of heating on the supra-molecular structure. In the photo of the unheated sample, many long rods were observed while in the 50° preheated sample, the rods became shorter with some smaller "doughnut shaped" ring structures close by (Fig. 3.24). For the samples that were heated to 80° and 100°, there were no signs of "rod-like" structure, only many circular rings of various sizes were observed (Fig. 3.25).

Fig. 3.24 The rod-like and some doughnut rings of unheated [Pt(di-*tert*-butylbipy)H_2L]Cl complex. (x37000)

Fig. 3.25 Various sizes of doughnut shaped rings after [Pt(di-*tert*-butylbipy)H_2L]Cl complexes being heated for 80° – 100°C. (x 73000)

These observations lead to speculation of possible modes of aggregation. The [Pt(diimine)H_2L]Cl complexes consist of a hydrophilic and a hydrophobic end, with the diimine ligand most likely being the hydrophobic and the 2-hydroxyethyl group of the benzoylthiourea ligand being hydrophilic. The complex can be represented as follows:

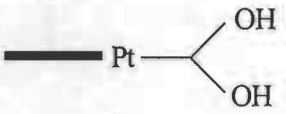

 = diimine ligand

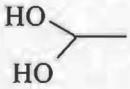 = *N,N*-dihydroxyethyl-*N'*-benzoylthiourea ligand

 = π-π interaction

By comparison, lipids are molecules which also consist of hydrophilic "heads" and long hydrophobic alkyl chain.[19] They have been found to self-aggregate to various different structures. Their "tails" always aggregate due to the hydrophobic effect, and the bilayer can form either low curvature structures such as planar sheets, twisted ribbons and scrolls or highly curved micelle structures such as sphere, disks and rods.

We can suggest that these [Pt(diimine)H_2L]Cl complexes aggregate in similar fashion to these of the lipid bilyers and therefore the aggregates that formed may be sheets that rolled up to be rods or disk-like structure. (Fig. 3.26) These structures are clearly evident from the transmission electron micrographs.

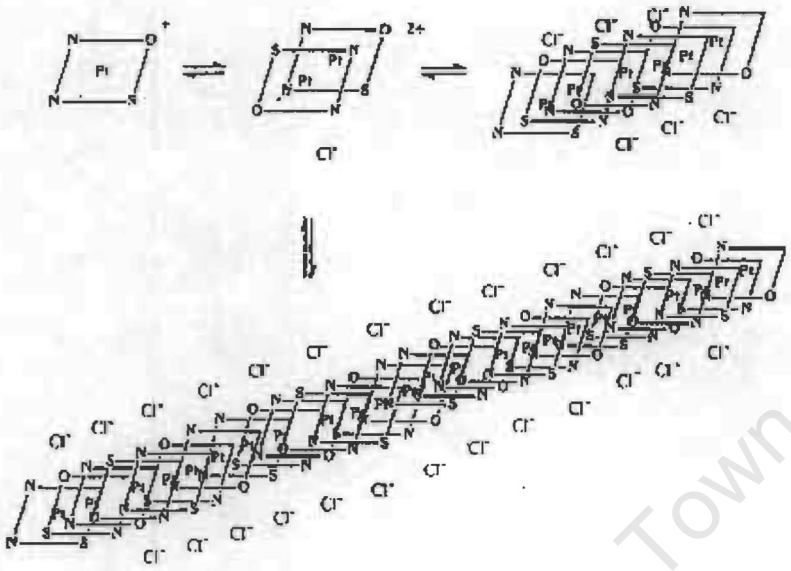

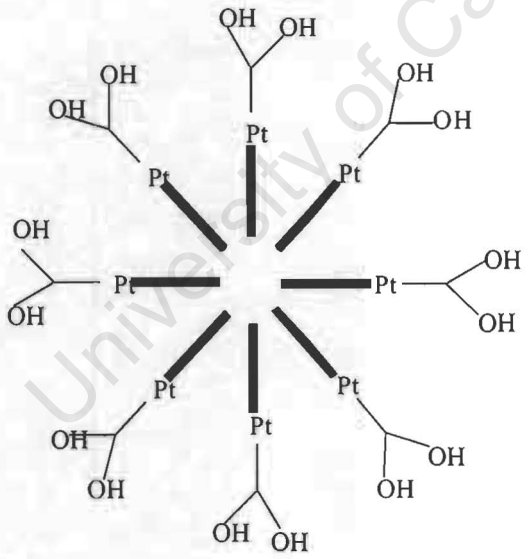

Fig. 3.26 Schematic diagram showing the possible manner in which [Pt(diimine)H_2L]Cl can self-associate to form ribbon-like or "doughnut" like structure.

REFERENCES

1. W. Saenger, *Principles of Nucleic Acid Structure,* Springer-Verlag: New York, 1984, 140.
2. J. C. Kendrew, *Side Chain Interactions in Myoglobin*, Brookhaven Symp., 1962, **15**, 216.
3. F. Espejo, M. Cubillos, L. M. Salazer, F. Guzman, M. Urquiza, M. Ocampo, Y. Silva, R. Rodriguez, E. Lioy and M.E. Patarroyo, *Angewandte Chemie, Int. Ed.*, 2001, **40**(24), 4654.
4. B. Ganem, Y. T. Li and J. D. Henion, *J. Am. Chem. Soc*, 1991, **113**(16), 6294.
5. A. Bernard and H. R. Bosshard, *Eur. J. Biochem*., 1995, **230**(2), 416.
6. H-S. Scgbeuder, *Angew. Chem. Int. Ed. Engl.*, 1991, **30**, 1417.
7. L. P. G. Wakelin, *Med. Res. Rev*. 1986, **6**, 275.
8. C. A. Hunter, P. Leighton and J. K. M. Sanders, *J. Chem. Soc., Trans. Perkin1*, 1989, 547.
9. G. R. Desiraju and A. Gavezotti, *J. Chem. Soc., Chem. Commun.* 1989, 621.
10. R. J. Abraham, F. Eivazi, H. Pearson and K. M. Smith, *J. Chem., Soc., Chem. Commun*. 1976, 698.
11. C. A. Hunter and J. K. M. Sanders, *J. Am. Chem. Soc*., 1990, **112**, 5525.
12. J. H. Williams, *Acc. Chem., Res*., 1993, **26**, 593.
13. J. Pawliszyn and S. Scheiner, *J. Phys. Chem*., 1984, **88**, 1726.
14. K. W. Jennette, J. T. Gill, J. A. Sadownick and S. J. Lippard, *J. Am. Chem. Soc.*, 1976, **98** (20), 6159.
15. G. Arena, L. Monsu Scolaro, R. F. Pasternack and R. Romeo, *Inorg. Chem.* 1995, **34**, 2994.
16. K. R. Koch, C. Sacht and C. Lawrence, *J. Chem. Soc., Dalton Trans*., 1998, 689.
17. I. Horman and B. Dreux, *Helv. Chem. Acta*, 1984, **67**, 754.
18. S. A. Hofstadler, R. Bakhtiar and R. D. Smith, *J. Chem. Educ.* 1996, **73**(4), A82.
19. J-H. Fuhrhop and J. Köning, *Membranes and Molecular Assemblies: The Synkinetic Approach*, Cambridge University Press: Cambridge UK, 1994.

4.1 INTRODUCTION

It is generally known that the fused aromatic systems which also carry a positive charge such as ethidium and acridine orange intercalate between DNA base pairs. This information was used to design metallointercalators including metalloporphyrins and other metal complexes. The first well known metallointercalator was the complex (2-hydroxyethanethiolato) (2,2':6',2"-terpyridine)platinum(II) or normally referred to as $[Pt(terpy)(HET)]^+$.[1] The x-ray fiber diffraction pattern of its DNA complex supports the neighbour exclusion binding model of intercalation.[2] The study then was expanded to include complexes such as 2,2'-bipyridine(ethylenediamine)-platinum(II) $[Pt(bipy)(en)]^{2+}$ and 1,10-phenanthroline-(ethylenediamine)platinum(II) $[Pt(phen)(en)]^{2+}$.[3] For all these complexes, the aromatic ligands lie strictly in the square planner coordination plane of the metal atom so facilitating intercalation. In the case of a closely related complex bis(pyridine)(ethylenediamine)platinum(II) $[Pt(py)_2(en)]^{2+}$, no intercation was observed due to the nonbonded steric repulsions between adjacent pyridine rings perpendicular to the coordination plane, preventing the required coplanarity. Crystal studies of terpyridylplatinum(II) species stacked with nucleotides showed that the entire planner metal complex, not only the aromatic ligand, intercalates between the base pairs.[4,5]

Srivastava *et al.* extended the study by incorporating diimine and amino acids into mixed-ligand platinum(II) complexes.[6-8] In contrast to comp lexes reported by Lippard *et al.*, no intercalation was found for [Pt(2,2'-bipyridyl)(Amino Acid)]Cl complexes. Further experiments led to a conclusion that the DNA-platinum binding for this series of complexes are stabilised by hydrogen bonding rather than intercalation.

In related study on the ruthenium(II) mixed-ligand complexes, the effects of hydrophobicity, size, geometry, dipole moment and hydrogen-bonding ability on the intercalation interaction were examined.[9] The hydrophobic nature of these complexes was found to be an important factor in determining their binding affinity for DNA. With increasing hydrophobicity of the complexes, self-association tends to compete with DNA binding resulting in a reduced DNA binding affinity. Results from the study also highlight the importance of the complex geometry. Molecular shape was found to be the

most important factor, as those complexes in which the van der Waals interactions between DNA and the complex are maximised, displayed the highest binding affinity. Therefore, cations with ligands that have extended hydrophobic surfaces are usually good intercalators.

The observed effect of geometry on the binding of metal complexes to DNA lead to the development of stereoselective complexes.[10-12] Chiral metal complexes such as Δ-$Ru(phen)_3^{2+}$ and Λ- $Ru(phen)_3^{2+}$ were found to have different binding affinities to DNA. The stereoselectivity was demonstrated by equilibrium dialysis and helix unwinding studies. The basis for the chiral discrimination of these metal complexes became evident when viewing the models of the interaction. With one ligand intercalated, for the Δ isomer, the remaining ligands lie along the groove of the right handed DNA double helix, complementing the groove in terms of disposition. For Λ isomer, however, with one ligand intercalated, steric repulsion was evident between the non-intercalated phenathroline hydrogen atoms and phosphate oxygen atoms. Thus the Δ isomer is more favoured in binding to a right-handed DNA.

There is a great deal of interest in complexes which combine metals and planar aromatic ligands. It was believed that, with the addition of an intercalating agent, DNA interaction can be maximised. Lippard *et al.*[13] combined a classical antitumour drug *cis*-diamminedichloroplatinum (cisplatin), which binds covalently to DNA, with the known intercalator ethidium. The unwinding angle of the DNA upon formation with complex *cis*-$[Pt(NH_3)_2(ethidium)Cl]^{2+}$ was found to be much greater than that of *cis*-diammine-dichloroplatinum but smaller than the unwinding angle caused by unbound intercalator ethidium bromide. This is a good evidence that the ethidium ligand interacts substantially with the double helix upon covalent binding of the platinum complex, strengthening the case for a combination of intercalative and covalent binding modes.[14]

In this study, the large flat π surfaces on the diimine ligands, [Pt(diimine)H_2L]Cl complexes were designed to be potential DNA intercalators. As described in chapter 3,

these complexes were also found to self associate in aqueous solution to form ribbon-like polymeric structure.

Over the years, studies using different physical techniques have been done in an attempt to elucidate different binding modes for molecules binding to nucleic acids. The following section is a brief introduction to those techniques:

4.1.1 Thermal Denaturing (melting of DNA)

DNA is well known to exist as a double helix in solution. When the solution is heated, the attractive forces that produce the three dimensional structure of molecules, such as the hydrogen bonding between DNA base pairs, become fairly weak and easily disrupted.[15] The double-stranded DNA thus dissociates into two single stranded DNA (denatured DNA) molecule. (Fig. 4.1) The most convenient way to monitor the denaturing of DNA is by UV spectrophotometry. When DNA denatures, its UV absorbance, which is almost entirely due to the degeneracy of the stacked aromatic bases, increases by *ca.* 40% at λ_{260nm}. This phenomenon, known as the "hyperchromic effect", is due to the fact that the aromatic bases in DNA interact via their π electron clouds when stacked together in the double helix. Since the UV absorbance of the bases is a consequence of π electron transitions, and since the potential for these transitions is diminished when the bases stack, the bases in duplex DNA absorb apparently less 260nm radiation than expected from the sum of the absorbance of the monomeric subunits. Unstacking alleviates this suppression of UV absorbance.[16]

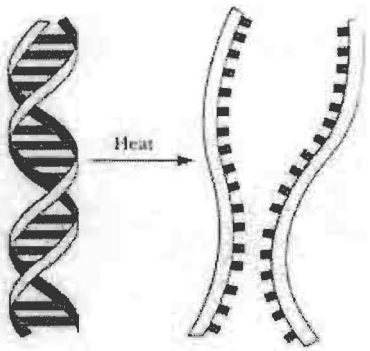

Fig. 4.1 The thermal denaturation of DNA.

The DNA molecule is a helix before the increase in temperature, as all bases are H-bonded to their complementary base forming a base pair and all base pairs being stacked. As the temperature increases, the base pairs in various segments of the molecule are broken and the number of broken base pairs is directly proportional to the increase in temperature. The unstacking of consecutive base pairs is a cooperative process, characteristically described by a sigmoidal curve.[17] At the upper temperature plateau, there remain only a few base pairs holding the two strands together and eventually at a critical temperature, the strands are finally separated completely. The hyperchromic absorbance change of DNA, as monitored at a particular wavelength (usually at 260nm), occurs over a narrow temperature range. The temperature at which 50% of the double strand DNA has dissociated into its two single strands or in other words 50% of the absorbance change has occurred is referred to as the melting temperature (T_m) of DNA. AT and GC base pairs are held together by two and three hydrogen bonds respectively and, therefore, higher temperature is required to disrupt GC pairs. For this reason, the melting temperature T_m is generally dependent linearly on the base composition of DNA.

4.1.2 Circular Dichroism[18]

Light is constituted by electromagnetic wave consisting of a combination of an oscillating electric field (E) and a magnetic field (H). Both of them can be represented by mutually perpendicular vectors. The plane of E vector is called the plane of polarisation. When two plane-polarised wave differing in phase by one quarter wavelength, with their E vectors perpendicular to one another, are superimposed, the resultant E vector rotates and its tip follows a helical path. The light associated with this is called circularly polarised light. (Fig. 4.2)

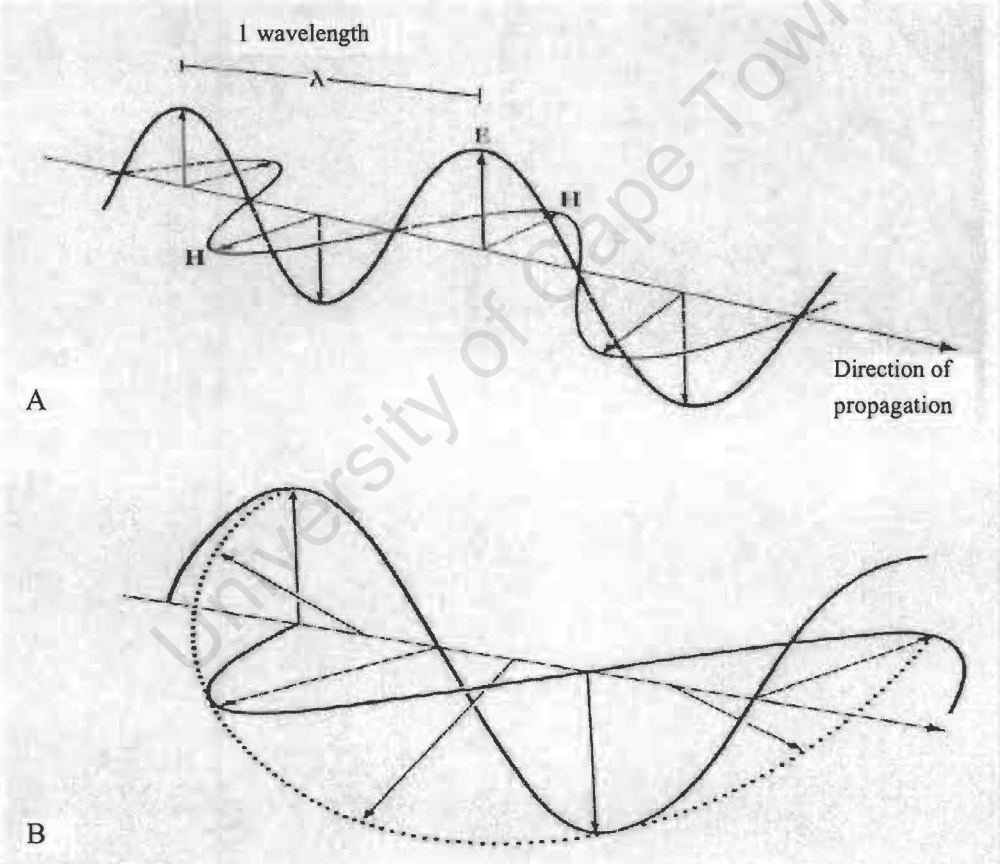

Fig. 4.2 A. Propagation of an electromagnetic wave.
B. Generation of circularly polarized light.

If the E vector rotates clockwise, it is referred to as being **right** circularly polarised and opposite for **left** circularly polarised light. When a right and left circularly polarised wave, both of equal amplitude, are superimposed, the E vectors will sum up to give a plane polarised wave. However, when they differ in amplitude, the tip of the resultant E vector will follow an elliptical path and this light is elliptically polarised. The parameter, θ, called ellipticity, is often used to describe the elliptical polarisation. (Fig. 4.3)

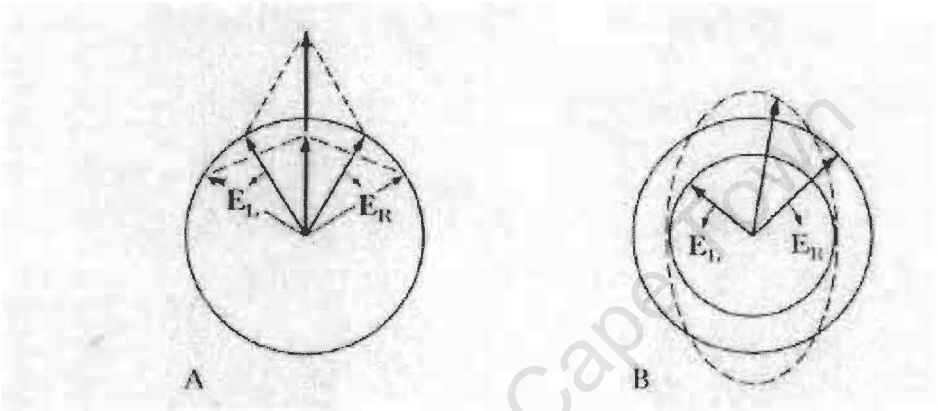

Fig. 4.3 Diagrams showing how right and left circularly polarised light combine. A. when two waves have equal amplitude and B. when their amplitudes differ, resulting in elliptically polarized light.

When polarised light passes through a solution, its properties change. If a substance retards both left (L) and right (R) polarised light equally, the L and R waves will recombine in such a way that the light passing through form plane-polarised light. However, for an optically active compound, L and R waves travel through the substance at different speeds, resulting in a rotated plane of polarisation. (Fig. 4.4) **Circular Dichroism** is a measure of intensity of each or these waves that pass through an optically active media. It is defined as $\Delta\varepsilon$, the difference of the extinction coefficients for L and R light. (ε_L and ε_R). Ellipticity θ is normally plotted *vs.* wavelength. It is related to $\Delta\varepsilon$ as $\theta = 3300\,\Delta\varepsilon$.

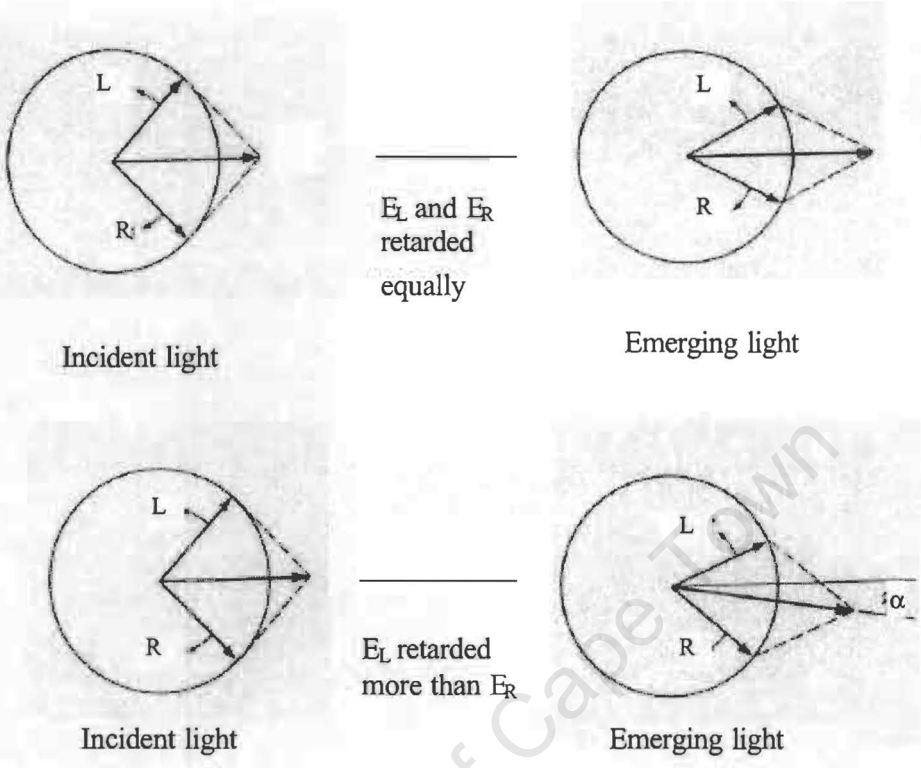

Fig. 4.4 Diagram showing the change in polarised light after passing through optically inactive and active substrates.

The rotational strength as shown in a CD curve is a measure of the degree of asymmetry of the solute. An agent that changes this parameter usually does so by exhibit an increased or decreased asymmetry. Although CD analysis rarely gives absolute information about structure, it is extraordinarily sensitive to *changes* in conformational change. For example, it is used to determine the relative content of various secondary structures of protein : α-helical form, β-sheet, and random coil. It can also be used to study conformational changes of nucleic acids. Purines and pyrimidines as such are symmetrical chromophores. They become optically active when attached to sugar by means of an *N*-glycosidic bond. The optical activity increases even more when they become part of a helical structure. Circular Dichroism is therefore extremely sensitive in

detecting a) the loss of helicity of single-stranded polymers or double stranded DNA due to the influence of various agents; b) the transition from single to double stranded polynucleotides and vice versa; c) structural changes in helical structures introduced by binding of cations, peptides and proteins etc. (Fig. 4.5)

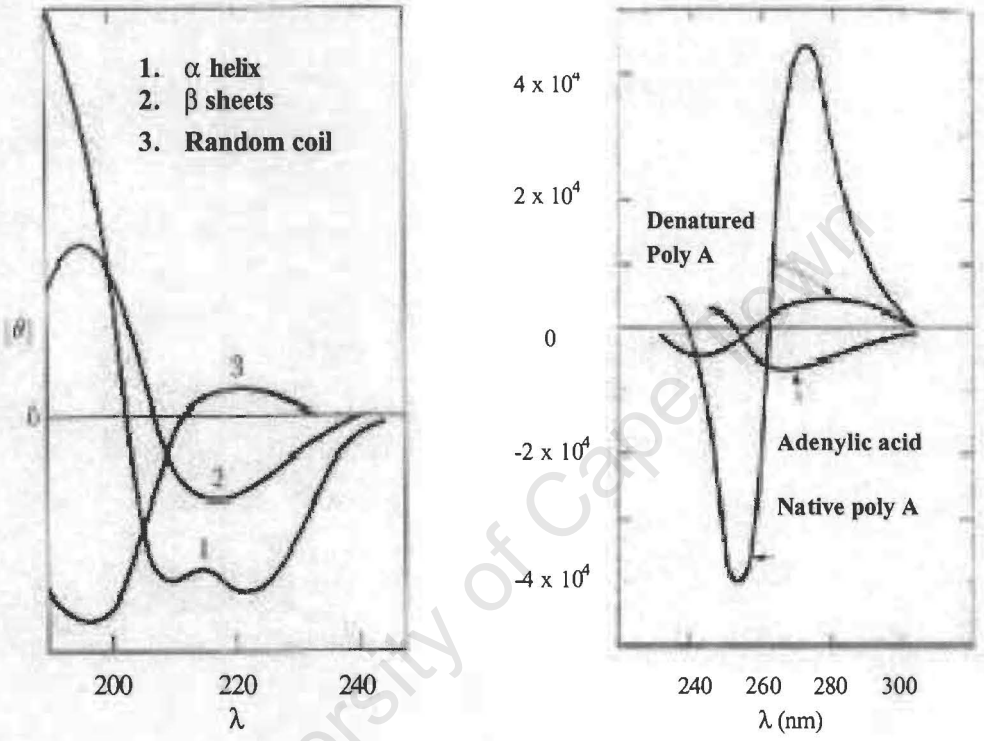

Fig. 4.5 CD spectra for poly-L-lysine in different conformations due to pH and the thermal denaturation of polyadenylic acid[18].

4.1.3 DNA Binding and Topology

Covalently closed circular plasmid DNA can be described as the double stranded DNA coiled on itself or being supercoiled.[19] Since left-handed twisting of right-handed, double stranded DNA along the helical axis tends to untwists DNA, the system compensates by the formation of supercoils. When one strand in supercoiled DNA is nicked by an

enzyme, the structure relaxes. In case that it is treated with either a covalently binding drug or an intercalator, the supercoils untwist step by step until it becomes a relaxed DNA (Fig. 4.6). If both strands of supercoiled DNA are being nicked close to each other, the DNA becomes linearised and loses all supercoiling. Due to the differences in topology and size for supercoiled, relaxed circular and linear DNA, their mobility in agarose gel are very different. Quantification of drug-mediated unwinding of supercoiled DNA using gel electrophoresis is a useful tool for studying the effects of intercalating and a covalently binding molecules on DNA topology.

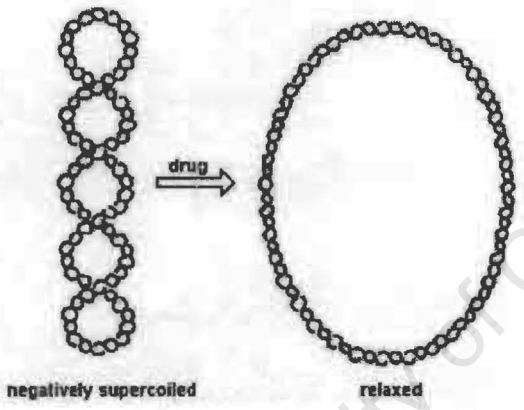

Fig. 4.6

Negatively supercoiled DNA becomes relaxed after treatment of drugs

4.1.4 DNA Damage and Repair

When bacteria are exposed to radiation by UV light or ionising irradiation or they are exposed to various chemicals which act on their DNA, they lose the ability to form colonies. This loss of viability can be expressed graphically by plotting the fraction of the initial population that survives various doses of exposure to the radiation or the chemicals against some measure of exposure. Such a dose-response graph is called a survival curve. Some bacteria (eg. *E.coli*) have ability to repair DNA damage and so increase their chance of survival.

One of the major pathway for dealing with DNA damaging agents causing distortions in the DNA helix is called nucleotide excision repair. In this process, the DNA in cells exposed to UV radiation or chemical agents was repaired in the manner which the damaged bases such as pyrimidine dimers and photoproducts are enzymatically excised from DNA as intact nucleotides. The enzyme-catalyzed incision of damaged DNA during nucleotide excision repair in *E.coli* requires three proteins: UvrA, UvrB and UvrC. Under physiological condition, UvrA protein associates with UvrB protein to form a $(UvrA)_2$ $(UvrB)_1$ complex. This complex is responsible for the damage specific recognition process. It has been suggested that the role of UvrA protein in nucleotide excision repair is to function as a "molecular matchmaker" which delivers UvrB protein to sites of distortive damage in DNA by the formation of a transient $(UvrA)_2(UvrB)_1$–DNA complex. The UvrA protein then rapidly dissociates, with the aid of ATP hydrolysis, establishing a stable $UvrB_1$-DNA complex. The UvrC protein binds near UvrB, activating the nuclease activity of UvrB. UvrB nicks the DNA about 4 nucleotides downstream from the damage and thus activates the nuclease activity of UvrC, possibly as a result of a DNA conformational change. UvrC then nicks the DNA about 7 nucleotides upstream of the damage. DNA helicase II uses energy from ATP hydrolysis to unwind the oligonucleotide from between the two nicks, leaving a gap of about a dozen nucleotides. At the same time, the UvrC protein is displaced. The gap is filled in by DNA polymerase I or II, using the non-damaged strand as template. UvrB is now also displaced. The resulting nick is sealed by DNA ligase. (Fig. 4.7) Experiments have shown that bacteria that did not contain either *uvrA*, *uvrB* or *uvrC* genes, especially the *uvrA* and *uvrB* mutants, are defective in repairing radiation damage and many types of chemical damage.

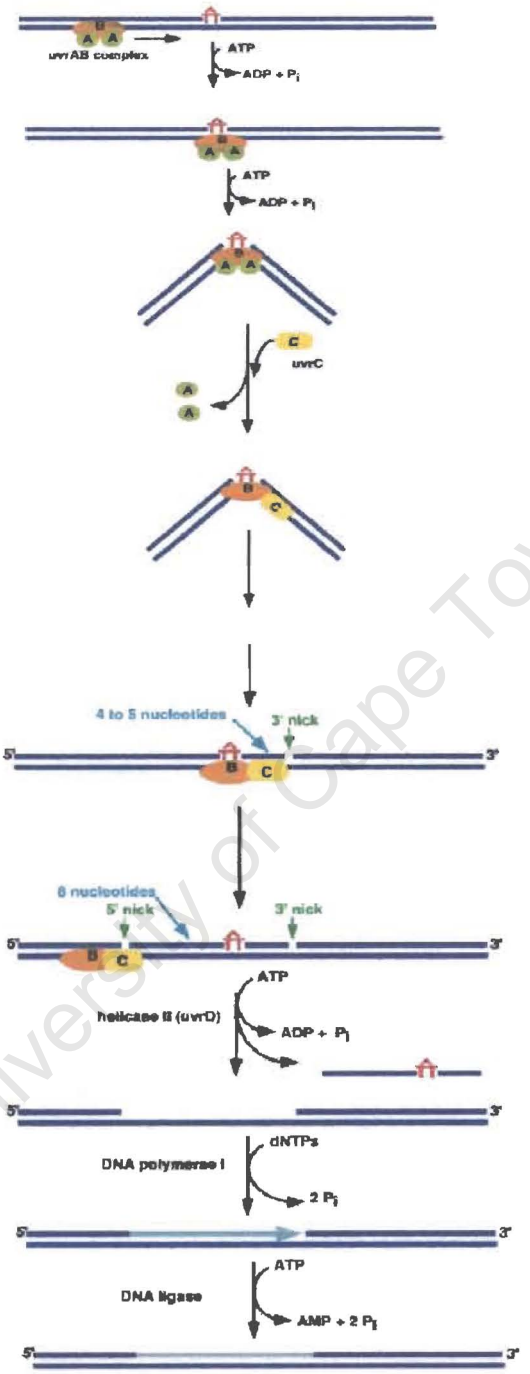

Fig. 4.7 Excision repair mechanism by UvrABC.

4.2 EXPERIMENTAL

4.2.1 Measurement of T_m

A completely sealed metal compartment that can accommodate a standard quartz cuvette was equipped with nitrogen inlet and outlet tubes and connections to a water bath that was built to fit into a HP8452A Diode-array UV-Visible spectrophotometer. A thermal couple was also attached to the cell leading to a temperature controller to control the temperature and desired temperature changes.

Calf thymus DNA and the synthetic polynucleotide polydA-polydT were bought from Sigma-Aldrich (Pty) Ltd. For experiments with polydA-polydT, 10µl of 2M sodium acetate buffer (pH7) were used to stabilise the double helix. The melting curve was obtained at λ_{260nm} from 30°C to 100°C using the Diode-array UV spectrophotometer. The melting curves of polydA-polydT after addition of various aliquots of [Pt(bipy)H_2L]Cl solution were also obtained in the same way. An optimum DNA concentration was selected for the melting study of complexes [Pt(diMebipy)H_2L]Cl, [Pt(di-*tert*-butylbipy)H_2L]Cl or [Pt(phen)H_2L]Cl with either polydA-polydT or calf thymus DNA.

The experiments with calf thymus DNA were carried out in 10mM cacodylate buffer at different temperature intervals. At each set temperature a complete spectrum was recorded.

4.2.2 Circular Dichroism (CD)

Aliquots of polydA-dT DNA was diluted into 1 ml of 20mM sodium acetate pH 7 buffer solution to approximately OD_{260}=0.25. CD spectra of control solutions of polynucleotides alone and various platinum complexes were performed at room temperature using a Jasco 810 spectropolarimeter with a 1cm path length cell. For [Pt(bipy)H_2L]Cl, [Pt(diMebipy)H_2L]Cl, [Pt(di-*tert*-butylbipy)H_2L]Cl and [Pt(phen)H_2L]Cl experiments, various aliquots of 100 µg ml^{-1} platinum solutions from 10 µl up to 170 µl are added to

the 1 ml DNA solution. For ethidium bromide experiments, 10-120 µl of 7.4 x 10^{-5} µg ml^{-1} ethidum bromide solution was added. All the experiments were carried out at room temperature.

4.2.3 Bacterial Growth and plasmid purification

All *Escherichia coli* strains (Table 4.1) were routinely propagated on LB agar.

E.coli JM109 containing pBluescript KS (Stratagene Cloning Systems) was inoculated into a starter culture of 5ml LB broth medium containing 0.1 µg ml^{-1} ampicillin. The culture was incubated for approximately 8 hours at 37 °C with vigorous shaking. The culture (5 ml) was inoculated into 25ml of LB medium which contained 0.12 µg ml^{-1} ampicillin and incubated at 37 °C overnight with shaking. The bacterial cells were then harvested by low speed centrifugation in a Beckman centrifuge JA-20 (6000 rpm for 10 minutes at 4°C). The supernatant from the centrifugation was discarded and the plasmid DNA isolated using the QIAGEN Plasmid preparation kit according to the manufacturer' s specification.

Strain	Relative repair genotypic characteristics	Reference
JM109	recA	Yanisch-Perron *et al*. 1985
AB1157	DNA repair wild type	ATCC 29055
AB1886	uvrA	Howard-Flanders *et al*. 1966

Table 4.1 *E.coli* strains used in this chapter.

DNA mobility in agarose gels

$[Pt(bipy)H_2L]^+$ and $[Pt(di\text{-}tert\text{-}butylbipy)H_2L]^+$ solutions were titrated against undigested plasmid DNA (600ng) at a platinum to base pair ratio of 0.05, 0.10, 0.15, 0.20 and 0.25. Plasmid DNA was restriction endonuclease digested according to manufacturer's instructions using *Eco*RI restriction enzyme to create linear plasmid DNA for reference purpose. The solutions were then loaded onto a 1% agarose gel and ran at ca. 50V for 4 hours.

Survival Curves

Both *uvrA*$^-$ and wild type *E.coli* (AB1886 and AB1157) cells were cultured overnight (approximately 16 hours) in LB medium at 37°C with shaking. The cells were diluted 10 fold in 1.8 ml of sterile water, harvested by centrifugation in an ependorf microfuge and the cell pellets resuspended in 0.5 ml sterile water. Pt solution (0.5 ml from 3 mg ml^{-1} stock solution) was added to the cell suspensions to give a final concentration of 0.1 ml of the mixture was taken out from the cell-Pt complex suspension into 0.9 ml of previously dispensed sterile water. The cell suspensions were sampled at different time intervals, including the starting time, and the surviving fraction of bacteria determined by dilution in sterile H_2O and plating out on LB agar plates, counting of the surviving colonies. The surviving colonies were counted after 24 hour incubation at 37°C.

4.3 RESULTS

4.3.1 Thermal Melting

PolydA-polydT was chosen for the T_m experiments due to its homogeneity in composition. The melting temperature T_m of an unplatinated polydA-polydT DNA in 20mM pH 7 sodium acetate buffer solution was highly cooperative, and found to be *ca.* 72.3°C. After the addition of different aliquots of $[Pt(bipy)H_2L]Cl$ to the polynucleotide, different shapes of melting profiles and changes in the melting temperature of the

polydA-polydT were observed. On changing the Pt concentration from $2.27x10^{-8}$ M to $1.13x10^{-6}$ M of [Pt(bipy)H_2L]Cl, no significant change in either the melting temperature nor the melting profile in comparison to the original polydA-polydT melting curve was observed. When the concentration of [Pt(bipy)H_2L]Cl increased from $1.13x10^{-6}$ M to $2.26x10^{-6}$ M, the melting point increased from 73.6°C to 78.8°C. As the platinum solution reaches $7.54x10^{-6}$ M, the polydA-polydT was found to melt at an even higher temperature (80°C). This same phenomenon was observed with both [Pt(diMebipy)H_2L]Cl and [Pt(phen)H_2L]Cl upon their addition to polydA-polydT. At the same Pt^{II} concentration, addition of [Pt(diMebipy)H_2L]Cl gave the same melting temperature as [Pt(bipy)H_2L]Cl. [Pt(di-*tert*-butylbipy)H_2L]Cl did not shift the T_m as compared to the unplatinated polydA-polydT. Adding [Pt(phen)H_2L]Cl gave the largest effect. It shifted the T_m from 72.3°C to 90°C. (Table 4.2, Fig. 4.8)

Complexes added	Concentration (M)	T_m (±0.5 °C)
DNA only	-	72.3
[Pt(bipy)H_2L]Cl	2.27×10^{-8}	72.6
[Pt(bipy)H_2L]Cl	4.52×10^{-8}	72.0
[Pt(bipy)H_2L]Cl	9.08×10^{-8}	72.0
[Pt(bipy)H_2L]Cl	2.26×10^{-7}	73.0
[Pt(bipy)H_2L]Cl	4.52×10^{-7}	72.3
[Pt(bipy)H_2L]Cl	1.13×10^{-6}	73.6
[Pt(bipy)H_2L]Cl	2.26×10^{-6}	78.8
[Pt(bipy)H_2L]Cl	4.52×10^{-6}	79.3
[Pt(bipy)H_2L]Cl	6.03×10^{-6}	77.6
[Pt(bipy)H_2L]Cl	7.54×10^{-6}	80.0
[Pt(diMebipy)H_2L]Cl	7.23×10^{-6}	80.6
[Pt(di-*tert*-butylbipy)H_2L]Cl	6.43×10^{-6}	73.0
[Pt(phen)H_2L]Cl	7.27×10^{-6}	90.3

Table 4.2 The melting temperature (T_m) of different complexes at various concentrations.

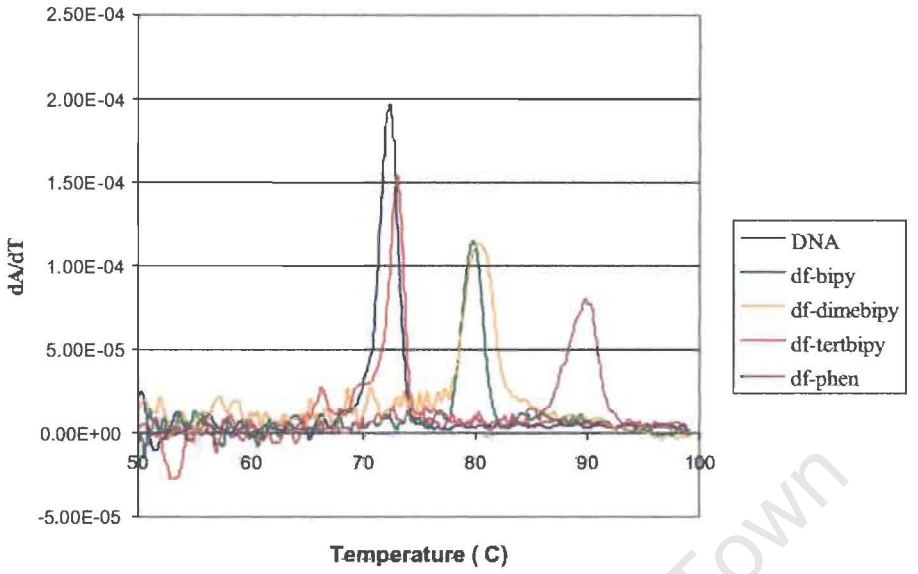

Fig. 4.8 The first derivative dA_{260}/dT *vs.* T curves of polydA-polydT on addition of various Pt(II) complexes.

Thermal melting experiments were also carried out with calf thymus DNA. Spectra were recorded simultaneously from 190nm to 820nm at selected temperature (Fig. 4.9a). Theoretical spectra (Fig. 4.9b) were calculated by manual addition of the separate component spectra both of calf thymus DNA and of the Pt(II) complex solutions. For [Pt(bipy)H_2L]Cl binding to calf thymus DNA, there was a distinctive change in the measured UV spectral profile after 90°C. At temperatures lower than 70°C, the spectral profiles are more "DNA like". As the temperature increases, more [Pt(bipy)H_2L]Cl characteristics were observed (the small fingerprint absorbance at wavelength 320nm).

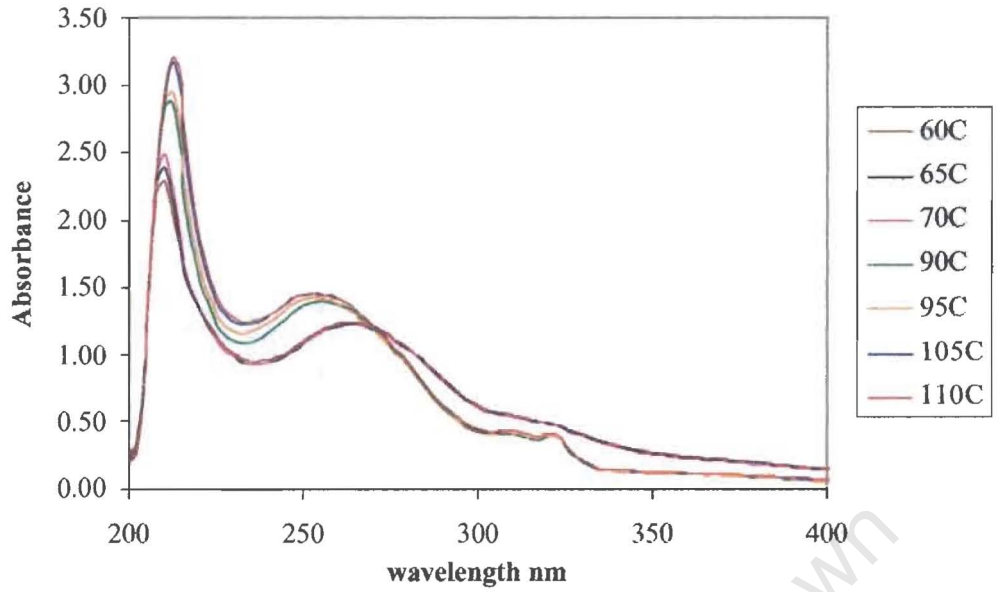

Fig. 4.9a Spectra of calf thymus DNA with 125µg ml^{-1} [Pt(bipy)H_2L]Cl solution taken after various temperatures.

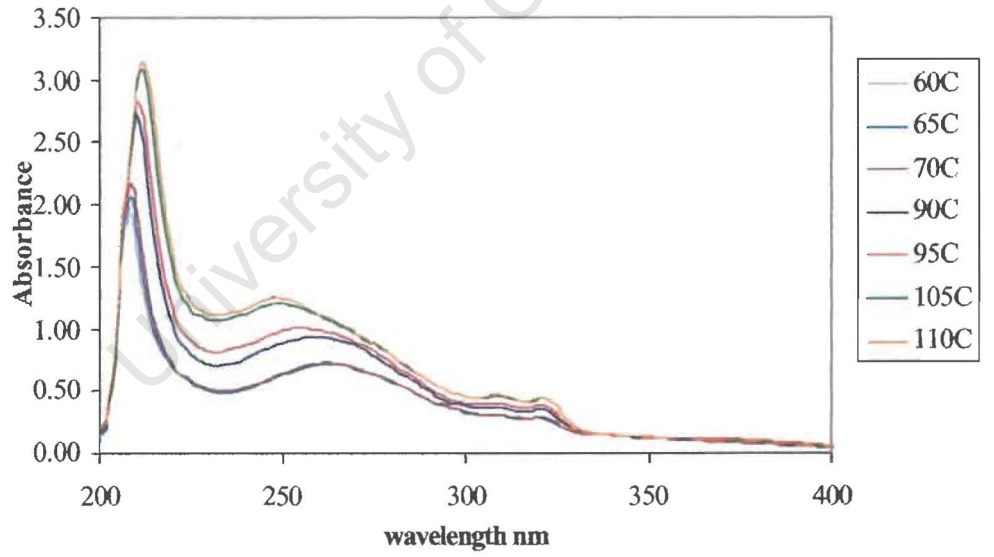

Fig. 4.9b Simulated Spectra of calf thymus DNA with 125µg ml^{-1} [Pt(bipy)H_2L]Cl solution taken after various temperatures.

4.3.2 Circular Dichoism

The circular dichroism spectrum of polydA-polydT shows three positive peak bands at 220nm, 260nm and 285nm respectively. There were also two negative bands with minima at 248nm and 270nm. The spectra of both Pt(II) complexes and the buffer solution showed no peak at all under experimental conditions. Addition of [Pt(bipy) H_2L]Cl into the solution of polydA-polydT induced changes in the UV circular dichroic spectrum (Fig. 4.10). The intensities of both the positive and negative ellipticity bands of the DNA decreased. From concentration of $1.5x10^{-6}$M to $7.5x10^{-6}$M, the changes in the intensities of the ellipticity bands were small. Between $1.2x10^{-5}$M and $1.8x10^{-5}$M, the changes increased significantly and after $1.8x10^{-5}$M, the changes became small again. The profile of the spectra, however, appeared to remain the same as for polydA-polydT alone with isosbestic points at wavelengths 210nm, 235nm, 255nm, 265nm and 275nm. Although the basic profile and isosbestic points remain unchanged, quenching of the peak maxima were observed as the concentration of the [Pt(bipy)H_2L]Cl increased. Similar trends were observed in the spectra of ethidium bromide (Fig. 4.11) and [Pt(phen)H_2L]Cl (Fig. 4.12). The CD spectra obtained after addition of [Pt(diMebipy)H_2L]Cl to polydA-polydT solution were slightly different. Upon the first few additions, the entire profile seemed to shift to higher intensities without intercepting the original spectrum (Fig. 4.13a). However, as the Pt(II) concentration increased, the spectra began to behave in the manner as observed for [Pt(bipy)H_2L]Cl (i.e. intercepting the original DNA curve with decreased intensity of peaks) (Fig. 4.13b). The spectra of [Pt(di-*tert*-butylbipy)H_2L]Cl showed the most upward shift with no intercepts on the original curve at all (Fig. 4.14). Concentrations of greater than $6.28x10^{-6}$M were not measured due to inaccuracy of the instrument in measuring high intensity peaks.

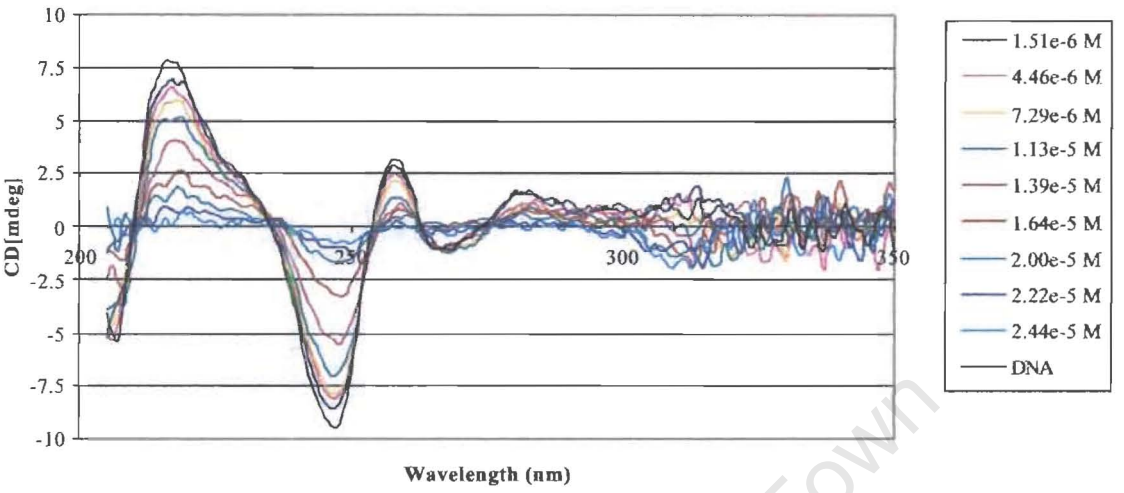

Fig. 4.10 CD Spectra of [Pt(bipy)H_2L]Cl binding to polydA-dT DNA

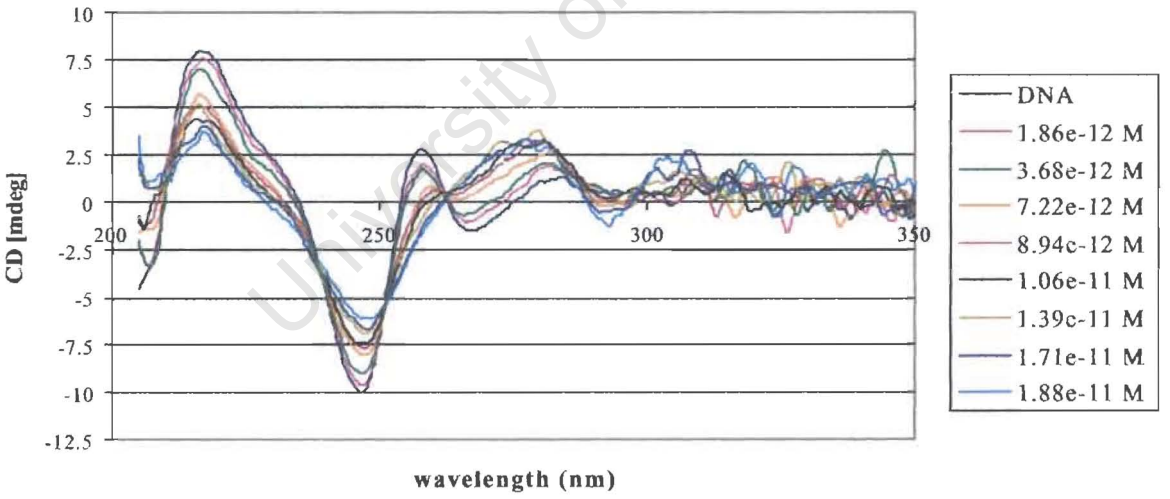

Fig. 4.11 CD Spectra of Ethidium bromide binding to polydA-dT DNA.

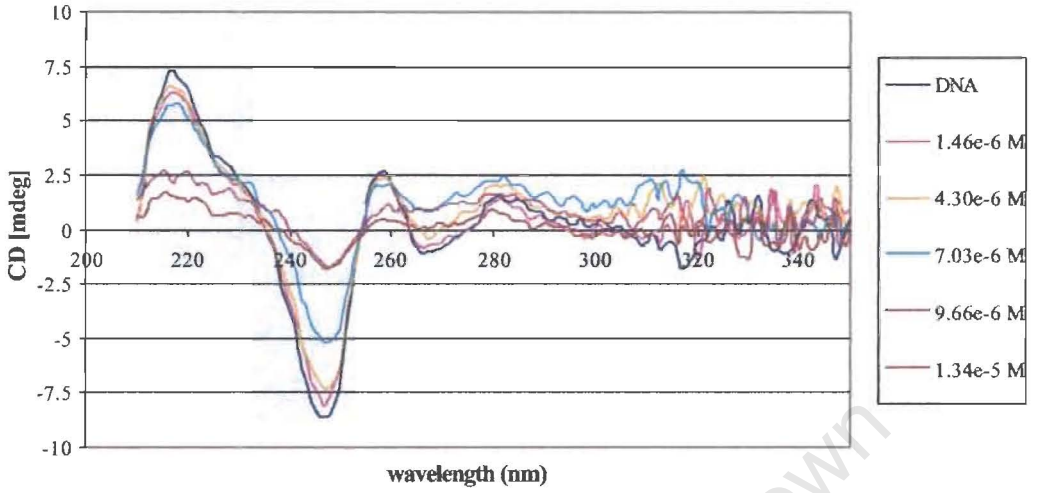

Fig. 4.12 CD spectra of [Pt(phen)H2L]Cl interacting with polydA-dT DNA

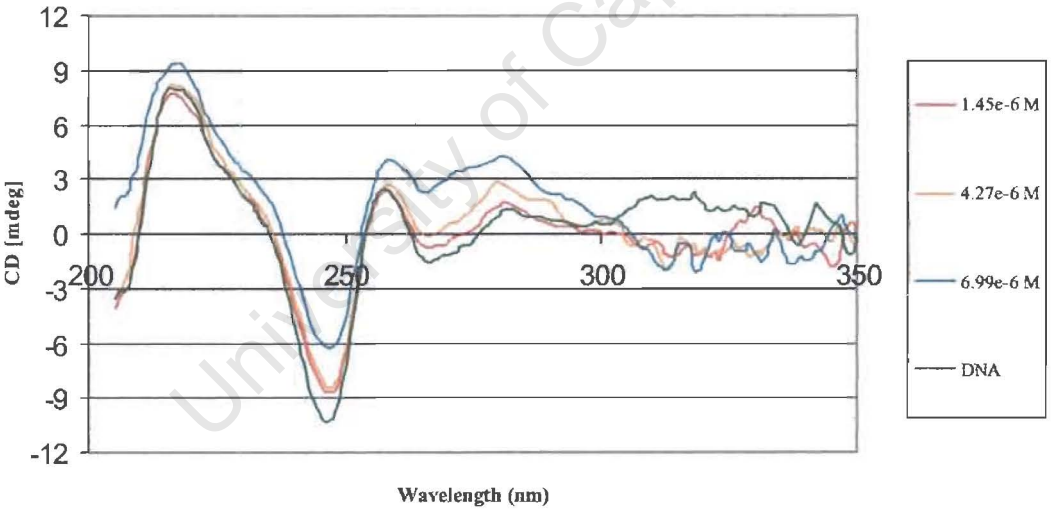

Fig. 4.13a CD Spectra of [Pt(diMebipy) H2L]Cl interacting with polydA-dT DNA for the first three concentration

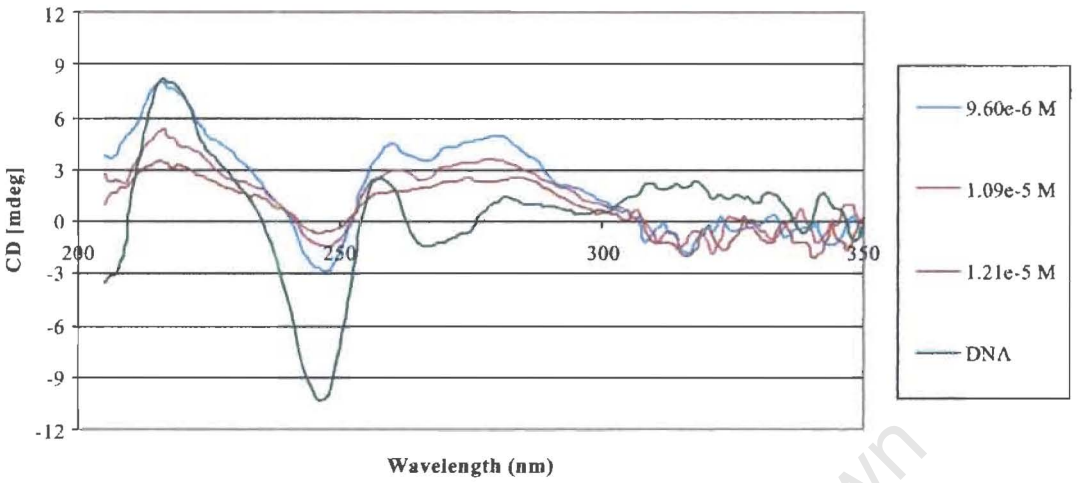

Fig. 4.13b CD Spectra of [Pt(diMebipy)H_2L]Cl interacting with polydA-dT DNA for the last three concentration

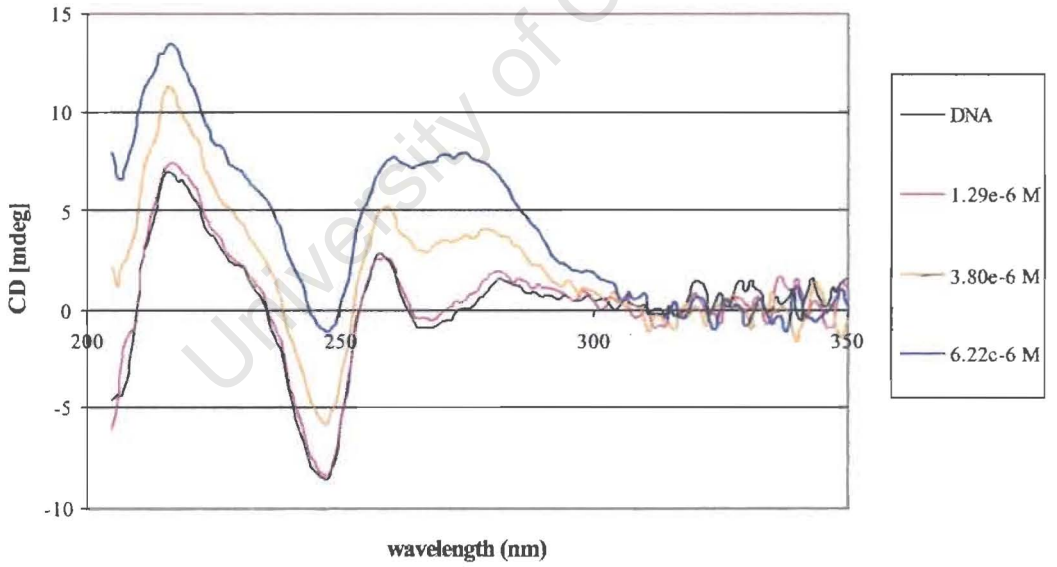

Fig. 4.14 CD spectra of [Pt(di-*tert*-butylbipy)H_2L]Cl with polydA-dT DNA

4.3.3 DNA Mobility in Agarose Gel

In experiments to test the effect of the binding of compounds to pBluescript(KS) plasmid DNA, no ethidium bromide was added to the agarose gel. When [Pt(bipy)H_2L]Cl was added to plasmid DNA in the Pt to DNA base pair ratio of 0, 0.25, 0.5, 0.75 and 1, some retardation in DNA mobility was observed. Above the ratio of 0.5, no more changes were observed (results not shown). The furthest band away from the well was the supercoiled plasmid DNA followed by linear DNA, and the relaxed circular DNA travels the slowest due to its topology. The supercoiled band was not observed after Pt to DNA base pair ratio 0.25, instead, a broad band was seen all the way to the relaxed circular band. In the gel electrophoretogram of plasmid DNA with [Pt(bipy)H_2L]Cl : base pair ratio of 0, 0.05, 0.1, 0.15, 0.2 and 0.25, one can see a gradual change in mobility of the DNA (Fig. 4.15A) even before ethidium bromide staining. When no [Pt(bipy)H_2L]Cl was added, a narrow supercoiled and a relaxed circular band were observed. As [Pt(bipy)H_2L]Cl to base pair ratio increased to 0.05, the narrow supercoiled band seemed to shift slightly upward (meaning travels slightly slower). When the ratio became 0.1, there was no more distinctive band but a broad "smear" band. The original narrow supercoiled band no longer appears and the broad band seems to travel towards the relaxed circular band. For another platinum complex [Pt(di-*tert*-butylbipy)H_2L]Cl, addition of the solution does not show any effect to the plasmid DNA at all. (Fig. 4.15B)

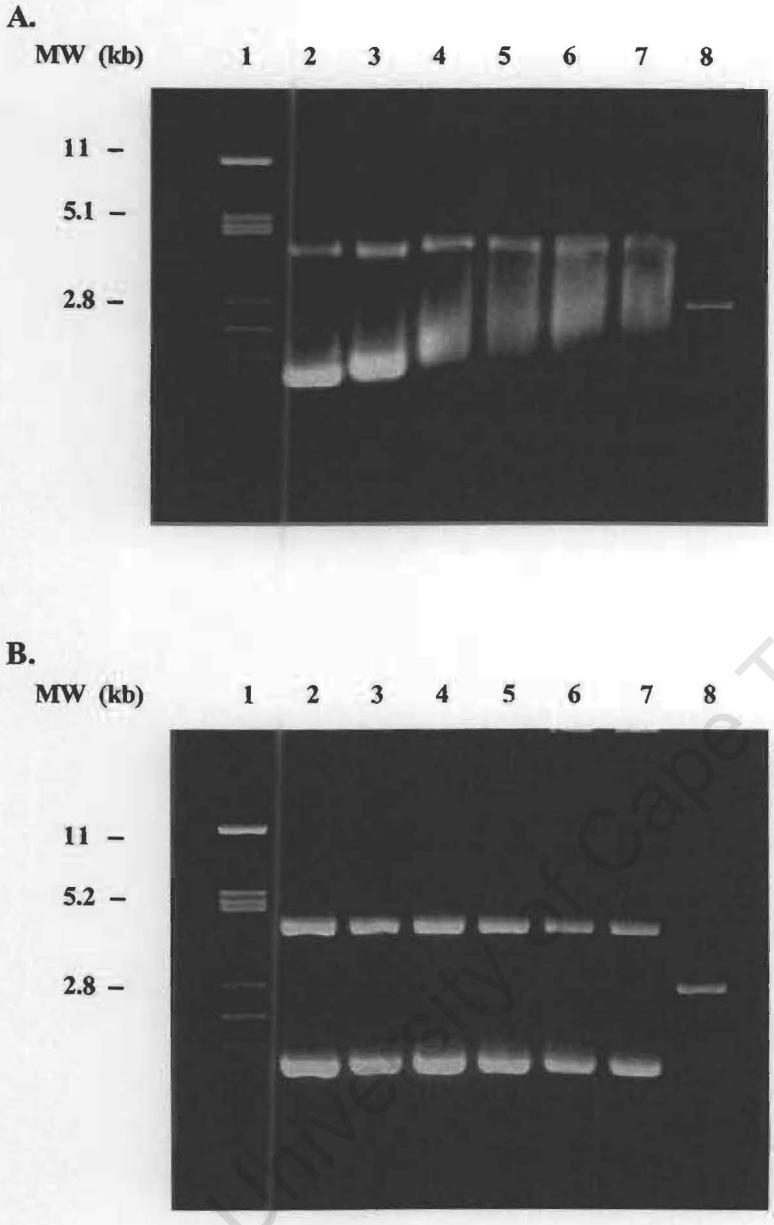

Fig. 4.15 Electrophoretogram of plasmid DNA before and after exposing it to various concentration of A. [Pt(bipy)H_2L]Cl and B. [Pt(di-*tert*-butylbipy)H_2L]Cl. lane 1, λ (*PstI*) DNA digested with PstI restriction endonuclease; lane 2-7, plasmid DNA after treated with A. [Pt(bipy)H_2L]Cl and B. [Pt(di-*tert*-butylbipy)H_2L]Cl, at the Pt / base pair ratio of 0, 0.05, 0.10, 0.15, 0.20, 0.25; lane 8, plasmid DNA after *Eco*RI digestion.

4.3.4 *In vivo* activity of Pt(II) compounds

Experiments were performed to determine whether the Pt(II) complexes had an effect *in vivo* and whether they targetted the DNA. *E.coli* AB1886 (*uvrA*$^-$), which has a mutated *uvrA* gene was used. This strain is unable to carry out excision repair of DNA damages and thus dies more rapidly compared to the wild type *E.coli* when Pt complex solution was added.

Previous work (chapter three) showed that in a 50:50 mixture of acetonitrile and water, the Pt(II) compounds became homogeneous in approximately 40 minutes. Since the compound was dissolved in water for the biological tests, 1.5 hours were allowed for a homogeneous solution to be achieved.

Survival Curves

Both wild type and *uvrA*$^-$ strain of *E.coli* were treated with 3 mg ml^{-1} of [Pt(bipy)H_2L]Cl, [Pt(phen)H_2L]Cl, [Pt(diMebipy)H_2L]Cl and [Pt(di-*tert*-butylbipy)H_2L]Cl solutions. Fig. 4.16 shows the average surviving fraction after exposing the cells to each of the Pt(II) solutions.

Fig. 4.16A showed any biological activity and only [Pt(bipy)H_2L]Cl resulted in a decrease in cell survival. After 60 minutes of exposure, the surviving fraction of uvrA$^-$ *E. coli* cells was more than 100 fold less than the wild type. Since the wild type and uvrA$^-$ *E. coli* cells only differ in one gene, the differences in their response to [Pt(bipy)H_2L]Cl solution suggested that this platinum complex targets DNA, and that the damage is partially repaired in the wild type as compared to the repair deficient *uvrA*$^-$ mutant. Interestingly, structurally similar complexes such as [Pt(phen)H_2L]Cl, [Pt(diMebipy)H_2L]Cl, and [Pt(di-*tert*-butylbipy)H_2L]Cl (Fig. 4.16 B, C, D) had no inhibitory effect on either *E. coli* strains at the same concentration.

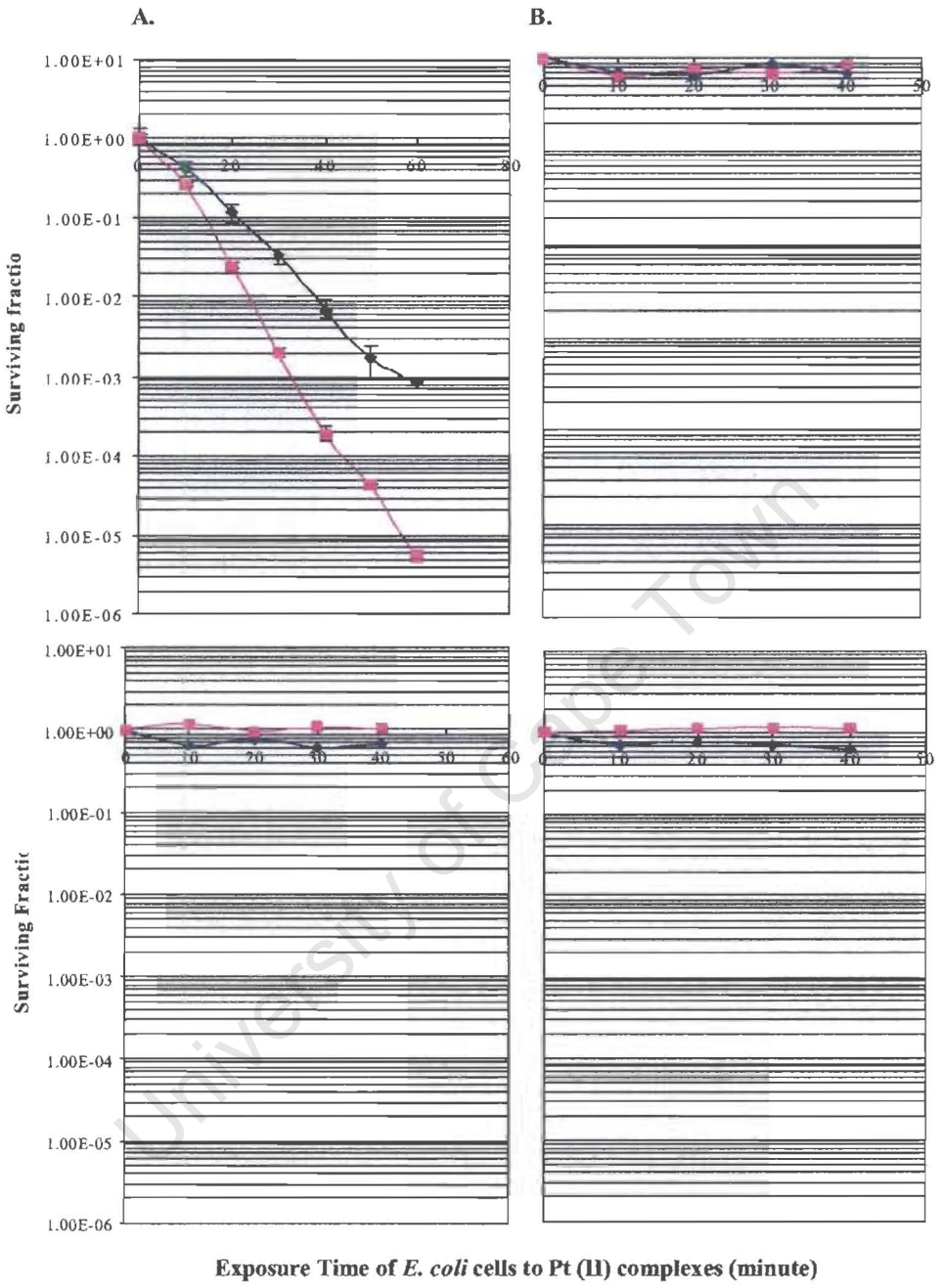

Fig 4.16 The surviving fraction of *wt*/*uvrA*⁻ *E. coli* cells after treatment with **A.** [Pt(bipy)H_2L]Cl, **B.** [Pt(phen)H_2L]Cl, **C.** [Pt(diMebipy)H_2L]Cl and **D.** [Pt(di-*tert*-butylbipy)H_2L]Cl complex. ◆ = *E. coli* AB1157 (wild type)
■ = *E. coli* AB1886 (*uvrA*⁻)

4.4 DISCUSSION

The interactions of nucleic acids with metal complexes have been extensively studied. In the case of interaction with cationic porphyrins, three possible binding modes were proposed[20,21]:

1) Intercalation can be characterised by the following observations. The intercalated DNA helix is stabilised against thermal denaturation. The characteristic Soret band of porphyrins displays substantial hypochromicity. There is often a negative induced CD band in the Soret region and the ellipticity in the near ultraviolet region is also altered. An increase in the solution relative viscosity is observed which indicates a lengthening of the persistence length of the DNA chain. Moreover, intercalation of the porphyrin results in an unwinding of covalently closed superhelical DNA.

2) Outside binding without porphyrin stacking displays a moderate bathochromic shift and hypochromicity/hyperchromicity of the Soret band. It also causes a positive induced CD band . However, there is no increase in the solution' s relative viscosity of linear DNA and no unwinding of DNA is observed.

3) Outside binding with the porphyrin stacking produce variable effects on the Soret band. In the CD spectrum, conservative signals are indicative of outside binding with stacking.

Many cationic water-soluble porphyrins undergo self-stacking in water and as described in Chapter 3, [Pt(diimine)H_2L]Cl complexes also self-associate strongly in aqueous solution. Thus the interaction of cationic porphyrins with DNA can aid in elucidating the mode of interaction of [Pt(diimine)H_2L]Cl complexes with DNA.

In this study, an increase in thermal stability of DNA was found after the binding of all the Pt(II) complexes. In the case of covalent binding of Pt(II) complexes, both interstrand cross links and intrastrand cross links that were induced by platinum coordination

significantly distort/destabilise the conformation of DNA.[16] This accounts for the decrease in melting temperature for cisplatin type of complexes as the platinum concentration increases. Even with positively charged platinum(II) complexes, the stabilisation on the DNA double helix can not overcome the distortion from the covalent binding. The Pt(II) complexes used in this study therefore are very unlikely to bind to DNA via covalent binding. The increase in T_m by addition of complexes [Pt(bipy)H_2L]Cl and [Pt(phen)H_2L]Cl can possibly be explained by intercalation or outside binding. As it could be seen in later experiments, binding through intercalation is the most likely interaction between [Pt(diimine)H_2L]Cl and DNA since an outside binding does not usually cause any DNA unwinding. Both bipyridine and phenathroline ligands after coordinating to Pt(II) possess planar π surfaces that are capable of intercalating between the stacked base pairs of the DNA double helix. When polydA-polydT was used, the shape of the DNA melting curve is almost the same after addition of [Pt(bipy)H_2L]Cl in the ligand concentration range from 2.27×10^{-8} M to 1.13×10^{-6} M, which suggests that the interaction with these low concentrations of Pt(II) complexes has no effect on the stability of the DNA structure. However, when the concentration was increased from 1.13×10^{-6} M to 2.26×10^{-6} M, a significantly broader melting temperature range was observed. This indicates that polydA-polydT is not in an uniform state with the [Pt(bipy)H_2L]Cl complex most likely bound to a portion of the DNA, resulting in a higher melting temperature than for untreated DNA. When we compare this result with the binding of dimethyl substituted bipyridine complex, we found that [Pt(diMebipy)H_2L]Cl complex gives an even broader melting profile, although they almost start to melt at the same temperature.

The change in the intensity of CD spectra can be viewed as a three stage process. At first, the gradual change in intensity up to a certain platinum to base pair ratio can be considered as the effect of the positively charged metal complexes which bind to the negatively charged DNA phosphate backbone by electrostatic force. After a critical platinum to base pair ratio, the reduction in the CD peak intensity became significantly larger. A reduction of CD spectra intensity generally indicates a more symmetrical (achiral) structure being formed. By comparing the CD spectra of polydA-polydT after

titrating with a concentration series of a known intercalator, ethidium bromide, one can confirm that the mode of binding for the complex [Pt(bipy)H_2L]Cl is by intercalation. The large reduction in both positive and negative ellipticity bands indicated a large change in helical structure of DNA. More specifically, the DNA loses its helicity and hence responds with a difference in absorbance of left and right polarised light. This is consistent with the assumption of intercalation: the insertion of an intercalating agent between the base pairs causes a spacing between the consecutive base pairs and the DNA double helix was unwound. As the concentration of [Pt(bipy)H_2L]$^+$ binding to the DNA phosphate backbone reaches a critical point, the bipyridine chromophore of [Pt(bipy)H_2L]$^+$ with its large π surface began to intercalate between two adjacent base pairs of the DNA double helix. If we look at the plot of ellipticity versus [Pt(bipy)H_2L]$^+$ to base pair ratio, it is not difficult to describe the intercalation as being a co-operative process. As the concentration of [Pt(bipy)H_2L]$^+$ increased to 1.64×10^{-5} M, the decrease in ellipticity became small again. This could indicate the saturation in the intercalation of Pt(II) complex to DNA. The CD spectra of [Pt(phen)H_2L]$^+$ was similar to that of [Pt(bipy)H_2L]$^+$. The loss of helicity observed is most probably due to intercalation. However, the binding affinity of the phenanthroline moiety seemed to be higher than the bipyridine since [Pt(phen)H_2L]$^+$ complex reached its saturation for intercalation at the lower concentration than [Pt(bipy)H_2L]$^+$. The upward shift of the spectrum [Pt(diMebipy)H_2L]$^+$ was surprising since one would expect the complex to behave in a similar way as [Pt(bipy)H_2L]Cl. The shift indicated that there was no change in the helicity of DNA and hence no intercalation observed between the compound and DNA at that concentration. At higher concentration of [Pt(diMebipy)H_2L]$^+$, the decrease in both the positive and the negative ellipticity bands were again observed. This suggests that at higher [Pt(diMebipy)H_2L]$^+$ concentration, the equilibrium favours intercalation despite the steric hindrance of methyl substituents on the bipyridine ligand. The tertiarybutyl group on the other hand is much more sterically demanding than the methyl group and therefore as expected, only a large upward shifts of the CD spectrum was observed.

Intercalating agents are known to relax supercoiled plasmid DNA. The first experiment included lanes with Pt: DNA base pair ratio (r_b) of 0, 0.25, 0.5, 0.75 and 1.0 showed

almost the same effect as the competition study. As the concentration of platinum increases, the bands became fainter. It suggests that the binding of Pt^{II} complex to the DNA substitutes for ethidium bromide, and makes the staining less effective. The retardation of bands could be due to the relaxation of plasmid DNA. The retardation was clearly observed at lower platinum to base pair ratios. There was a gradual upward shift of supercoiled band when r_b changes from 0 to 0.05. This can be explained by intercalation of [Pt(bipy)H_2L]Cl into the supercoiled plamid DNA. As the platinum to base pair ratio increases, the degree of intercalation also increases. At a critical point, there will be no more supercoiled DNA. Since [Pt(bipy)H_2L]Cl randomly populate the intercalation sites, it was expected when streaky bands were observed at r_b 0.1, 0.15, 0.20,0.25. The electrophoretogram of [Pt(di-*tert*-butylbipy)H_2L]Cl binding to plasmid DNA at the same r_b values showed no difference to the unplatinated DNA. This suggested that at those concentration level, [Pt(di-*tert*-butylbipy)H_2L]Cl complex does not intercalate due to the steric constrain of the tertiary butyl residues.

Amongst all the complexes tested, [Pt(bipy)H_2L]Cl, [Pt(diMebipy)H_2L]Cl, [Pt(di-*tert*-butylbipy)H_2L]Cl and [Pt(phen)H_2L]Cl, [Pt(bipy)H_2L]Cl was the only one that showed significant killing for both wild type *E.coli* and *uvrA*- mutant. This may be due to the different solubility property of these complexes and also their permeability for entering the cell membrane of *E.coli*. There is a hundred fold difference between the killing of wild type *E.coli* and the *uvrA*$^-$ mutant strain. As we have discussed earlier in the chapter, *uvrA*$^-$ strain *E.coli* is incapable of repairing chemical or ultra violet light damage by excision repair mechanism. When there is no difference between the survival of wild type and *uvrA*$^-$ strain *E.coli*, the chemical agent is known to be generally toxic to cells. However, if one can see a substantial difference between the two survival curves, then it suggests the chemical agent causes damage that is directed towards the DNA.

REFERENCES

1. K. W. Jennette, S. J. Lippard, G. A. Vassiliades and W. R. Bauer, *Proc. Natl. Acad. Sci. U.S.A.* 1974, **71**, 3839.
2. P. J. Bond, K. W. Jenette and S. J. Lippard, *Proc. Natl. Acad. Sci. U.S.A.*, 1975, **72**, 4825.
3. S. J. Lippard, P. J. Bond, K. C. Wu, and W. R. Bauer, *Science*, 1976, **194**, 726.
4. A. H. Wang, J. Nathans, G. van der Marel, J. H. van Boom and A. Rich, *Nature*, 1978, **276**, 471.
5. Y-S. Wong and S. J. Lippard, *J. Chem. Soc., Chem. Commun.*, 1977, 824
6. L. Kumar, N. R. Kandasamy and T. S. Srivastava, *Inorganica Chimica Acta*, 1982, **67**, 139.
7. N. Jain, R. Mital, S. Ray, T. S. Srivastava and R. K. Bhattacharya, *J. Inorganic Biochemistry*, 1987, **31**, 57.
8. R. Mital, K. S. Ray, T. S. Srivastava and R. K. Bhattacharya, *J. Inorganic Biochemistry*, 1986, **27**, 133.
9. A. M. Pyke, J. P. Rehmann, R. Meshoyner, C. V. Kumar, N. J. Turro and J. K. Barton, *J. Am. Chem. Soc.*, 1989, **111**, 3051.
10. H-Y. Mei and J. K. Barton, *Proc. Natl. Acad. Sci. U.S.A.*, 1988, **85**, 1339.
11. J. K. Barton, *Science*, 1986, **233**, 727.
12. J. K. Barton, A. T. Danishefsky, J. M. Goldberg, *J.Am.Chem.Soc.*, 1984, **106**, 2172.
13. T. Ren, D. P. Bancroft, W. I. Sundquist, A. Masschelein, M. V. Keck and S. J. Lippard, *J. Am. Chem. Soc.*, 1993, **115**(24), 11341.
14. M. V. Keck and S. J. Lippard, *J. Am. Chem. Soc.*, 1992, **114**(9), 3386
15. D. Freifelder, *Microbial Genetics*, Jones and Bartlett Publishers, Inc., 34
16. Garret and Grisham, *Biochemistry*, Saunders Co llege Publishing,1995, 229
17. D. and J. G. Voet, *Biochemistry*, John Wiley & Sons, 208
18. D. Freifelder, *Physical Biochemistry*, W. H. Freeman and Company, Chapter 13.
19. J. M. Veal and R. L. Rill, *Biochemistry*, 1991, **30**, 1132-1140.
20. N. E. Mukundan, G. Pethö, D. W. Dixon, M. S. Kim, and L. G. Marzilli, *Inorg. Chem.* 1994, **33**, 4676.

21. R. F. Pasternack, E. J. Gibbs, and J. J. Villafranca, *Biochemistry,* 1983, **22**, 2406.

22. H-Y. Mei and J. K. Barton, *Proc. Natl. Acad. Sci. U.S.A.*, 1988, **85**, 1339.

23. J. K. Barton, *Science*, 1986, **233**, 727.

24. J. K. Barton, A. T. Danishefsky, J. M. Goldberg, *J.Am.Chem.Soc.*, 1984, **106**, 2172.

5. CONCLUSION

A series of water soluble [Pt(diimine)(*N,N*-dihydroxyethyl-*N'*-benzoylthioureato)]$^{+}$A^{-} complexes have been successfully synthesised and characterised. The ^{1}H NMR spectra of these complexes in water showed considerable peak broadening, which indicated that these complexes undergo self-association to form aggregates in aqueous solution. The concentration dependence of ^{1}H NMR for these complexes and D_2O also indicated that they interact with each other to form at least dimers in 50% (v/v) acetonitrile-d_3 solution.

From the concentration dependence of the ^{1}H NMR spectra, the dimerisation constant K^D can be estimated. These dimerisation constants allowed us to examine the extent of dimer formation in the mixed solvent system. The results suggested that [Pt(diMebipy)H_2L]Cl self-associate most strongly (K^D = 36.4 ± 11.8 dm^3 mol^{-1}) followed by [Pt(bipy)H_2L]Cl and [Pt(di-*tert*-butylbipy)H_2L]Cl (K^D = 21.6 ± 2.7 dm^3 mol^{-1} and 22.3 ± 5.2 dm^3 mol^{-1}). This may be explained by the contribution of both inductive and steric effects, where the methyl substituents on bipyridyl ring of [Pt(diMebipy) H_2L]Cl contribute positively towards the formation of dimer and at the same time does not pose a steric constrain.

The dimer species were also confirmed by electrospray ionisation mass spectroscopy as molecular ions such as {[Pt(diimine)H_2L]$_2$Cl}$^{+}$ were observed.

The solvent composition was also found to influence the dimerisation of these Pt(II) complexes. As the water content increases in the acetonitrile/water mixture, the K^D value also increases. This could be explained by the fact that in a more water like solvent mixture, the interaction between the aggregates and the solvent is also maximised.

Hunter and Sanders' model of π-π interaction was used to explain the dimerisation of [Pt(diimine)(*N,N*-dihydroxyethyl-*N'*-benzoylthioureato)]$^{+}$A^{-} complexes in the acetonitrile/H_2O mixed solvent and a possible dimer structure was being proposed.

In pure aqueous solution, [Pt(diimine)(*N,N*-dihydroxyethyl-*N'*-benzoylthioureato)]$^+A^-$ complexes were found to form larger aggregates as observed by the transmission electron microscope. Both [Pt(bipy)H_2L]Cl and [Pt(diMebipy)H_2L]Cl showed ribbon like structures while rod-shaped structure was observed for [Pt(di-*tert*-butylbipy) H_2L]Cl. When the solution of [Pt(di-*tert*-butylbipy) H_2L]Cl was heated up to 50° and 80°, the rod-like structure gradually disappeared and "doughnut" shaped rings of various sizes started to form. These findings lead to reasonable speculation that the stacking of these complexes can be presented in the following way:

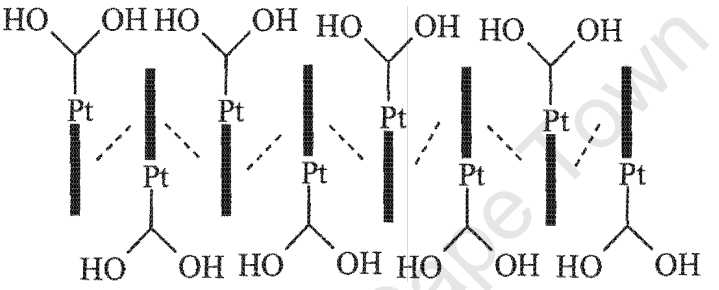

= diiimine ligand

HO
HO
= *N,N*-dihydroxyethyl-*N'*-benzoylthiourea ligand

-------- = π-π interaction

The [Pt(diimine)(*N,N*-dihydroxyethyl-*N'*-benzoylthioureato)]$^+A^-$ complexes were designed to be a potential DNA intercalators due to their planar structure. From the aggregation study, these complexes are postulated to form ribbon like structures, which is likely to be a positively charged supra molecular aggregate. Since the DNA phosphate backbone is negatively charged, it is possible for the aggregated compound to attach itself along the DNA backbone by electrostatic interation. This way, the compound would have also bind to DNA through a grove binding mode. Studies therefore were undertaken to elucidate the mode of binding of these complexes to DNA.

Several methods were designed to study the mode of binding, these including DNA melting spectrophotometry, Circular Dichroism and DNA mobility study. The DNA melting experiments showed significant increase in melting point of DNA upon the addition of [Pt(diimine)H_2L]Cl complexes. This indicated that these complexes interact with DNA and stabilise the double helical structure. The spectra of circular dichoism (CD) also confirmed the binding complexes [Pt(bipy)H_2L]Cl, [Pt(diMebipy)H_2L]Cl and [Pt(phen)H_2L]Cl to DNA by intercalation. The reduction on the CD peaks suggest the unwinding of DNA double helix. This result was consistent after comparing to the known intercalator, ethidium bromide. [Pt(di-*tert*-butylbipy)H_2L]Cl, however, showed no binding at all. This was expected since the tertiary butyl groups on the bipyridine ligand may provide steric hindrance to the intercalating site. The gel mobility study compared the two complexes [Pt(bipy)H_2L]Cl and [Pt(di-*tert*-butylbipy)H_2L]Cl confirming the intercalation was restricted by the bulky tertiary butyl substituents on the bipyridine moiety. This is illustrated in Fig. 5.1 and Fig. 5.2.

Finally these complexes were also tested *in vivo* system to determine whether they show any biological activity. A wild type strain *E.coli* and a excision repair deficient mutant strain *uvrA*$^-$ were used for the survival study. It was found that [Pt(bipy)H_2L]Cl complex was the only complex that showed significant toxicity and the rest of compounds were found inactive. This may be due to their permeability for entering the cell membrane of *E.coli*. There is a hundred fold difference between the killing of wild type *E.coli* AB1157 and *uvrA*$^-$ mutant AB1886 by [Pt(bipy)H_2L]Cl complex. The *uvrA*$^-$ strain showed the inability to repair the damage by [Pt(bipy)H_2L]Cl while the wild type strain with a normal excision repair mechanism showed much less toxicity indicates that the complex causes damages directly to the DNA.

Fig 5.1 The three dimensional representation of [Pt(bipy)H_2L]Cl complex intercalating into DNA double helix.

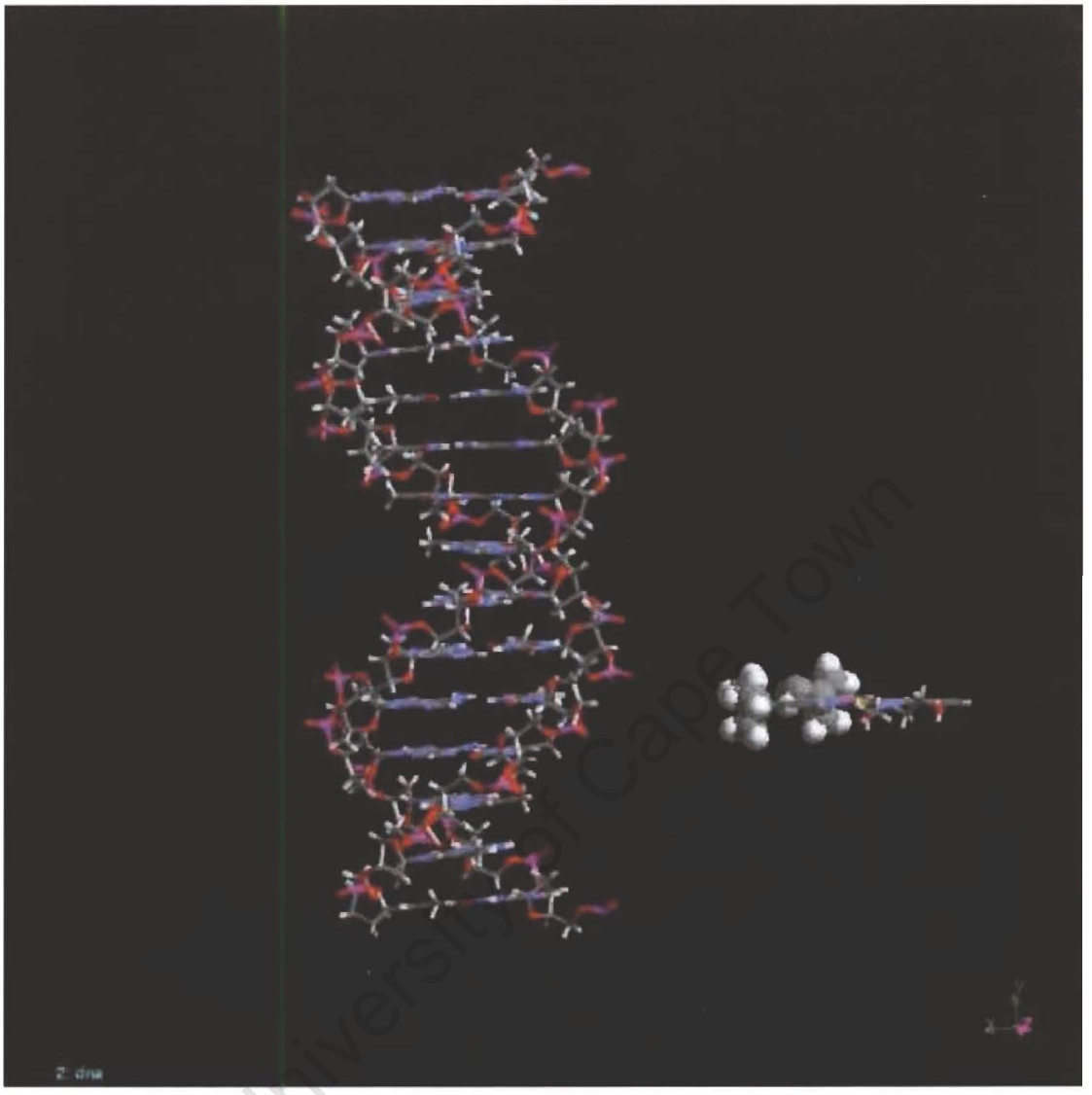

Fig. 5.2 The three dimensional representation showing the tertiary butyl groups on the bipyridyl rings poses steric hindrance for DNA intercalation.